Over-expression, purification and characterization of Adh5p from *Saccharomyces cerevisiae.*

by

Michael Ernst Henn

May 2010

University of the Free State
Universiteit van die Vrystaat

Over-expression, purification and characterization of Adh5p from *Saccharomyces cerevisiae.*

by

Michael Ernst Henn

Submitted in fulfillment of the requirements
for the degree

MAGISTER SCIENTIAE

In the Faculty of Natural and Agricultural Sciences
Department of Microbial, Biochemical and Food Biotechnology
University of the Free State
Bloemfontein
South Africa

May 2010

Study Leader: Prof. J. Albertyn
Co-study Leaders: Dr. O. de Smidt
Prof. J.C. du Preez

TABLE OF CONTENTS

LIST OF FIGURES AND TABLES

Fig 6: This illustration depicts the two main domains in Adh. Adh1p, Adh2p and Adh3p bind four moles of NAD^+ and four atoms of zinc. A zinc atom is crucial for maintaining the quaternary structure of the enzyme, as well as sharing catalytic function (taken from Vallee and Falchuk, 1993).

Fig 7: Active site of alcohol dehydrogenase I. The proton relay system illustrates the protonation and deprotonation of amino acid residues important in transferring protons from the active site to the surface of the protein (taken from Leskovac et al. 2002).

Fig 8: The chemical reaction catalyzed by Adh, occurring when protons are shifted during the proton relay system (Klinman, 1974).

Fig 9: Scheme 1 illustrates the uptake of a proton prior to acetaldehyde reduction. Scheme 2, contradictory to scheme one, suggests that proton uptake takes place subsequent to aldehyde reduction (taken from Klinman, 1974).

Fig 10: Gel electrophoresis of *ADH5* amplicons. *ADH5* PCR product with a 6X N-terminal His-tag (**lane 1**) and *ADH5* amplified with a 6X C-terminal His-tag (**lane 2**)**.** Lane **GR** represents a 1 Kb DNA ladder (Fermentas).

Fig 11: Restriction profiles of transformed *ADH5* clones in dam^- competent *E. coli* cells ligated into pGEM®-T Easy. (**Lane 1** and **2**), pGEM®-T Easy::*ADH5* N-terminal His-tag. (**Lane 3** and **4**), pGEM®-T Easy::*ADH5* C-terminal His-tag. The ~3 kb band is represented by the pGEM®-T Easy backbone, and the ~1.1 kb band is represented by the *ADH5* gene. The ~4 kb band represents partially digested plasmid DNA.

Fig 12: Restriction profiles of three clones representing the successful shuttling of the His-tagged *ADH5* ORF from pGEM®-T Easy into pYES2. Two clones represent constructs with the *ADH5* N-terminal His-tag (**lane 1** and **lane 2**) and the other the construct harbouring the C-terminal His-tag (**lane 3**). The ~6 kb fragment represents the pYES2 backbone and the ~1.1 kb fragment the His-tagged *ADH5* ORF.

Fig 13: Plasmid map of the pYES2 vector indicating the *GAL1* inducible promoter region, selection is based on the *URA3* yeast marker. *ADH5* containing the 6X His-tag with restriction sites *Hind*III and *Xba*I is also annotated and visible on the map.

Fig 14: SDS-PAGE illustrating the expression levels of Adh5p in both *S. cerevisiae* CEN PK42 and *S. cerevisiae* W303-1A at various time intervals. Adh5p is located at 40 kDa. **A**: *S. cerevisiae* W303-1A at time 2 hours, (**lane 1** and **2**) and *S. cerevisiae* CEN PK42 at time 2 hours (**lane 3** and **4**). Maximum expressions for these strains are represented in **B:** *S. cerevisiae* W303-1A harvested at 8 hours (**lane 1** and **2**) and *S. cerevisiae* CEN PK42 harvested at 8 hours (**lane 3** and **4**).

Fig 15: N-terminal hybridization of *S. cerevisiae* Invsc, *S. cerevisiae* CEN PK42 and *S. cerevisiae* W303-1A after 8 hours of expression. Harvested cellular fractions extracted from all three strains indicate a band at approximately 40 kDa. *S. cerevisiae* Invsc (**lane 1**), *S. cerevisiae* CEN PK42 (**lane 2**) and *S. cerevisiae* W303-1A (**lane 3**). The reference (**lane 4**) represents the expression level at nil hours, immediately after inoculation into 2% galactose.

Fig 16: Western blot hybridization of Adh5p in *S. cerevisiae* strain W303-1A and *S. cerevisiae* Invsc. The 40 kDa purified Adh5p expressed in *S. cerevisiae* Invsc is represented in (**lane 1**) while the expression of *S. cerevisiae* Invsc at time 0 is represented in (**lane 2**). Purified Adh5p expressed in *S. cerevisiae* strain W303-1A (**lane 3**). Lysed *S. cerevisiae* W303-1A cells expressed for 8 hours (**lane 4**) and expression in *S. cerevisiae* W303-1A at time 0 (**lane 5**). Prestained page blue protein ladder (Fermentas) (**lane 6**).

Fig 17: SDS-PAGE analysis of purified Adh5p using Ni-NTA Spin Columns, illustrating Adh5p at 40 kDa, harvested at 8 hours expression (**lane 1**). *S. cerevisiae* W303-1A lysed after 8 hours of Adh5p expression (**lane 2**). Sample taken prior to induction of *S. cerevisiae* W303-1A with *GAL1* promoter (**lane 3**). Fermentas unstained protein ladder can be interpreted in lane (**PL**).

Fig 18: Adh5p elution profile. The blue line represents the A_{280} and the pink line the linear gradient of imidazole. When the conductivity reached 20% the protein shifted to mobile phase. This resulted in the elution of Adh5p, to be used in down-stream kinetic experiments.

Fig 19: **A:** Western blot analysis of purified Adh5p after dialysis illustrating the purified Adh5p at 40 kDa after 8 hours expression (**lane 1**). The prestained protein ladder was compared to the unstained protein ladder from SDS-PAGE. Prestained protein ladder has a tendency to denature resulting in false band sizes (**lane 2** and **lane 3**). **B**: Purified Adh5p (**lane 1**) and unstained protein ladder (**lane 2**).

Fig 20: BCA standard curve. The theoretical absorbance is annotated on the Y axis and the protein concentration on the X axis. Curve was constructed from dilution range provided by the manufacturer. The graph represents a linear curve recorded at A_{562}.

Fig 21: Data profile illustrating the relative activity in percentage towards the four co-factors utilized in YADHs. NAD^+ was plotted as 100% and the other co-factors conversion rates are plotted against NAD^+.

Fig 22: Optimum pH of Adh5p determined at 30°C with ethanol as substrate and NAD^+ as co-factor. The data demonstrates the optimum pH at 8.8 with a rapid decline visible when the pH exceeds 9. The error bars indicate the standard deviations calculated from triplicate experiments to be less than 10%.

Fig 23: Optimum temperature of Adh5p determined at 30°C with ethanol as substrate and NAD^+ as cofactor. The optimum activity was plotted as 100% and the rest of the data plotted relative to it with standard deviation less than 10%.

Fig 24: Illustration of the substantial difference in relative activity in % of Adh5p when exposed to alcohols increasing in chain length. Standard deviations calculated are less than 12%.

Fig 25: Kinetics of Adh5p towards ethanol as substrate in mM, specific activity is expressed in µMol min^{-1} mg^{-1}. The data follows Michaelis-Menten steady state kinetics. Parameters were kept at 30°C, pH 8.8. The graph indicates a clear turnover of substrate to product. Enzyme saturation occurred at relatively low concentrations, approximately 3 mM ethanol.

Fig 26: Enzyme kinetics illustrating the 1st and 2nd order reaction progress curve of the characterization based on NAD^+ as substrate at fixed ethanol concentration. Parameters were kept at 30°C, pH 8.8. The graph indicates a clear turnover of substrate to product. Enzyme saturation occurred at relatively low concentrations, approximately 5 µM NAD^+. The V_{max} determined in the NAD^+ characterization is much lower than characterization data presented in **Fig 25**.

Fig 27: Enzyme kinetics illustrating the 1st and 2nd order reaction progress curve of the characterization based on propan-2-ol as substrate at fixed co-factor concentration. Parameters were kept at 30°C, pH 8.8. Enzyme saturation occurred at low concentrations, approximately 3 mM propan-2-ol. The enzyme proved a very insufficient catalyst of propan-2-ol. This is due to the branched backbone of the alcohol.

Fig 28: 1st and 2nd order reaction progress curve of the characterization based on NAD^+ as substrate. Parameters were kept at 30°C, pH 8.8. Enzyme saturation occurred at low concentrations, approximately 3 mM NAD^+. The enzyme proved a very insufficient catalyst of propan-2-ol. This is due to the branched backbone of the alcohol.

Fig 29: Kinetics of butanol as substrate in mM, the specific activity was calculated in µMol min^{-1} mg^{-1} Adh5p. Enzyme saturation occurred at approximately 3 mM butanol. Parameters were kept at 30°C, pH 8.8. The activity towards butanol is higher than towards propan-2-ol. This signifies the effect of branched alcohols

on the activity of Adh5p. Butanol chain length is longer than propan-2-ol. However, butanol is not branched.

Fig 30: 1st and 2nd order reaction progress curve of the characterization based on NAD^+ as substrate. Enzyme saturation occurred at approximately 3 mM NAD^+. Parameters were kept at 30°C, pH 8.8.

Fig 31: Kinetics of pentanol as substrate in mM, the specific activity was calculated in µMol min^{-1} mg^{-1} Adh5p. Enzyme saturation occurred at approximately 3 mM pentanol. Parameters were kept at 30°C, pH 8.8. The activity towards pentanol is higher than towards propan-2-ol. However, ethanol is the preferred substrate.

Fig 32: 1st and 2nd order reaction progress curve of the characterization based on NAD^+ as substrate. Enzyme saturation occurred at approximately 3 mM NAD^+. Parameters were kept at 30°C, pH 8.8.

Fig 33: Kinetics of hexanol as substrate in mM, the specific activity was calculated in µMol min^{-1} mg^{-1} Adh5p. Enzyme saturation occurred at approximately 2 mM hexanol. Parameters were kept at 30°C, pH 8.8. The activity towards hexanol is higher than towards propan-2-ol. However, ethanol is the preferred substrate.

Fig 34: 1st and 2nd order reaction progress curve of the characterization based on NAD^+ as substrate. Enzyme saturation occurred at approximately 3 mM NAD^+. Parameters were kept at 30°C, pH 8.8.

Fig 35: Kinetics of decanol as substrate in mM, the specific activity was calculated in µMol min^{-1} mg^{-1} Adh5p. Enzyme saturation occurred at approximately 3 mM decanol. Parameters were kept at 30°C, pH 8.8. The enzyme is not capable of oxidizing decanol. This alcohol has a 10-carbon chain length. The affinity towards decanol is the lowest from all the substrates used in this study. The K_m is double that recorded for ethanol.

Fig 36: 1st and 2nd order reaction progress curve of the characterization based on NAD^+ as substrate. Enzyme saturation occurred at approximately 3 mM NAD^+. Parameters were kept at 30°C, pH 8.8. The reduction of NAD^+ was extremely low. No significant signs of reduction were recorded.

Fig 37: PCR amplicons representing the a*dh1*∆::*LEU2* ~4 kb fragment amplified with primer set *ADH1*-1F and *ADH1*-1R. Lane **GR** is represented by a 1 kb DNA ruler supplied by Fermentas.

Fig 38: PCR profile of clones screened for a*dh1*∆::*LEU2* replacement. 1 kb DNA ruler (**GR**) and gel electrophoresis of clones screened for a*dh1*∆::*LEU2* (**lane 1 – 13**) delivering a ~1.7 kb fragment when amplified with *ADH1-2F/*LEU2-1R . Visualization of this band indicates the deletion of *ADH1* by replacing the gene with a selective marker (*LEU2*).

Fig 39: **A:** Gel electrophoresis illustrating PCR profiles of triple deletion mutant clones screened for the a*dh3*∆::*TRP1* deletion (**A**) and intact *ADH4* and *ADH5* genes. **B:** Multiplex PCR reaction, containing primer sets to amplify *ADH1* – *ADH5* ORFs. As expected no amplification was visible for the *ADH1*, *ADH2* and *ADH3* genes, while the intact *ADH4* and *ADH5* genes were represented by amplicons of ~1.4 kb for *ADH4* and ~1.1 kb for *ADH5* in length respectively (**lane 1 – 6**).

Fig 40: PCR results applied to genomic DNA extracted from triple deletion mutant, lacking *ADH1, ADH2* and *ADH3*. Primers were used to amplify the a*dh2*∆::*URA3* deletion identified at ~1.5 kb. . Visualization of this band indicates the deletion of *ADH2* by replacing the gene with a selective marker (*URA3*).

Fig 41: Gel electrophoresis illustrating PCR profiles using *ADH1*-MH-R (*Hin*dIII) and *ADH1*-MH-F (*Xba*I). 5 kb amplicon containing the 1 kb *ADH1* promoter region, 1 kb *ADH1* terminator region and pGEM®-T Easy backbone can be seen in (**lane 1**). DNA gene ruler (**GR**) (Fermentas).

Fig 42: Gel electrophoresis of two clones (pGEM®-T Easy plus promoter, terminator and *ADH5* gene). The 5 kb band represents the pGEM®-T backbone illustrated in **Fig 41**. The *ADH5* gene is represented by the ~1.1 kb bands visualized in both **lanes 1** and **2.** DNA gene ruler (**GR**) (Fermentas).

Fig 43: Gel electrophoresis of two clones after ligation into pRS413 and pRS423 respectively. Clones were digested with *Bam*HI. pRS413, delivered a ~2.5 kb and ~5.5 kb band respectively (**lane 1**). pRS423, delivered a ~2.1 kb and ~6.5 kb band respectively (**lane 2**).

Fig 44: pRS413::*ADH5.* Finalized vector in circular configuration with *ADH5* flanked with the *ADH1* promoter and *ADH1* terminator regions. *HIS3* is the selective marker utilized by both pRS413 and pRS423. The transformed strain has the capability to grow in histidine deficient media, due to vector's capability for selection on histidine.

Fig 45: pRS423::*ADH5.* Finalized vector in circular configuration with *ADH5* flanked with the *ADH1* promoter and *ADH1* terminator regions. *HIS3* is the selective marker utilized by both pRS413 and pRS423. The transformed strain has the capability to grow in histidine deficient media, due to vector's capability for selection on histidine.

Fig 46: Growth profiles of *S. cerevisiae* W303-1A, *S. cerevisiae* Q1, *S. cerevisiae* *T*∆*123*::*ADH5*_S and *S. cerevisiae* *T*∆*123*::*ADH5*_M on glucose or ethanol as carbon sources. Strains were grown in chemically defined medium in shake flasks at 30°C. **A**: *S. cerevisiae* W303-1A (**green**), *S. cerevisiae* Q1 (**blue**), *S. cerevisiae* *T*∆*123*::*ADH5*_S (**red**) and *S. cerevisiae* *T*∆*123*::*ADH5*_M (**orange**) grown on 7 g l^{-1} ethanol. **B**: Illustrates growth of *S. cerevisiae* W303-1A (**green**), *S. cerevisiae* Q1 (**blue**), *S. cerevisiae* *T*∆*123*::*ADH5*_S (**red**) and *S. cerevisiae* *T*∆*123*::*ADH5*_M (**orange**) on 8 g l^{-1} glucose as carbon source.

Fig 47: Curves **A+B**, illustrates biomass (**blue**) over time, on ethanol (**green**) as carbon source. **A:** Growth of *S. cerevisiae* Q1 on ethanol as carbon source indicates an increase in biomass with a decrease in ethanol to approximately

0.07 g l^{-1}. **B**: Growth of *S. cerevisiae* W303-1A on 7 g l^{-1} ethanol, ethanol depletion takes place at a quicker rate than that of *S. cerevisiae* Q1.

Fig 48: Graphs **A** and **B** represent the growth studies performed on both *S. cerevisiae T∆123*::*ADH5*_S and *S. cerevisiae T∆123*::*ADH5*_ M. **A:** Biomass formation (**blue**) and ethanol consumption (**green**) of *S. cerevisiae T∆123*::*ADH5*_S. Biomass yield is tenfold lower than that of *S. cerevisiae* W303-1A and *S. cerevisiae* Q1. 2 g of ethanol was utilized. **B:** Biomass formation (**blue**) and ethanol consumption (**green**) of *S. cerevisiae T∆123*::*ADH5*_M.

Fig 49: Graphs **A** and **B** represent the growth studies performed on both *S. cerevisiae* W303-1A and *S. cerevisiae* Q1 with 8 g l^{-1} glucose as carbon source. Biomass (**blue**) vs. ethanol (**green**) formation and glucose (**purple**) depletion. Ethanol pathway was activated as glucose concentration decreased. Adh1p and Adh2p is primarily responsible for the ethanol metabolism in *S. cerevisiae* W303-1A (**A**). Adh1p is responsible for the ethanol metabolism in *S. cerevisiae* Q1 (**B**).

Fig 50: Graphs **A** and **B** represent the growth studies performed on both *S. cerevisiae T∆123*::*ADH5*_S and *S. cerevisiae T∆123*::*ADH5*_ M, 8 g l^{-1} glucose as carbon source. Biomass (**blue**) vs. ethanol (**green**) formation and glucose (**purple**) depletion. For both the singlecopy vector (**A**), and multicopy expression (**B**). Glucose depletion took place after approxiamtly 20 hours, where max biomass yield was identified. Ethanol production started after 7 hours of incubation. The ethanol formation rate in the multicopy expression is slightly higher.

Fig 51: Analysis curves, illustrating acetaldehyde (**blue**) and glycerol (**purple**) accumulation. Both in *S. cerevisiae T∆123*::*ADH5*_S (**A**) and *S. cerevisiae T∆123*::*ADH5*_ M (**B**). Acetaldehyde concentrations increased in both strains. A clear indication that acetaldehyde is being formed and not catalyzed by Adh5p. The glycerol concentrations also increased in both strains.

Table 1. Strains used in this study

Table 2. Chemically defined medium components

Table 2a. Vitamin solution composition

Table 2b. Amino acid composition

Table 2c. Trace element solution

Table 3. List of primers used in this study

Table 4. Kinetic parameters of Adh5p calculated per active site. Enzymatic activities were measured in 50 mM Sodium Phosphate, pH 8.8. K_m and V_{max} values were determined by interpretation of steady state kinetic curves.

Table 5. Data retrieved from different studies, the purpose of this table is to compare data between the various K_m and V_{max} values of Adh1p, Adh2p and now characterized Adh5p to ethanol as substrate.

Table 6. *S. cerevisiae* strain W303-1A, *S. cerevisiae* Q1, *S. cerevisiae T∆123*::*ADH5*_S and *S. cerevisiae T∆123*::*ADH5*_M. Growth parameters are listed below.

Table 7. Growth parameters of *S. cerevisiae* W303-1A, *S. cerevisiae* Q1, *S. cerevisiae T∆123*::*ADH5*_S and *S. cerevisiae T∆123*::*ADH5*_M in bioreactor batch cultures grown on glucose.

Table 8. Expression of Adh5p and Adh1p on ethanol and glucose as carbon sources respectively.

CHAPTER 1: LITERATURE STUDY

1 INTRODUCTION

Alcohol dehydrogenases are oxidoreductase enzymes which participate in the metabolism of alcohols and the detoxification of bile salts. In the yeast *Saccharomyces cerevisiae* five of these enzymes (Adh1p - Adh5p) have been identified and classified in playing a role in either the reduction of acetaldehyde to ethanol, or the oxidation of ethanol to acetaldehyde. They are ubiquitous in nature and can be isolated from plants, mammals, insects, yeast and bacteria.

1.1 Classification of Adh

Alcohol dehydrogenases are classified under two main categories, namely short chain dehydrogenases (SDR) and medium chain dehydrogenases (MDR). *S. cerevisiae,* Adh1p – Adh5p fall under the MDR category. Two additional alcohol dehydrogenase enzymes, Adh6p and Adh7p, fall under a different group and are classified as cinnamyl Adhps (CAD). The cellular functions of the two enzymes are not known. These two enzymes also share high homology with plant cinnamyl Adh (Gonzalez et al. 2000: Larroy et al. 2002b).

1.2 Short chain dehydrogenase

Short chain dehydrogenases (SDR) are enzymes consisting of approximately 250 amino acid residues catalyzing NAD(P)(H^+) dependent redox reactions. The first concept of SDRs was established in 1981 (Jornvall et al. 1981). At that time the only known members of this group were the prokaryotic ribitol dehydrogenase as well as an insect alcohol dehydrogenase. There are currently at least 3000 members that represent the SDR group (Keller et al. 2006). These members originate from various species and include a wide substrate spectrum, ranging from alcohols, sugars, steroids to aromatic

compounds. SDR members are further divided into two large families, namely classical SDRs and extended SDRs. Classical SDRs consist of a typical residue length of about 250 amino acids whereas extended SDRs are approximately 350 residues in length (Kallberg et al. 2002).

The addition of new sequences to the superfamily is based on functional assignments and distinct characteristics of these sequences. Through analysis of these defined characteristics, the classical SDRs can further be subdivided into seven subfamilies and extended SDRs into three subfamilies. These defined characteristics can be used for functional predictions of further novel structures. This functional assignment system is implemented in human, *Dorosphila melanogaster, Saccharomyces cerevisiae, Arabidopis thaliana* and the mouse genome research (Kallberg et al. 2002). The illustration in **Fig 1** identifies the spheres indicating the co-enzyme deterministic position for oxidised/reduced nicotinamide adenine dinucleotide ($NAD(H^+)$) in red and oxidised/ reduced nicotinamide adenine dinucleotide phosphate ($NADP(H^+)$) in blue. The blue ribbons in **Fig 1** are used to identify various SDR members. The co-enzyme is coloured magenta as seen in **Fig 1** (Kallberg et al. 2002).

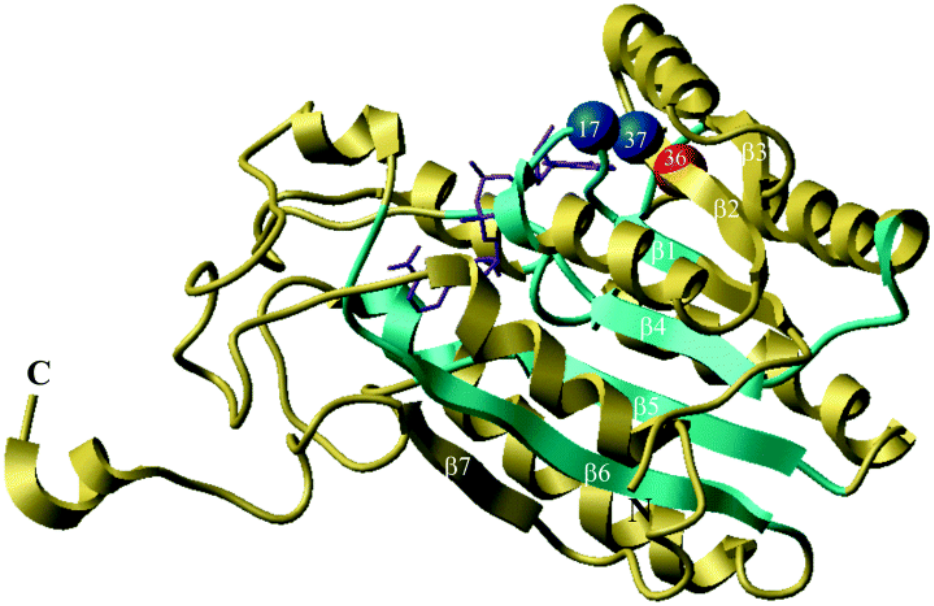

Fig 1: Classical SDR enzyme with motifs (taken from Kallberg et al. 2002).

1.3 Medium chain dehydrogenase

MDRs can sometimes be referred to as long chain dehydrogenases, and constitute a widespread enzyme superfamily with members found in Bacteria, Archaea and Eukaryota. Adhps are classified as MDRs due to the presence of either one or two zinc atoms at their active sites (Jornvall, 1994). The proteins associated with this class are predominantly basic metabolic enzymes either acting on alcohols or aldehydes, hence the crucial function in the detoxification or catabolism of various toxic compounds, protecting organisms from environmental stresses. The subunits of MDRs are typically made up of 350 amino acid residues which are divided into two domains, one being the catalytic domain and the other the co-factor binding domain.

1.4 Classical alcohol dehydrogenases

In *S. cerevisiae*, there are five genes encoding the classical alcohol dehydrogenases These five fall under the medium chain zinc-containing superfamily involved in ethanol metabolism, namely *ADH1 – ADH4* (Lutstorf and Megnet, 1968) and *ADH5* (Feldman et al. 1994). The diagram in **Fig 2** illustrates the phylogenetic characteristics of *ADH1 – ADH7,* bootstrap values allocated to each *ADH* indicate that *ADH1, ADH2, ADH3 and ADH5* share phylogenetic characteristics based on nucleotide alignment**.** The other two alcohol dehydrogenases, *ADH6* and *ADH7,* are not classified as classical *ADH*s. They share a strong resemblance with that of plant cinnamyl *ADHs* (Larroy et al. 2002a: Larroy et al. 2002b).

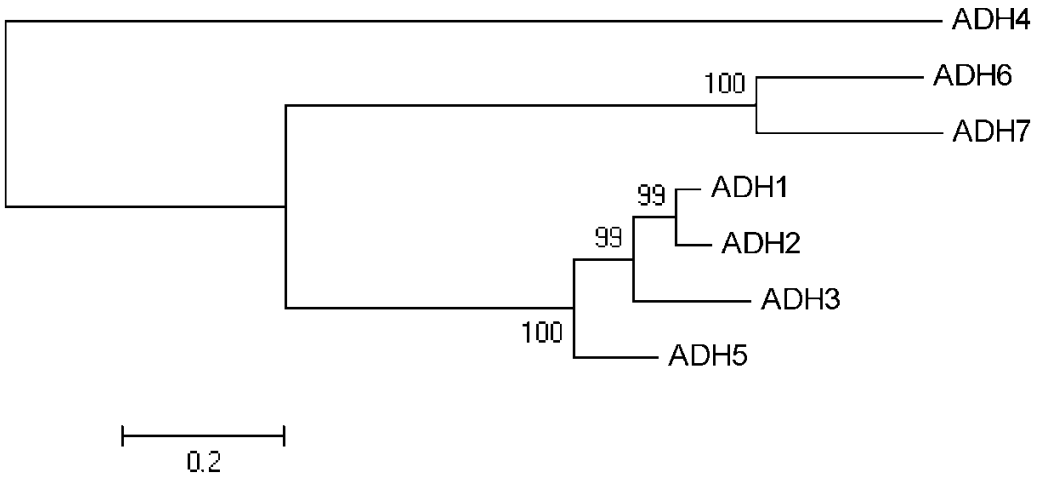

Fig 2: Phylogenetic tree incorporating all seven *ADHs* present in *S. cerevisiae*. Nucleotide alignment performed using CLUSTALX 1.83 (Thompson et al. 1997) and phylogenetic analyses were conducted with MEGA version 4 (Tamura et al. 2007) using the neighbour-joining method with the Kimura two parameter distance measure. Confidence values were estimated from bootstrap analysis of 1000 replicates. The tree has a common point of origin, dividing into three main branches. High bootstrap values at branch points indicate that *ADH1, ADH2, ADH3* and *ADH5* can be grouped together, as can *ADH6* and *ADH7*. *ADH4* shares no resemblance with any other of the YADHs.

1.4.1 Alcohol dehydrogenase 1

Alcohol dehydrogenase I (Adh1p) is the major enzyme responsible for the reduction of acetaldehyde to ethanol through the subsequent oxidation of NADH to NAD^+ (**Fig 3**) (Leskovac et al. 2002). Adh1p localized in the cytoplasm is catalytically active under high glucose stress. When *S. cerevisiae* is grown on a fermentable carbon source such as glucose, Adh1p will be expressed and subsequently ethanol will be produced and NADH regenerated (Leskovac et al. 2002: Thomson et al. 2005). A study conducted by De Smidt (2007) proved that Adh1p has the capability of oxidizing ethanol to

acetaldehyde as well. Mutants expressing only Adh1p were able to function at relatively normal metabolic rates when compared to a wild type strain.

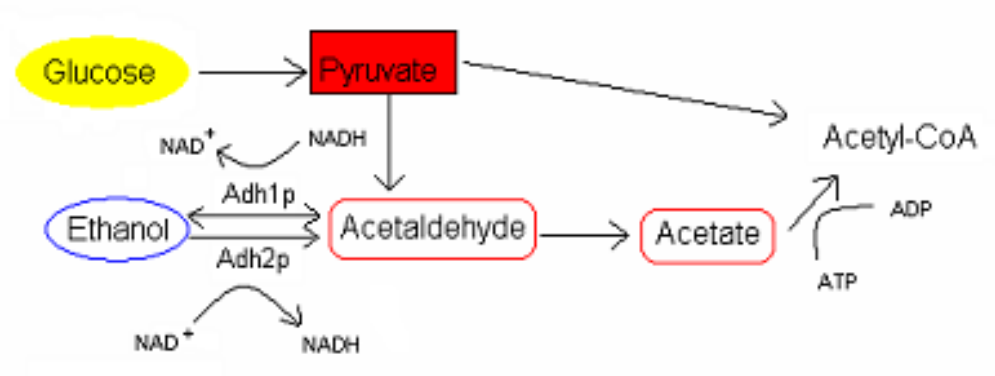

Fig 3: Metabolic pathway illustrating the reduction of acetaldehyde to ethanol catalyzed by Adh1p with the subsequent oxidation of NADH to NAD^+ and the oxidation of ethanol back to acetaldehyde with reduction of NAD^+ to NADH, catalyzed by Adh2p and Adh1p.

Through physico-chemical methods it was determined that Adh1p has a molecular weight of 150 kDa. It was further noted that the active site of the enzyme contained four identical reactive sites (Harris, 1964). Jornvall (1977) established that many amino acid residues unevenly distributed in the protein, proline and cystine residues are over-represented in the N-terminal, which can be correlated to the evolutionary and functional relationships. Jornvall (1977) further established that almost 60% of all valine residues are adjacent to those of branched-chain amino acids.

Adh1p from *S. cerevisiae* is stabilized by Ca^{2+}. This is achieved by preventing the dissociation of the reduced form of the enzyme as well as preventing the unfolding of the oxidized form. This makes yeast alcohol dehydrogenase (YADH) an excellent model for studying the stability of complex enzymes (De Bolle et al. 1997).

1.4.2 Alcohol dehydrogenase 2

By the early 1980s, both structural genes coding for Adh1p and Adh2p were identified genetically, cloned and their DNA sequences determined (Williamson et al. 1980; Bennetzen and Hall, 1982; Russell et al. 1983). Adh2p is primarily responsible for the oxidative reaction, thus converting ethanol back to acetaldehyde by reducing NAD^+ to NADH as illustrated in **Fig 3**. Even though Adh2p is responsible for the reverse reaction, it shares high similarity with that of Adh1p which is evident at nucleotide sequence level and amino acid sequence, 90% and 95% respectively. These two proteins differ by only 22 out of 347 amino acids although none of these residues has been proven to be responsible for the oxidation of ethanol to acetaldehyde or the reduction of acetaldehyde to ethanol (Ganzhorn et al. 1987; Walther and Schuller, 2001). *ADH2* expression and regulation is activated through the depletion of glucose in the media or growth on non-fermentable carbon sources such as ethanol or glycerol.

1.4.3 Alcohol dehydrogenase 3

Adh3p from *S. cerevisiae* is responsible for the reduction of acetaldehyde to ethanol in the mitochondrial matrix and couples this reaction to the generation of proton motive force as illustrated in **Fig 4** (Bakker et al. 2000). Adh3p is present in respiratory deficient mutants and superimposes a tetrameric structure (Harris, 1964; Wiesenfeld et al. 1975). Due to the localization of Adh3p, protons need to be shuttled across membranes, and since ethanol and acetaldehyde can diffuse freely across biological membranes, the net result of ethanol-acetaldehyde shuttling would be the exchange of NADH and H^+ for NAD^+.

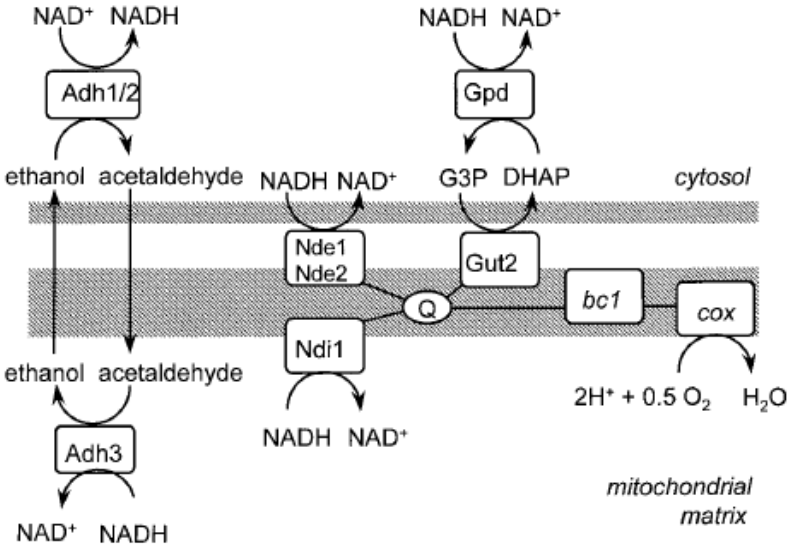

Fig 4: Schematic illustration of the respiratory system of *S. cerevisiae*. The diagram focuses on the acetaldehyde-ethanol shuttle, located in and across the mitochondrial matrix and cytosol. Adh3p functions as the main enzyme responsible for regeneration of mitochondrial NADH and reduction of acetaldehyde to ethanol (taken from Bakker et al. 2000).

Young and Pilgrim (1985) isolated and sequenced the *ADH3* gene, and nucleotide sequence analysis indicated 73% and 74% identity with Adh1p and Adh2p respectively. At amino acid level, Adh3p is 79% identical to Adh1p and 80% identical to Adh2p. All co-factor binding sites, active site and non-catalytic zinc binding site for *S. cerevisiae* Adh1p (Jornvall, 1977) are conserved in Adh2p and Adh3p (Young and Pilgrim, 1985).

1.4.4 Alcohol dehydrogenase 4

The sequence of *ADH4* is significantly different from those of *ADH1, ADH2* and *ADH3*, however, it was found to be similar to the Adh2p of *Zymomonas mobilis.* Sequence analysis showed that Adh4p has no resemblance to Adh1p and Adh2p amino acid residues important for structural and functional support. The strong homology between Adh4p and the iron-activated Adhp from *Z. mobilis* suggests that *ADH4* encodes an alcohol dehydrogenase, but different than those described in eukaryotes (Williamson and Paquin, 1987). Another significant difference between Adh1p/Adh2p in respect to Adh4p is that Adh1p is capable of oxidizing ethanol to acetaldehyde as well as reducing acetaldehyde to ethanol, while Adh4p is a dimeric protein and only occurs at low concentrations in lab strains. Drewke and Ciriacy (1988) purified Adh4p by over-expression of the *ADH4* gene on a multicopy plasmid. This study contradicted the suggestion made by Williamson and Paquin in 1987 that Adh4p is an iron-containing dehydrogenase.. Adh4p, like the other MDRs, is activated by zinc ions in the active site of the protein, coordinating with amino acids in the proton relay system and catalytic pocket.

1.4.5 Alcohol dehydrogenase 5

After the sequencing of *S. cerevisiae* chromosome II by Feldman and co-workers (1994), it was apparent that there is an additional *ADH* not previously identified. The additional *ADH* was subsequently named *ADH5.* Adh5p is 76% and 77% identical to Adh1p and Adh2p respectively (**Fig 5**). Adh5p is localized in the cytoplasm of *S. cerevisiae* and the expression levels are known to be notably lower than that of Adh1p (Hue et al. 2003). However, no other data is available on Adh5p.

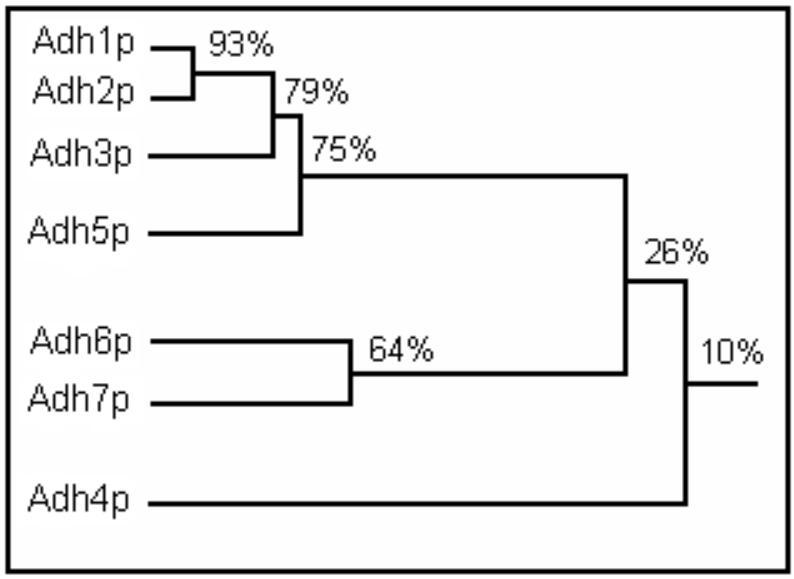

Fig 5: Homology tree based on amino acid alignment of the seven Adh proteins from *S. cerevisiae*. The classical Adhs share high similarity with one another based on the alignment of amino acids. Adh1p and Adh2p are 93% similar on amino acid alignment. Adh6p and Adh7p share 26% similarity with the other Adh proteins but 64% with each other. Adh4p on the other hand shares only 10% similarity with any of the other Adh proteins.

1.4.6 Cinnamyl alcohol dehydrogense 6 and alcohol dehydrogense 7

The *ADH6* gene codes for a dimeric protein. Unlike the classical tetrameric Adhp, however, Adh6p shares a zinc-signature, co-enzyme binding domain and amino acid sequence characteristics with the zinc-containing MDRs (Gonzalez et al. 2000). This homodimeric protein has a molecular weight of 71.3 kDa and is highly specific for NADPH as a co-factor. The enzyme accepts a wide range of substrates, most importantly branched-chain primary alcohols, aldehydes and cinnamyl alcohols. The specificity of substrate and co-factor relationships strongly suggests that Adh6p primarily functions as an aldehyde reductase rather than an alcohol oxidizer (Gonzalez et al. 2000).

The role of Adh6p in *S. cerevisiae* is difficult to ascertain due to its close structural resemblance to plant cinnamyl ADHs (CAD). However, the potential

role of Adh6p can either be the involvement in the biosynthesis of the monomeric precursors of lignin from their cinnamyl aldehydes, or implicated in plant-defence reactions. An alternative role for Adh6p arises from the ability to convert veratraldehyde and anisaldehyde into their corresponding alcohols (Larroy et al. 2002a).

Adh7p, much like Adh6p, is a cinnamyl or CAD protein and its role in yeast cells is difficult to ascertain. Characterization studies performed by Larroy and co-workers (2002b) proved that cinnamaldehyde is the primary substrate. These results and the specificity for NADP(H^+) further suggest that the enzyme would act as an aldehyde reductase rather than an alcohol dehydrogenase. The catalytic efficiencies shown for the reductive reaction are similar to those of Adh6p (Larroy et al. 2002b).

2 Active centres of alcohol dehydrogenases

Alcohol dehydrogenases are separated into two domains, one being a co-enzyme binding domain and the other the catalytic domain (**Fig 6**). Known relationships from tertiary structures of dehydrogenases show that the two domains consist of constituent monomers. The domains are further separated by a cleft containing a deep pocket which, in turn, accommodates the substrate and the co-factor. One domain is responsible for binding the co-enzyme and the other provides ligands to the catalytic zinc and most of the other groups that are involved in the control of substrate specificity (Vallee and Falchuk, 1993; Leskovac et al. 1998).

After solving the three-dimensional structure of *S. cerevisiae* Adh1p, the presence of a hydrogen-bonded proton relay system was evident, stretching from His-51 on the surface of the enzyme to the active site zinc atom in the substrate binding site (Leskovac et al. 1998). The active tetramer is capable of forming an independent active site within the quaternary structure, based on the fact that each individual chain contains one reactive sulphydryl group by

binding one atom of zinc and one mole of NAD^+/$NADP^+$ (Harris, 1964; Ganzhorn et al. 1987). The only known difference between Adh1p, Adh2p and Adh3p with regard to their active sites is apparent where Adh1p has a methionine residue at position 294, while the same position is occupied by leucine in Adh2p and Adh3p (Ganzhorn et al. 1987).

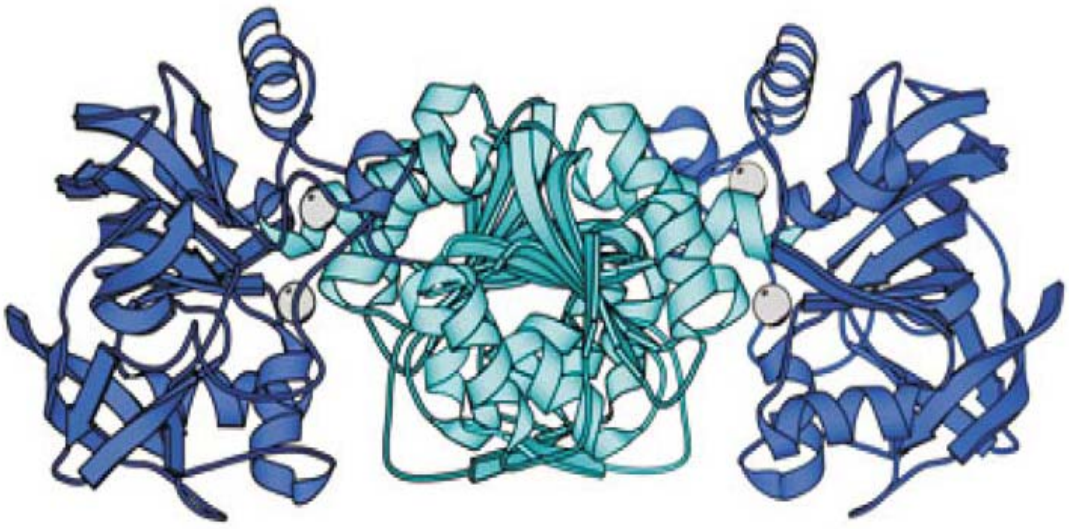

Fig 6: This illustration depicts the two main domains in Adh. Adh1p, Adh2p and Adh3p that bind four moles of NAD^+ and four atoms of zinc. A zinc atom is crucial for maintaining the quaternary structure of the enzyme, as well as sharing catalytic function (taken from Vallee and Falchuk, 1993).

In a study performed by Magonet and co-workers (1992) they showed that one zinc atom is essential for catalytic activity and the other for maintaining structural conformation of the tertiary and quaternary structure of the protein. The experimental data showed that treatment of yeast alcohol dehydrogenase (YADH) Adh1p with Dichorodiphenyltrichloroethane (DTT) had no effect on the activity of the enzyme. However, at high DTT concentrations one of the two zinc atoms was removed, resulting in the appearance of a highly heat sensitive enzyme that denatures at high temperatures. It is best interpreted that at high DTT concentrations the structural zinc is removed leading to inactivation. This is due to the peptide chain unfolding and leading to denaturation. The active

site zinc is imbedded deeper in the skeleton of the protein and disulfide bonds keep it from chelating, whereas the structural zinc atom is localized closer to the surface of the protein and more easily removed (Magonet et al. 1992).

3 Proton relay system involved in catalysis

In the early 1960s, Sund and Theorell (1963) confirmed the presence of the zinc atom in the active site of Adh1p, as well as a water molecule bound as a fourth ligand, demonstrating that the zinc atom is arranged in a tetrahedral arrangement. The zinc atom coordinates with two cystines (Cys 43 and Cys 153), and one histidine to form the catalytic centre (Zn^{2+}, Cys 2, His 1) which is essential for the conversion of ethanol and other primary alcohols to the corresponding aldehydes. The numbering allocated to each of the above-mentioned amino acids indicate the position assigned to each of these amino acids numerically in the structural bone of the proton relay system. The second zinc atom coordinates with four cystine residues assuming a conformational role rather than a catalytic function. These six cystine residues are highly conserved in all yeast alcohol dehydrogenases (Blumberg et al. 1987; Men and Wang, 2006). **Fig 7** illustrates the active site of Adh1p, with the proton relay system, as well as important amino acid residues located on the backbone of the system (Leskovac et al. 2002).

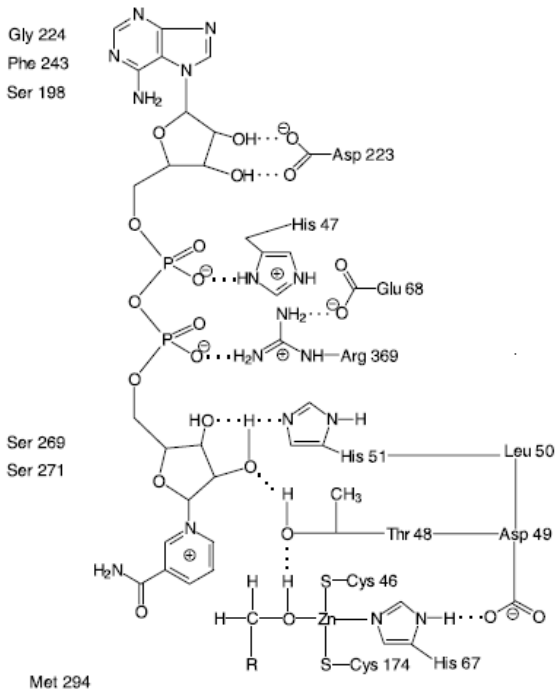

Fig 7: Active site of alcohol dehydrogenase I. The proton relay system illustrates the protonation and deprotonation of amino acid residues important in transferring protons from the active site to the surface of the protein (taken from Leskovac et al. 2002).

4 Catalytic mechanisms

Two different mechanisms have been suggested with regard to the deprotonation of the alcohol. The first mechanism, as suggested by Branden and co-workers (1975), zinc-bound water dissociates when NAD^+ binds to these enzymes. This will result in the deprotonation of the alcohol *via* the remaining $-OH^-$. The alcohol is then bound to the zinc ion.

The second mechanism, suggested by Cook and Cleland (1981), assumed that the zinc-bound water is substituted by the alcohol. Through substitution the alcohol will subsequently become deprotonated and then the alcoholate becomes bound to the zinc as a fourth ligand. Through Fourier transform infrared difference spectroscopy performed by Nadolny and Zundel (1997). It was suggested that deprotonation takes place through the addition of an extra

ligand. Due to the very strong interaction of the zinc ion with ligands, a tetrahedral coordination is necessary. If no coordination takes place, no hydrids between three-dimensional orbitals and orbitals of the fourth shell would be able to form. Under these conditions the water molecule, which is bound to zinc, is in a tetrahedral arrangement and will become acidic. A proton relay system is important to establish a shift of a positive charge away from the zinc. Such a shift occurs in hydrogen-bonded chains with large proton polarizability due to collective proton motion (Eckert and Zundel, 1988). Brzezinski and Zundel (1996) stated that these hydrogen-bonded chains will only show large proton polarizability if a largely symmetrical proton potential is present in these chains.

The above-mentioned hydrogen-bonded pathway becomes largely symmetrical due to strong covalent interaction of the zinc ion with the tetrahedrally conformed water molecule. The protonated His-51 is comparably basic to the water proton (Orgel, 1960; Zundel, 1969). This coupled proton motion is responsible for the symmetrical potential of the protons in the hydrogen-bonded chain, this potential causes the shift of the positive charge on the NAD^+ ring to His-51, facilitating a proton shift or transfer (**Fig 8**).

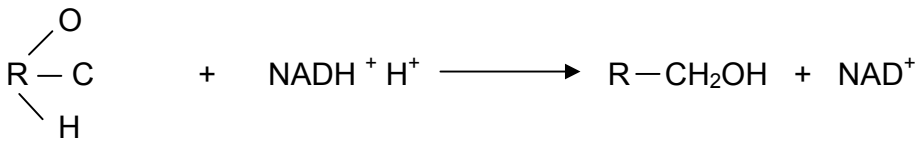

Fig 8: The chemical reaction catalyzed by Adh, occurring when protons are shifted during the proton relay system (Klinman, 1974).

The actual incorporation and function of substrate and proton uptake in the active site can occur when the proton is directly absorbed from solution through catalytic residues at the enzyme's active site that functions as an acid-base catalytic mechanism. It is possible to postulate various methods of proton uptake into the enzyme's active site. In **Fig 9**, scheme one (A and B) proton uptake takes place prior to aldehyde reduction. Whereas in scheme two it is

illustrated that actual proton uptake takes place subsequent to aldehyde reduction. The only difference between scheme 1A and 1B is the discrepancy between whether or not proton transfer from the catalytic residue to substrate takes place prior to, or concomitant with the hydrid transfer step (1A) or after the hydrid transfer step (1B) (Klinman, 1974).

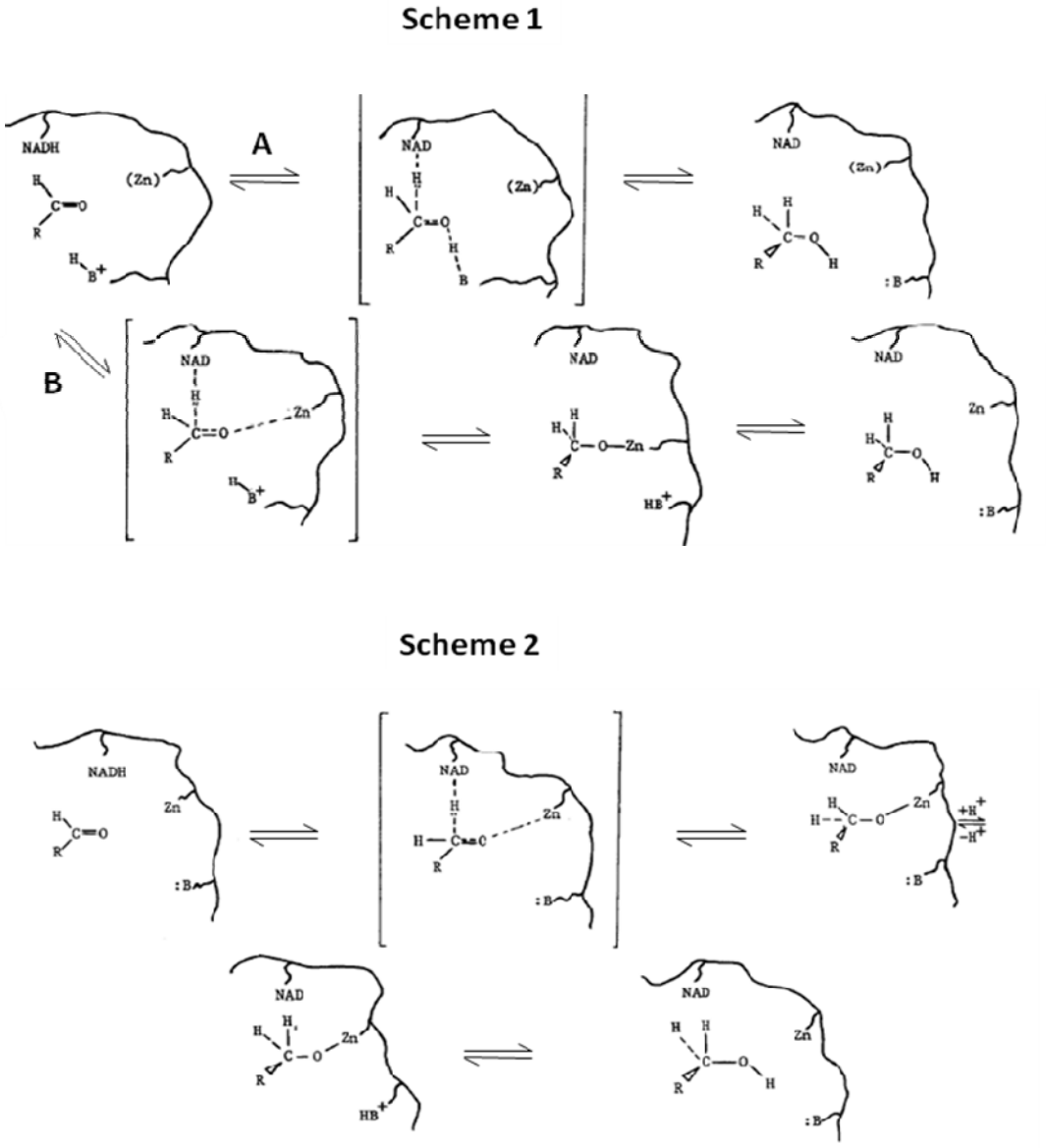

Fig 9: Scheme 1 illustrates the uptake of a proton prior to acetaldehyde reduction. Scheme 2, contradictory to scheme one, suggests that proton uptake takes place subsequent to aldehyde reduction (taken from Klinman, 1974).

5 Substrate specificity

According to Heick and co-workers (1969), Adh1p and Adh2p both favoured the reduction of acetaldehyde, however, under high ethanol concentrations these enzymes tend to favour the oxidation of ethanol back to acetaldehyde. The K_m of Adh1p towards ethanol is between 17 000-20 000 µmol l^{-1} making acetaldehyde its primary substrate. This was later confirmed by Thomson and co-workers (2005). Adh2p can produce acetaldehyde at a faster rate at low ethanol concentrations (Wills et al. 1982). Ethanol is the primary substrate during the oxidizing pathway. Adh1p is also capable of oxidizing all primary alcohols with chain lengths of between two and ten carbon atoms (Schopp and Aurich, 1976).

Kinetic investigations established that there is a direct correlation between the increases in carbon chain length leading to a decrease in enzyme activity. The specificity of Adh1p is limited to primary un-branched aliphatic alcohols. When shorter branched alcohols are presented to the active site the efficiency of the enzyme decreases rapidly (Ganzhorn et al. 1987; Leskovac et al. 2002). Some substrates, such as β-mercaptoethanol, may completely inhibit protein function.

Adh2p, unlike its close relative Adh1p, has a dramatically lower K_m towards ethanol, ranging between 600-800 µmol l^{-1} and is active under aerobic growth conditions, corroborating its role as primary ethanol oxidizer (Thomson et al. 2005). More recent research showed that the K_{cat} s^{-1} is three-fold faster than those of Adh1p. This data is based on kinetic characterization of Adh1p and Adh2p by determining their specificity constants for a number of long chain alcohols (Dickinson and Dack, 2001; Leskovac et al. 2002).

6 Substrate and co-factor binding

The hydrophobic side chains located in the inner wall of the catalytic pocket of yeast Adh1p, (Trp-57, Trp-93, Asn-110, Leu-132, Tyr-141, Met-294, Ala-296 and Ile-318), are amino acid residues that line the inner pocket and these residues are from the same subunit as the zinc ligands. The interactions of two of the residues, Trp-93 and Thr-48 result in the narrowing effect of the substrate-binding site near the zinc ion. The side chains of a number of residues also contribute to the narrower substrate-binding site. At the bottom of the pocket, a zinc atom is coordinated to three protein ligands and two thiolates from Cys-174 and Cys-46, the third ligand is nitrogen from His-67. The catalytic pocket is highly hydrophobic. The only polar groups occurring in the pocket are located close to the zinc, and they form the zinc ligands, side chain of Thr-48 and the nicotinamide moiety of the enzymes (Leskovac et al. 2002).

Co-factor binding takes place in a cleft located in the interior of the protein, close to the centre of the molecule. The one side of the NAD^+ ring interacts with Thr-178, Leu-203 and Met-294. While the other side faces the active site situated close to Cys-46 and Cys-174. Val-319's main-chain nitrogen atom is then hydrogen-bonded to the oxygen atom on the carboxamide group. The carboxyl oxygens of Val-292 and Ser-317 become hydrogen-bonded to the nitrogen atom's carboxamide group. To ensure that the nucleotide remains in the right stereo-chemical position, the side chain of Thr-178 helps as stabilizer. The Thr-178 residue is highly conserved in all known homologous Adhps (Fan and Plapp, 1999; Leskovac et al. 2002).

Through various studies researchers came to the conclusion that Adh follows the steady-state random ordered mechanism on the alcohol side of the reaction and as a steady-state ordered mechanism on the aldehyde side of the catalytic cycle (Dickinson and Monger, 1972; Leskovac et al. 2002).

Product-inhibition studies performed by Wratten and Cleland (1963) claimed that the mechanisms of YADH catalysis with ethanol as substrate could be described as a compulsory-order reaction mechanism. The enzyme reacted first with the co-enzyme to form the enzyme-co-enzyme complex. They effectively ruled out the possibility of rapid-equilibrium random-order reaction mechanism suggested by Mahler and Douglas (1957). However, later studies performed by Dickinson and Monger (1972) suggested that the compulsory-ordered mechanism might not be totally satisfactory.

7 Conclusion

Throughout the past few decades a great deal of experimental work has been conducted to broaden the knowledge scope into Adh research. The predominant research focused on Adh1p and Adh2p in terms of the kinetic characterization and gene regulation of these two alcohol dehydrogenases. From these studies it can be deduced that Adhp has an important if not crucial role in metabolism. These roles imply the initiation of ethanol fermentation, and the detoxification of various toxic compounds such as acetaldehyde. These toxic compounds can lead to the cessation of cellular functions.

The classical Adhps are closely related. The most studied belong to Adh1p and Adh2p. They are highly homologous to each other and share 77% and 76% homology with Adh5p, respectively. *ADH5* is situated on chromosome II and is expressed at much lower levels than that of Adh1p. Furthermore, it shares remarkable resemblance with Adh1p and Adh2p based on sequence homology. A previous study showed that a deletion mutant of *S. cerevisiae,* with only *ADH5* intact in the genome, was still able to produce ethanol when grown on glucose as a substrate (De Smidt, 2007). The mutant was, however, unable to grow on ethanol as a carbon source.

8 Aim of the study

The study reported in this dissertation focuses on the *in vitro* characterization of Adh5p from the yeast *S. cerevisiae*.

8.1 Objectives

1. To construct an expression system capable of over-expressing Adh5p in *S. cerevisiae* followed by purification of this enzyme.
   1.1. To purify the protein and kinetically characterize it on the following parameters:
      1.1.1. Optimization towards the preferred co-factor, pH, substrate and temperature.
      1.1.2. To determine the efficiency of Adh5p towards substrates.
2. To investigate the impact of *ADH5* expression on ethanol metabolism by *S. cerevisiae*.
   2.1. To place *ADH5* under the transcriptional control of *ADH1* promoter.
   2.2. To monitor growth characteristics.

CHAPTER 2: MATERIALS AND METHODS

1 Stains and media

The strains relevant to this study are listed in table 1.

Table 1. Strains used in this study

Strain	*Genotype*	*Reference*
W303-1A	*MAT(a),his3,leu2,trp1,ura3*	Thomas and Rothstein, 1989
Invsc	SC1: *MATα;* his3Δ1, leu2 trp1-289, ura3-52, MATAlpha his3Δ1 leu2 trp1-289, ura3-52	Invitrogen
By4742	By4742; *MATα,* his 3Δ1; Leu2Δ0; ura3Δ0; YDR242w::kanMX4	Invitrogen
CEN PK42	W303-1A ,*MAT*α: Ura3-52: Leu2-3/112, trp 1-289: his 3Δ1; MAL2-8c SUC3	Entian and Kotter, 1998
Q_1	W303-1A, *MATa, adh2Δ::URA3, adh3Δ::TRP1, adh4Δ, adh5Δ::LEU2*	De Smidt, 2007
TΔ123::*ADH5*_S	W303-1A, *MATα, adh1Δ::LEU2, adh2Δ::URA3, adh3Δ::TRP1*	This study
TΔ123::*ADH5*_M	W303-1A, *MATα, adh1Δ::LEU2, adh2Δ::URA3, adh3Δ::TRP1*	This study
TΔ123	W303-1A, *MATα, adh1Δ::LEU2, adh2Δ::URA3, adh3Δ::TRP1*	This study
DΔ23	W303-1A, *MATα, adh2Δ::URA3, adh3Δ::TRP1*	De Smidt, 2007
E. coli XL-10 Gold	Tet^r *D(mcrA)183 D(mcrCB-hsdSMR-mrr)173 endA1 supE44 thi-1 recA1 gyrA96 relA1 lac* Hte [F' *proAB lacI^{q}ZDM15 Tn10* (Tet^r) Amy Cam^r]^a	Stratagene

For yeast transformation purposes, strains were grown in YPD media (10 g l^{-1} yeast extract, 20 g l^{-1} peptone, 20 g l^{-1} glucose), 15 g l^{-1} agar was added for plating purposes. Bacterial transformation was performed into *Escherichia coli* XL-10 Gold (Stratagene) cells and dam$^-$ *E. coli* cells. Selective LB plates were used for blue/white selection (5 g l^{-1} yeast extract, 10 g l^{-1} tryptone, 10 g l^{-1} NaCl, 10 μg ml^{-1} ampicillin, 20 mg ml^{-1} X-Gal and 4.8 mg ml^{-1} IPTG). Transformants were inoculated into LB media supplemented with 10 μg ml^{-1} ampicillin (AMP). For expression the *ADH5* gene was transformed into *S. cerevisiae* W303-1A, *S.*

cerevisiae CEN PK42 and *S. cerevisiae* Invsc (**table 1**). The inoculants were grown in a selective media. Yeast nitrogen base (YNB) uracil drop out media, (6.7 g l^{-1} yeast nitrogen base 20 g l^{-1} glucose, 0.6 g l^{-1} amino acid supplement (BIO 101). 50 mg l^{-1} histidine, 50 mg l^{-1} tryptophan and 400 mg l^{-1} leucine at pH 6 were added. Components of the chemically defined medium used for the growth studies are shown in **table 2a, b** and **c**.

Table 2. Chemically defined medium components

Component	***Concentration***	
Citric acid	0.25 g l^{-1}	
NH_4SO_4	5 g l^{-1}	
$MgSO_4.7H_20$	0.4 g l^{-1}	
$CaCl_2.2H_20$	0.02 g l^{-1}	
NaCl	0.1 g l^{-1}	
KH_2PO_4	10 g l^{-1}	
Glucose	8 g l^{-1}	
Vitamins	1 ml l^{-1}	See table 2a
Amino acid stock	20 ml l^{-1}	See table 2b
Trace elements	1 ml l^{-1}	See table 2c

Table 2a. Vitamin solution composition

Component	***Concentration***
0.1M NaOH	10 ml l^{-1}
dH_20	400 ml l^{-1}
Calcium panthatenate	500 mg l^{-1}
Nicotinic acid	500 mg l^{-1}
p-aminbenzoic acid	100 mg l^{-1}
Pyrodoxine, HCL	500 mg l^{-1}
Thiamine, HCL	500 mg l^{-1}
m-Inositol	12.5 g l^{-1}

Table 2b. Amino acid composition

Amino acid	*Stock solution (50x)*	*Final concentration*
Adenine	5 g l^{-1}	100 mg l^{-1}
Alanine	2.5 g l^{-1}	50 mg l^{-1}
Arginine	2.5 g l^{-1}	50 mg l^{-1}
Asparagine	2.5 g l^{-1}	50 mg l^{-1}
Aspartic acid	2.5 g l^{-1}	50 mg l^{-1}
Glutamic acid	2.5 g l^{-1}	50 mg l^{-1}
Glutamine	2.5 g l^{-1}	50 mg l^{-1}
Glycine	2.5 g l^{-1}	50 mg l^{-1}
Valine	2.5 g l^{-1}	50 mg l^{-1}
Isoleucine	2.5 g l^{-1}	50 mg l^{-1}
Lysine	2.5 g l^{-1}	50 mg l^{-1}
Methionine	2.5 g l^{-1}	50 mg l^{-1}
Phenylalanin	2.5 g l^{-1}	50 mg l^{-1}
Proline	2.5 g l^{-1}	50 mg l^{-1}
Serine	2.5 g l^{-1}	50 mg l^{-1}
Threonine	2.5 g l^{-1}	50 mg l^{-1}
Tryptophane	2.5 g l^{-1}	100 mg l^{-1}
Cysteine	NA	50 mg l^{-1}
Leucine	NA	400 mg l^{-1}
Tyrosine	2.5 g l^{-1}	50 mg l^{-1}
Uracil	5 g l^{-1}	100 mg l^{-1}

Table 2c. Trace element solution

Elements	*Mass per 100 ml dH_20*
$FeSO_4.7H_2O$	3.5 g
$FeCl_2.6H_2O$	0.6 g
$MnSO_4.H_2O$	0.7 g
$ZnSO_4.7H_2O$	1.10 g
$CuSO_4.5H_2O$	0.1 g
$CoCl_2.6H_2O$	0.2 g
$Na_2MoO_4.2H_2O$	0.04 g
KI	0.04 g
H_3BO_3	0.2 g
$Al_2(SO_4)_3.18H_2O$	0.16 g

Table 3. List of primers used in this study

Primer name	Primer sequence (5' – 3')
ADH5-Forward-*Hin*dIII	CGA AGC TTA TCA TG GGT CCT TCG CAA GTC ATT CCT G
ADH5-Reverse-His-tag-*Xba*I	CGT CTA GAT CAG **TGA TGA TGA TGA TGA TGT** TTA GAA GTC TCA ACA ACA TAT CTA CC
ADH5-Forward-His-tag-*Hin*dIII	**CAT CAT CAT CAT CAT CAC** CGA AGC TTA TCA TGG GTC CTT CGC AAG TCA TTC CTG
ADH5-Reverse-*Xba*I	CGT CTA GAT CAT TTA GAA GTC TCA ACA ACA TAT CTA CC
1RT-R	GGA AGA ATT ATT CAG ATC CAT CGG TGG TG
ADH1-2F	TGC CGA AAG AAC CTG AGT GC
LEU2-1R	TTC GGC TGT GAT TTC TTG ACC
ADH2-3F	GAG CGT TGA ATC GGT GAT GC
2RT-*R*	TCG CCT TAG CAT ATT GAA CAG CCA
URA3-1R	TAG CTT GGC AGC AAC AGG ACT A
ADH3-3F	ATC GCT TAA CCT GGC TAG TTG
ADH3-4R	GAG TCT TAG GGA TTG CAG C
TRP-1R	AAT GGA CCA GAA CTA CCT GTG AA
ADH4-4F	ATG TCT TCC GTT ACT GGG
ADH4-4R	GGT TAG TCA AAT GGC AGG C
ADH5-3F	TGC GGT AGC GAC AGA TTG TAG
ADH5-4R	TTG TGA CAT CTG CTG ACG CG
ADH1-MH-R (*Hin*dIII)	GCA AGC TTT GTA TAT ATG AGA TAG TTG ATT GTA TGC
ADH1-MH-F (*Xba*I)	GCT CTA GAG GGA ATT TCT TAT GAT TTA TG

Bold characters indicate the histidine -tagged sequence engineered onto the primer.

Underlined characters in primer sequence indicate the introduced restriction sites (as indicated in the primer name).

2 Construction of plasmids pGEM®-T Easy::*ADH5*- N-terminal and pGEM®-T Easy::*ADH5*- C-terminal

ADH5 was amplified from *S. cerevisiae* genomic DNA. Two sets of primers were designed to amplify *ADH5* containing a 6X His-tag (CATCATCATCATCATCAC) on the N-terminal side (*ADH5*-Forward-*Hin*dIII, A*DH5*-Reverse-Histag-*Xba*I), and on the C-terminal side (*ADH5*-Forward-Histag-*Hin*dIII and *ADH5*-Reverse-*Xba*I). Both sets of primers were designed by including a *Hin*dIII restriction site on the forward primers and *Xba*I on the reverse primers (**table 3**).

The *ADH5* gene was PCR amplified using genomic DNA from *S. cerevisiae* W303-1A as template in an Applied Biosystems Thermocycler (model 2720). Initial denaturation at 94°C for 2 min, followed by 30 cycles of denaturation at 94°C for 20 seconds, annealing at 50°C for 30 seconds and 72°C for 1 minute. Final elongation was allowed at 72°C for 7 minutes. In a standard 50 µl reaction, 0.4 µl of a 1 unit/µl concentration of KAPA HiFi DNA Polymerase (KAPA Biosystems, RSA), 41.6 µl dH_2O, 5 µl 10 x polymerase buffer, 1 µl of both primers and 1.5 µl dNTPs (10 mM) were used together with 0.5 µl genomic DNA from *S. cerevisiae* W303-1A. The expected 1053 bp amplicon was visualized on a 1% agarose gel and the PCR product purified using a Biospin gel extraction kit (Bioflux). DNA was eluted with 30 µl of elution buffer (10 mM hydroxymethylaminomethane (Tris), 0.1 mM ethylenediaminetetraacetic acid (EDTA) at pH 8.5) and used for downstream applications.

The PCR amplicon was ligated into pGEM®-T Easy. Ligation was performed at room temperature for 60 minutes. 1 µl 10x ligation buffer, 0.3 µl pGEM®-T Easy, 2.5 µl PCR product, 1 µl T4 DNA ligase (Fermentas) solution was made up to 10 µl with dH_2O. The ligation product was transformed into competent *E. coli* XL 10 gold cells using a standard chemical transformation protocol (Nishimura *et al.,* 1990). Transformants were plated out on 10 µg ml^{-1} ampicillin, 20 mg ml^{-1} X-Gal and 4.8 mg ml^{-1} IPTG plates, incubated at 37°C for 12-24 hours. White clones were selected for further application. Single colonies were inoculated into 5 ml LB media supplemented with 10 µg ml^{-1} ampicillin and grown overnight at 37°C. Plasmid was isolated from each culture using the Zymo-zippy plasmid extraction kit (Fermentas). Purified plasmid products were subjected to a second round of transformation. Dam^- competent *E. coli* cells were used to prevent methylation on the *Xba*I restriction site. The same transformation, selection and growth procedures were repeated and plasmid DNA was isolated from single colonies using the lysis by boiling method (Sambrook and Russell, 2001; Ehrt and Schnappinger, 2003). Constructs were verified by restriction analysis with enzymes *Xba*I and *Hin*dIII (Fermentas). Two N-terminal His-tag clones, and two

C-terminal His-tag clones. These selected clones were subjected to sequencing analysis (Inqaba biotechnologies).

3 Construction of a *ADH5* expression vector

After sequencing analysis two clones containing the N-terminal His-tag and one clone containing the C-terminal His-tag were selected for construction of the expression system. The modified *ADH5* fragment was excised from the pGEM®-T Easy::*ADH5*- N-terminal and pGEM®-T Easy::*ADH5*- C-terminal constructs. Using *Xba*I and *Hin*dIII and purified from a 1% agarose gel with a Biospin gel extraction (Bioflux). Purified *ADH5*- N-terminal product was then ligated into pYES2. Ligation was performed at room temperature for 60 minutes in 1 µl 10x ligation buffer, 0.3 µl pYES2, 2.5 µl *ADH5*- N-terminal, 1 µl T4 DNA ligase (Fermentas) solution was filled to 10 µl with dH_2O. The same procedure was repeated for the *ADH5*- C-terminal product. Ligated product was transformed into *E. coli* XL 10 gold competent cells, plated on ampicillin, IPTG and XGal selective media and grown overnight at 37°C. Plasmid was isolated using lysis by boiling and construct assembly was digested with *Xba*I and *Hin*dIII. Two clones, one representing the *ADH5* ORF with an N-terminal and the other clone representing the C-terminal His-tag, were individually employed for expression studies. Plasmid products were transformed into *S. cerevisiae* W303-1A, *S. cerevisiae* CEN PK42 and *S. cerevisiae* Invsc using the one step yeast transformation method (Chen et al. 1992). Transformants were plated out on YNB uracil dropout media and incubated overnight at 30°C. Transformants capable of growing on the selective media were then re-inoculated in 5 ml YNB and grown overnight at 30°C.

4 Adh5p expression utilizing pYES::*ADH5* construct

Transformants were inoculated into 5 ml YNB uracil dropout media, grown overnight at 30°C. Thereafter 5 ml of inoculum was passaged into four flasks containing 250 ml YNB and grown overnight at 30°C.

1 L of incubated cells was harvested by centrifugation at 10 000 x *g* for 20 minutes at 4°C (Beckman model J2-21). Harvested cells were resuspended in 50 ml YP (10 g l^{-1} Bacto-yeast extract and 20 g l^{-1} Bacto-peptone) media to remove all remaining traces of glucose. Harvested cells were inoculated into 200 ml YP media containing 2% Galactose (20 g l^{-1}) as a sole carbon source. Galactose was added to the YP media to initiate expression at promoter level (*GAL1* inducible promoter) of the gene integrated into the pYES2 vector. After inoculation, 10 ml samples were drawn at 0, 2, 4, 6, 8 hours, centrifuged at 10 000 x *g* at 4°C for 15 minutes. Thereafter 10 ml sample was resuspended in 0.5 ml phosphate buffer. Cells were homogenized with glass beads for purification of crude extract. One tablet of complete mini EDTA-free protease inhibitor (Roche) was added to prevent protein breakdown due to the presence of proteases.

Crude lysed extract was loaded onto a Sodium dodecyl sulfate polyacrylamide gel (SDS-PAGE). Resolution was verified by using the Bio-Rad mini-protean® tetra cell system, at 90 V while protein was settling in the stacking gel. Voltage was increased to 100 V separating the various natural and over-expressed proteins in the running gel. Protein was visualized following gel staining according to the method by Fairbanks et al. (1971).

5 Western blot analysis

All SDS-PAGE gels were performed in duplicate, one gel was stained with Coomassie blue. The other SDS-PAGE gel was transferred to a Nitrocellulose membrane submerged in pre-chilled transfer buffer (20 mM Tris, 150 mM Glycine, 20% MeOH, 0.038% SDS, pH 8.3). Protein was transferred at 30 V overnight at 4°C. All Western blot hybridizations were performed with the Super Signal® West HisProbe kit™ (Pierce) following the manufacturer's instructions. Western blot analysis was performed on crude extract isolated at various time intervals from *S. cerevisiae* CEN PK42, *S. cerevisiae* W303-1A and *S. cerevisiae* Invsc expressing the Adh5 protein.

Crude cellular extract containing 6X His-tag was also hybridized with a C-terminal specific signal. *S. cerevisiae* W303-1A, *S. cerevisiae* CEN PK42 and *S. cerevisiae* Invsc crude extracts were probed with Invitrogen Anti-His (C-term) antibody. The antibody was diluted 1:5000 ratio in phosphate-buffered saline (PSB) containing 0.5% Tween 20 and 5% skimmed milk. The nitrocellulose membrane was incubated in blocking solution for 60 minutes. The membrane was then incubated in blocking solution for 60 minutes, washed in fresh blocking solution and equilibrated in buffer 3 (0.1 M Tris HCL, 0.1 M NaCL, 0.05 M $MgCl_2$ at pH 9.5). One tablet of Nitro blue tetrazolium chloride/ 5-Bromo-4-chloro-3-indolyl phosphate, toluidine salt (NBT/BCIP) (Sigma Aldrich), was added for the development in a sealed developing cassette in the dark.

6 Preliminary purification of Adh5p

Protein was purified under native conditions with mini pre-packed Ni-NTA Spin Columns (Qiagen). pYES2::*ADH5* was transformed into *S. cerevisiae* W303-1A. Transformants were inoculated into 250 ml YNB uracil dropout media and grown overnight at 30°C. Cells were harvested, resuspended in 50 ml YP plus 2% galactose media. Protein was expressed for 8 hours at 30°C. Harvested cells were resuspended in 1 ml lysis buffer (50 mM NaH_2PO_4, 300 mM NaCl, 10 mM

Imidazole), pH 8 containing one tablet of complete mini EDTA free protease inhibitor (Roche). One unit (1 mg ml^{-1}) of lysozyme was added to the resuspended fraction. Cells were homogenized with 200 µl acid-washed glass beads (425 µm – 600 µm) (Sigma Aldrich), added to every 1 ml of cell culture. Cells were lysed by vortexing for 10 second time intervals for a total of 1 minute. Cell lysate was placed on ice for 5 seconds after every 10-second interval. Lysate was then centrifuged at 10 000 x *g* for 20-30 minutes at 4°C. Supernatant was collected and a 20 µl fraction frozen at -20°C for SDS-PAGE analysis. The Ni-NTA Spin Columns were equilibrated with 600 µl lysis buffer, and centrifuged for 2 minutes at 700 x *g*. After equilibration, 600 µl of cleared lysate containing Adh5p was added to the matrix and centrifuged at 700 x *g* for 2 minutes. Flow-through was collected in a 1.5 ml micro centrifuge tube and stored at -20°C for SDS-PAGE analysis. Ni-NTA Spin Columns were washed twice at 700 x *g* with 600 µl wash buffer (50 mM NaH_2PO_4, 300 mM NaCl, 20 mM imidazole at pH 8) and the protein eluted in 200 µl elution buffer (50 mM NaH_2PO_4, 300 mM NaCl, 20 mM Imidazole at pH 8). The eluted protein, together with the fractions collected at time 0 and 8 hours was analyzed with SDS-PAGE gel electrophoresis. Thereafter the membrane was hybridized for N-terminal 6X His-tag detection. The hybridization was performed under denatured conditions to identify if other contaminating proteins were present. Other proteins hybridized, containing a 6X His-tag, can cause improper purification of the target protein. The purification was performed on both the *S. cerevisiae* W303-1A and *S. cerevisiae* Invitrogen strains.

7 FPLC purification of Adh5p

Larger scale purification of Adh5p was performed using 5 ml HisTrap™ FF (Invitrogen) columns. Ni^{2+} affinity-based chromatography was applied to 20 ml lysate pre-equilibrated with 20 mM binding buffer (20 mM Na_2PO_4, 20 mM Imidozole, pH 7.4). Protein lysate was injected onto the His-trap columns using the ÄKTAprime™ system (GE Healthcare). A_{280} was measured at an increasing gradient of elution buffer (20 mM Na_2PO_4, 500 mM Imidazole, pH 7.4). Eluted

protein was pooled and imidazole was removed by dialysis. Native size of Adh5p was calculated by gel filtration with Sefadex H200 as gel matrix. Gel filtration standard supplied by Bio-rad set the reference point from 1.35 kDa to 670 kDa. Native size was calculated though the edifice of an elution profile of both the standards and the unknown Adh5p. Purified protein was visualized on SDS-PAGE gels following staining with either Coomassie blue or silver staining.

8 Adh5p characterization

Protein concentrations used for characterization purposes to calculate specific activity were assayed and determined with a Micro BCT™ protein assay kit supplied by Pierce (Smith et al. 1985). Through the edifice of a standard curve the protein concentration was calculated by dividing the A_{562} obtained by the gradient calculated from the standard curve, the coefficient was subtracted from the Y axis intercept and calculated as 1 mg ml^{-1}.

8.1 Co-factor optimization

Various parameters were optimized prior to protein characterization. All reactions were performed aerobically. Co-factor dependence/preference was determined with four co-factors, NAD^+, NADH, $NADP^+$ and NADPH, all co-factors were of the highest grade, supplied by Sigma Aldrich. Assays were performed with a micro-titre plate reader (Molecular devices, Spectra max M2). For the oxidation of ethanol, the co-factor preference was assayed at a temperature gradient ranging from 20°C to 35°C at various pH (6, 6.5, 7, 7. 5, 8, 8.5). A final concentration of 2 mM ethanol was added to the buffer cocktail (20 mM 2-(N-Morpholino)ethanesulfonic Acid, 20 mM N,N-Bis(2-hydroxyethyl) Glycine and 20 mM 3-(N-Morpholino) propanesulfonic Acid), 20 µl enzyme (1 mg ml^{-1}) was added and the reaction was initiated by adding 1 mM NAD^+ to the solution. Assays were monitored at A_{340} every 10 seconds. The reverse reaction was performed exactly the same way except ethanol was substituted with acetaldehyde but in this case NADH or NADPH was used as a co-factor.

8.2 pH optimization

After determining co-factor usage the optimum co-factor (NAD^+) was used to determine the optimum pH range at which catalysis takes place. The same buffer cocktail and parameters mentioned in the above section (section 8.1) was used, the only varying parameters were pH and two set temperatures (25°C and 30°C). Assays were monitored at A_{340} every 10 seconds.

8.3 Temperature optimization

Optimum temperature was determined at pH 8.8 (optimized) for NAD^+ as co-factor and ethanol as substrate. All parameters were kept constant. Temperature gradient was used to calculate optimum reaction rate with temperatures ranging from 17°C to 45°C.

9 Substrate specificity

9.1 Alcohols

Enzyme concentration was determined by interpreting a standard curve utilizing the Micro BCA™Protein assay kit. The activity of purified Adh5p was determined at 30°C by adding 65 µl of a 50 mM Sodium phosphate buffer (pH 8.8), 75 µl 15 mM NAD^+, 20 µl enzyme (1 mg ml^{-1}) and an ethanol dilution range was made of the alcohol substrate. Absolute ethanol (Sigma Aldrich) was used and diluted from 10 mM to 50 µM. The reaction was initiated by the addition of Adh5p to the solution. The reaction rate was monitored through the reduction of NAD^+ to NADH at A_{340}. A molar extinction coefficient for the reduced co-factor (6.22 mM) was used to calculate the specific enzyme activity in µMol min^{-1} mg^{-1} (Dickinson and Monger, 1972; Schopp and Aurich, 1976; Ganzhorn et al. 1987; Murali and Creaser, 1986; Leskovac et al. 2002; Trivedi et al. 2005).

9.2 Aldehydes

The above-mentioned method was adapted for the reverse reaction. Due to the wide spectrum of pH utilized in the reduction of acetaldehyde, a buffer cocktail was constructed covering a wider pH spectrum than that of the phosphate buffer. Buffer concentrations were increased to 100 mM (3-(N-Morpholino) propanesulfonic Acid (MOPS), 100 mM N,N-Bis(2-hydroxyethyl) Glycine (BICINE) and 100 mM 2-(N-Morpholino)ethanesulfonic Acid (MES) at pH ranging from 5.5 to 6.5). 10 mM of acetaldehyde was added to 0.1 mM NADH / NADPH respectively. The assay was initiated with a final enzyme concentration of 0.2 mg ml^{-1}. Assay conditions were held stable at 25°C for one assay and 30ºC for another assay (Dickinson and Monger, 1972; Schopp and Aurich, 1976; Ganzhorn et al. 1987; Murali and Creaser, 1986; Leskovac et al. 2002).

10 Construction of an *adh* triple deletion mutant

A *S. cerevisiae* double deletion strain, *adh2Δ::URA3, adh3Δ::TRP1* (*DΔ23,* De Smidt, 2007*)* was used to construct a triple deletion strain *adh1, adh2* and *adh3* (*TΔ123*). Primers *ADH1-1F* and *ADH1*-1R (**table 3**) re-amplifying the a*dh1Δ::LEU2* deletion construct (De Smidt, 2007) were used in a standard PCR reaction. Containing 1 µl of each primer, 2 µl template (*adh1Δ::LEU2*), 1 µl DNTPs, 25 µl dH_2O, 0.75 µl Taq and 10 µl buffer. PCR product was visualized on a 1% agarose gel under UV light and the remaining product purified using the Biospin gel extraction kit (Bioflux).

Purified *adh1Δ::LEU2* PCR product was transformed into the double deletion strain *DΔ23*. Transformants were plated out on YNB media lacking leucine (selective for *ADH1* deletion), tryptophan (selective for *ADH3* deletion) and uracil (selective for *ADH2* deletion). Transformants able to grow in the presence of all three selective elements were isolated and subjected to genomic DNA extraction (Labuschagne and Albertyn, 2007).

11 Triple deletion mutant screening for intact and deleted genes

Each clone was PCR screened for the deletion of *adh1, adh2* and *adh3* with primer pairs *ADH1-2F*/1RT-R, *ADH2-3F*/2RT-R and *ADH3-4F*/*ADH3-4R* respectively, where no amplification product indicates a deletion of each gene. A second round of conformational PCR was performed to confirm the deletion of each gene. In this case a*dh1*∆::*LEU2* deletions were confirmed with primer pair *ADH1-2F/*LEU2-1R, a*dh2*∆*::URA3* with pair *URA3 ADH2-3F/*URA3-1R and a*dh3*∆::*TRP*1 with *ADH3-4F/*TRP-1R. In each case a PCR product of the correct size indicated positive deletion of each gene. The presence of the remaining two *ADH* genes [*ADH4 (*~1.4 kb) *and ADH5* (~1.1 kb)] were confirmed through amplification with primer pairs *ADH4-4F*/*ADH4-4R* and *ADH5-3F/ADH5-4R* respectively. Verified triple deletion mutant (*T*∆*123*) strains were transferred to YNB (-Leu, -Trp, -Ura) agar and incubated at 30°C for 48 hours.

12 Amplification and integration of *ADH1* promoter and terminator regions

ADH1-MH-R (*Hin*dIII) and *ADH1*-MH-F (*Xba*I) primers were used in the targeting of a 1 kb fragment upstream and 1 kb fragment downstream flanking region of the ORF (open reading frame) of *ADH1*. An already constructed *ADH1*::pGEM®-T Easy vector (De Smidt, 2007) was used as a template to amplify the *ADH1* promoter and terminator regions. Following amplification, the PCR products were purified and further digested with *Dpn*I and the 5 kb product was then purified using the Biospin gel extraction kit (Bioflux) and thereafter restricted with *Hin*dIII and *Xba*I. *ADH5* was amplified with *ADH5*-Forward-*Hin*dIII and *ADH5*-Reverse-*Xba*I primers and subsequently ligated into pGEM®-T Easy containing the additional 1 kb 3' and 5' flanking regions. Ligated product was transformed into dam$^-$ competent *E. coli* cells. Plated on ampicillin, IPTG and XGal agar plates and incubated at 37°C for 24 hours. Transformants were

chosen and inoculated into 5 ml LB media supplemented with 10 μg ml^{-1} ampicillin for small-scale plasmid isolation.

13 Construct ligation into pRS423 and pRS413

After ligation of *ADH5* into pGEM®-T Easy, the insert, the 1 kb promoter and 1 kb terminator regions were removed from the vector by digestion with *Eco*R1. The inserts were then ligated into vectors pRS413 (singlecopy number) and pRS423 (multicopy number) and verified with *Bam*HI digestion. Expression constructs pRS413::*ADH5*_S and pRS423::*ADH5*_M were transformed into the constructed triple deletion mutant strain *TΔ123* (*adh1, adh2* and *adh3 null*). Transformants were plated out on YNB media lacking histidine (selection in pRS413 and pRS423). As well as leucine, tryptophan and uracil and incubated at 30°C for 72 hours. Single colonies selected from these transformations were designated stains *S. cerevisiae TΔ123::ADH5*_S and *S. cerevisiae TΔ123::ADH5*_M.

14 Growth studies

Chemicallydefined medium was prepared as described in **table 2a, b** and **c**. Cultivations were performed at pH 5.5 with either glucose (8 g l^{-1}) or ethanol (7 g l^{-1}) as carbon source. For the preparation of *S. cerevisiae* W303-1A pre-inoculum, cells were grown on YPD agar plates for 48 hours. Harvested and resuspended in 5 ml of chemically defined medium containing glucose. The resuspended cells were used to inoculate 50 ml of chemically defined media with glucose in 250 ml Erlenmeyer flask. An optical density (OD_{600}) value of 0.2 was recorded. The cells were then placed in a shaking incubator for 16 hours at 30ºC. The cells were re-inoculated in this manner twice more for 8 hours and 11 hours. This method of preparing the pre-inoculum for the wild type strain was also used for the ethanol-grown cells with the exception of a longer incubation period of 48 hours for the final flask.

For growth on glucose, *S. cerevisiae* W303-1A, *S. cerevisiae* Q1, *S. cerevisiae T*Δ*123*::*ADH5*_S and *S. cerevisiae T*Δ*123*::*ADH5*_M strains were used to inoculate 1 L Erlenmeyer flasks with 400 ml chemicallydefined medium to produce a initial OD_{600} value of 0.2. A sterile 4.50 cm stirrer bar was placed in each flask. Flasks were closed with cotton bungs and placed on stirrers set at 400 rpm, for aerobic cultivation. All cultivations were conducted at 30ºC. Samples of 1 ml were collected at 3-hour intervals for *S. cerevisiae* W303-1A. *S. cerevisiae T*Δ*123::ADH5*_S and *S. cerevisiae T*Δ*123::ADH5*_M were sampled at 4-hour intervals for further analysis.

For growth in 7 g l^{-1} ethanol as carbon source, strains were inoculated into 400 ml chemicallydefined medium to give a starting OD_{600} of 0.2. Flasks were covered with cotton bungs and placed on a 200 rpm shaking incubator at 30ºC for 24 hours. Samples of 500 µl were collected from each flask to measure OD_{600}.

15 Bioreactor cultivation

15.1 Inoculum preparation

For the growth studies in 8 g l^{-1} glucose as carbon source, pre-inocula were prepared by reviving cells from cryo-storage on YPD plates for 48 hours at 30°C. These cells were used to inoculate 1 L chemically defined medium, for the *S. cerevisiae* Q1 and *S. cerevisiae* W303-1A reference strains. A final OD_{600} value of 0.2 was achieved in 1 L media.

For the cultivation of *S. cerevisiae T∆123*::*ADH5*_S and *S. cerevisiae T∆123*::*ADH5*_M on ethanol, clones were plated out on YNB agar and grown at 30°C for 48 hours. Thereafter 2 ml of sterile dH_2O was added to the plate and cells were resuspended in the dH_2O. The resuspended cells were used to inoculate 1 L chemically defined media resulting in a final OD_{600} value of 0.2 in a bioreactor.

15.2 Cultivation conditions

Stirrer speed was kept at 201 rpm, dissolved oxygen (pO_2) was limited to 30%, and the pO_2 was regulated by an increase of stirrer speed. The airflow in the bioreactor was kept at 0.15 l m^{-1}. Temperature was kept constant at 30°C throughout each individual reactor run and optimum pH conditions were kept at 5.5 with KOH and H_2SO_4. Samples were drawn at 3-hour intervals.

15.3 Analysis

Growth was monitored over 48 hours and biomass, ethanol, glucose, glycerol and acetaldehyde content determined every 3 hours. Biomass concentration was calculated through wet weight sampling at mid and late exponential growth phase. 10 ml samples were centrifuged at 3000 x *g* for 15 minutes to impede

metabolic activity and to isolate cellular biomass, thereafter fractions were dried at 80ºC for 24 hours. Dry weight was calculated and biomass was determined through interpretation of standard curve, constructed from dilutions made from both mid and late exponential growth phase cellular fractions. Ethanol and acetaldehyde concentrations were determined with a 2010 gas chromatograph (Shimadzu, equipped with an SGE PBX-70 column (30 m x 0.25 ID) at an oven temperature of 180ºC using nitrogen gas at 30 ml min^{-1} as carrier. Glucose was determined with a Sugar Analyzer I high-performance liquid chromatograph equipped with a refractive index detector and a Waters Sugarpack I column (Waters Associates, Milford, MA, USA) operating at 85ºC with an eluent (degassed water) flow rate of 0.5 ml min^{-1}. Glycerol was determined with a Hewlett Packard 1100 high-performance liquid chromatograph equipped with a refractive index detector and a Phenomenex Luna 5u NH2 100A column operating at 35ºC with an eluent (degassed 75% acetonitrile) flow rate of 2 ml min^{-1}.

CHAPTER 3: RESULTS AND DISCUSSION

1 Construction of *pYES2::ADH5*

ADH5 primers flanked with 6X His-tag (CATCATCATCATCATCAC) were used in the PCR amplification of *ADH5* with KAPA HiFi DNA Polymerase (KAPA Biosystems, RSA). After which amplification of both products was visualized on a 1% agarose gel as seen in **Fig 10.** The expected ~1 kb fragment was obtained for both amplicons.

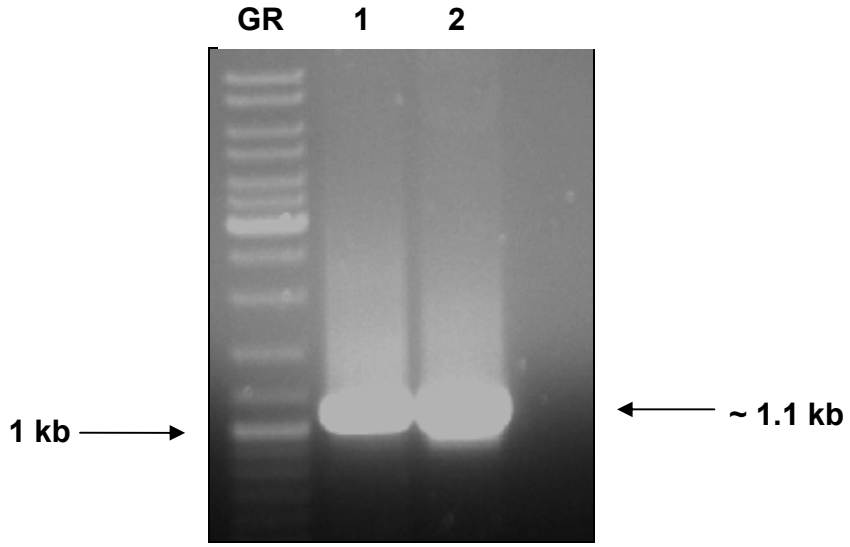

Fig 10: Gel electrophoresis of *ADH5* amplicons. *ADH5* PCR product with a 6X N-terminal His-tag (**lane 1**) and *ADH5* amplified with a 6X C-terminal His-tag (**lane 2**). Lane **GR** represents a 1 Kb DNA ladder (Fermentas).

ADH5:N-terminal Tag and *ADH5*:C-terminal Tag PCR products were ligated into pGEM®-T Easy, and transformed into competent *E. coli* XL 10 gold cells and dam⁻ competent *E. coli* cells. Restriction digests with *Xba*I and *Hin*dIII confirmed successful ligation with the presence of a ~3 kb plasmid backbone and ~1.1 kb insert (**Fig 11**).

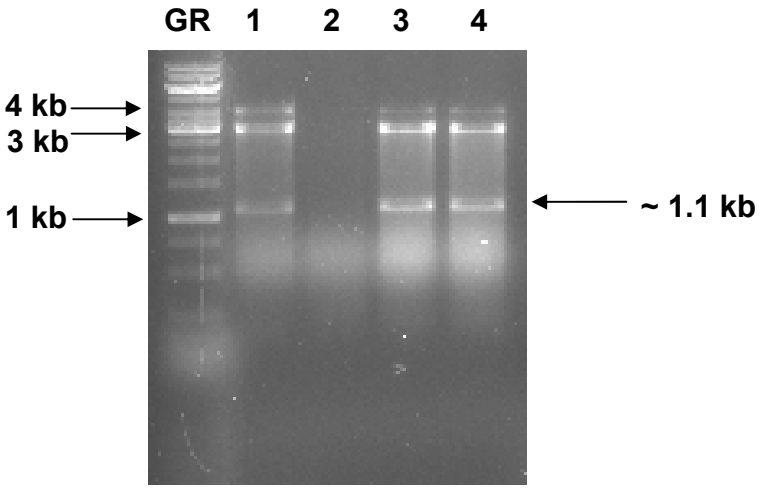

Fig 11: Restriction profiles of transformed *ADH5* clones in dam$^-$ competent *E. coli* cells ligated into pGEM®-T Easy. (**lane 1** and **2**), pGEM®-T Easy::*ADH5* N-terminal His-tag. (**lane 3** and **4**), pGEM®-T Easy::*ADH5* C-terminal His-tag. The ~3 kb band is represented by the pGEM®-T Easy backbone, and the ~1.1 kb band is represented by the *ADH5* gene. The ~4 kb band represents partially digested plasmid DNA.

The ~1.1 kb insert, representing *ADH5*:N-terminal Tag and *ADH5*:C-terminal Tag were excised from the gel, purified and cloned into the expression vector pYES2. **Fig 12** illustrates the restriction analysis verification of the pYES2::*ADH5*-N-terminal and pYES2::*ADH5*-C-terminal constructs.

pYES2::*ADH5* construct

After verification of His-tagged *ADH5* ORF (open reading frame) in pGEM®-T Easy. Two *ADH5* inserts containing the N-terminal His-tag and one harbouring the C-terminal His-tag was removed from pGEM®-T Easy, by excising it with *Xba*I and *Hin*dIII. The ~1.1 kb fragment was purified from the agarose gel and ligated into the expression vector pYES2 as seen in **Fig 12**.

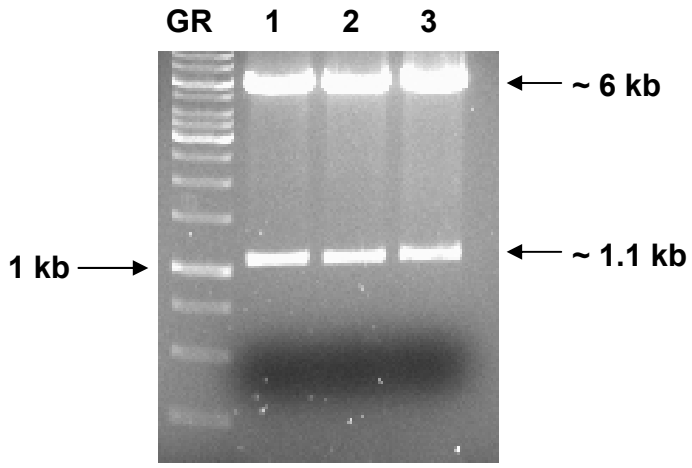

Fig 12: Restriction profiles of three clones representing the successful shuttling of the His-tagged *ADH5* ORF from pGEM®-T Easy into pYES2. Two clones represent constructs with the *ADH5* N-terminal His-tag (**lane 1** and **lane 2**) and the other the construct harbouring the C-terminal His-tag (**lane 3**). The ~6 kb fragment represents the pYES2 backbone and the ~1.1 kb fragment the His-tagged *ADH5* ORF.

2 *ADH5* expression

pYES2 was chosen as an expression vector because this plasmid was essentially designed for expression in *S. cerevisiae*, which is regulated by a *GAL1* inducible promoter (**Fig 13**). Transferring cells from glucose to galactose medium allows transcription to take place due to de-repression of the *GAL1* promoter. Three *S. cerevisiae* strains were chosen to quantify the efficiency of Adh5p expression, namely *S. cerevisiae* W303-1A, *S. cerevisiae* CEN PK42 and *S. cerevisiae* Invsc.

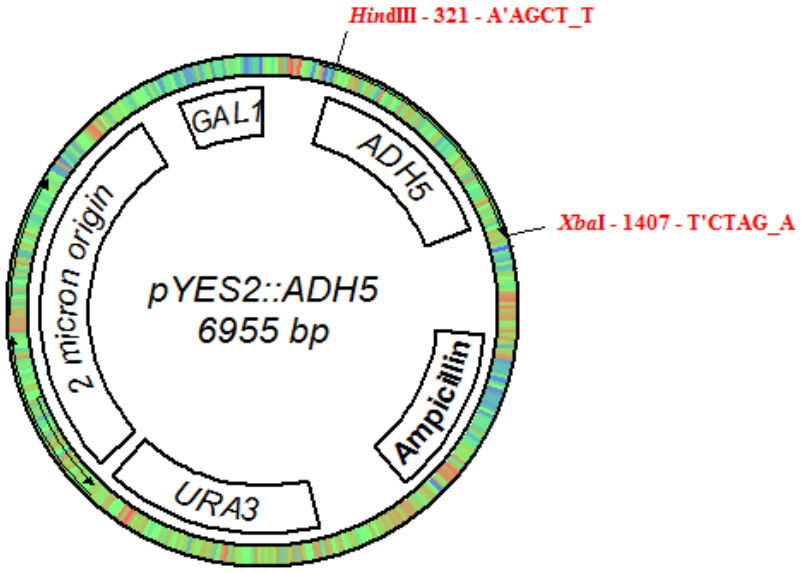

Fig 13: Plasmid map of the pYES2 vector indicating the *GAL1* inducible promoter region, selection is based on the *URA3* yeast marker. *ADH5* containing the 6X His-tag with restriction sites *Hind*III and *Xba*I is also annotated and visible on the map.

The three positive clones (two pYES2::*ADH5*-N-terminal and one pYES2::*ADH5*-C-terminal) were transformed into *S. cerevisiae* W303-1A and *S. cerevisiae* CEN PK42 strains. These transformants were inoculated into 5 ml yeast nitrogen-based uracil dropout media and grown overnight at 30°C. The inoculums were then re-inoculated in 250 ml YNB uracil dropout and grown overnight at 30°C. Cells were harvested, washed in 50 ml YP followed by resuspension into 200 ml YP plus 2% galactose inducing expression. The level and efficiency of Adh5p expression was verified with SDS-PAGE (**Fig 14**).

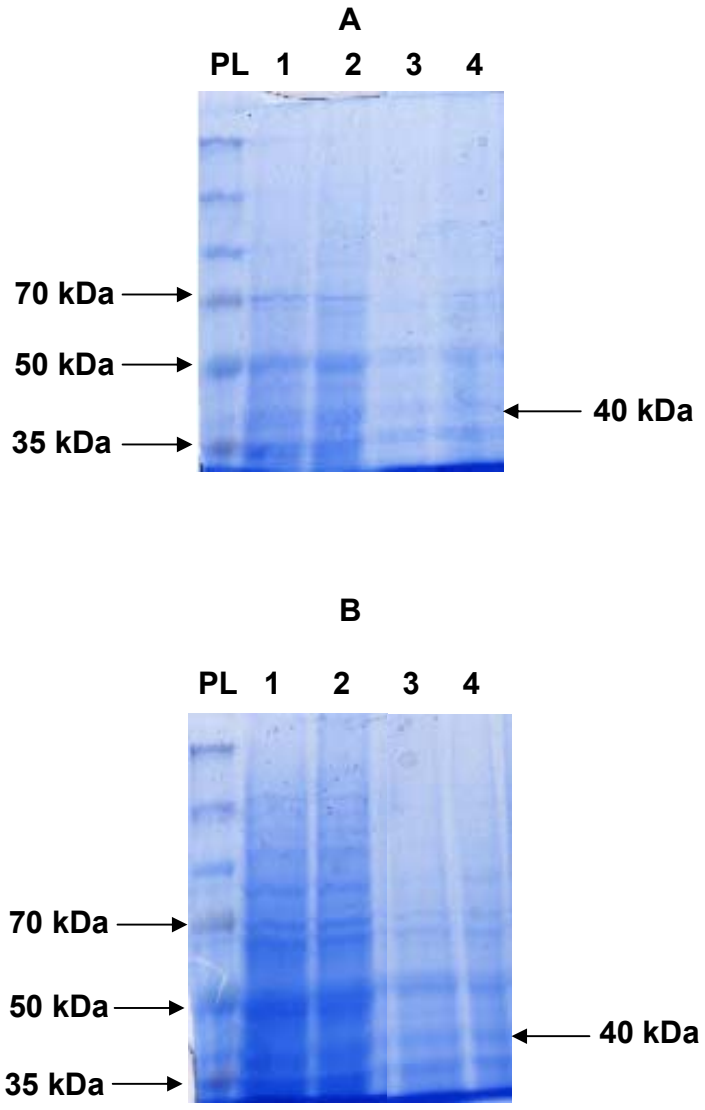

Fig 14: SDS-PAGE illustrating the expression levels of Adh5p in both *S. cerevisiae* CEN PK42 and *S. cerevisiae* W303-1A at various time intervals. Adh5p is located at 40 kDa. **A**: *S. cerevisiae* W303-1A at time 2 hours, (**lane 1** and **2**) and *S. cerevisiae* CEN PK42 at time 2 hours (**lane 3** and **4**). Maximum expressions for these strains are represented in **B:** *S. cerevisiae* W303-1A harvested at 8 hours (**lane 1** and **2**) and *S. cerevisiae* CEN PK42 harvested at 8 hours (**lane 3** and **4**).

N-terminal Western blot analyses were performed on *S. cerevisiae* W303-1A, *S. cerevisiae* Invsc and *S. cerevisiae* CEN PK42 crude cellular extract (**Fig 15**). This diagram illustrates the hybridization of all three crude extracts obtained from the three strains mentioned above after 8 hours of expression in YP plus 2% galactose. The Adh5p (40 kDa) can be seen as a black hybridized blot on the X-ray film (**Fig 15**). Antibody specific to the His-tag engineered onto the protein's N- or C-terminals were used as probe to detect the Adh5 protein. It was seen that the Western blot hybridization did not detect any of the expressed protein containing the 6X His-tag on the C-terminal. A C-terminal specific antibody was used, however this also did not allow detection of the Adh5 protein.

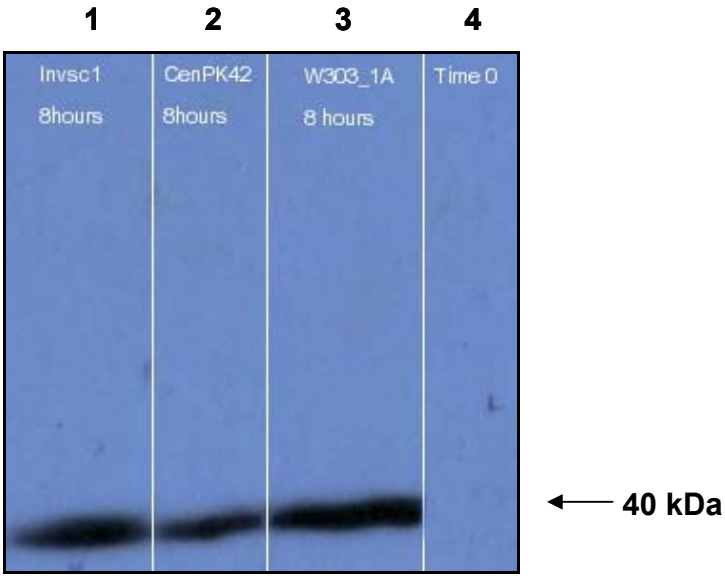

Fig 15: N-terminal hybridization of *S. cerevisiae* Invsc, *S. cerevisiae* CEN PK42 and *S. cerevisiae* W303-1A after 8 hours of expression. Harvested cellular fractions extracted from all three strains indicate a band at approximately 40 kDa. *S. cerevisiae* Invsc (**lane 1**), *S. cerevisiae* CEN PK42 (**lane 2**) and *S. cerevisiae* W303-1A (**lane 3**). The reference (**lane 4**) represents the expression level at nil hours, immediately after inoculation into 2% galactose.

Although positive results of the Western blot analyses were obtained, they were, however, performed under denaturing conditions. In the translated sequence of Adh5p there seems to be an abundant amount of proline residues. These residues are situated close to the N-terminal of the protein. Proline has a stringent degree of folding. This can cause the 6X His-tag to become imbedded into the protein, which can lead to unsuccessful purification of Adh5p.

A preliminary purification was thus performed with Ni-NTA Spin Columns provided by Qiagen. In addition, levels of expression were also tested between two *S. cerevisiae* strains (*S. cerevisiae* W303-1A and *S. cerevisiae* Invsc) to determine which of these strains would be the best host for the purpose of large-scale protein purification. *S. cerevisiae* CEN PK42 expression levels as seen in **Fig 15** were much less than *S. cerevisiae* W303-1A and *S. cerevisiae* Invsc. Thus the preliminary purification was performed on *S. cerevisiae* W303-1A and *S. cerevisiae* Invsc.

A clear band can be seen at approximately 40 kDa. These results indicate that firstly, the Adh5p could be purified using the N-terminal His tag. Secondly, the expression levels of Adh5p in *S. cerevisiae* strain W303-1A were significantly higher than those of *S. cerevisiae* Invsc.

Initial Western blot analysis (**Fig 15**) was performed on crude extract following 8 hours of induction. In this case the expression levels of strains *S. cerevisiae* W303-1A and *S. cerevisiae* Invsc were similar, while *S. cerevisiae* CEN PK42 showed the lowest expression levels. Protein concentrations were determined and equal concentrations were used. Preliminary purification using Ni-NTA Spin Columns were thus performed on *S. cerevisiae* strains W303-1A and *S. cerevisiae* Invsc crude extract. Results of purified Adh5p can be seen in **Fig 16**.

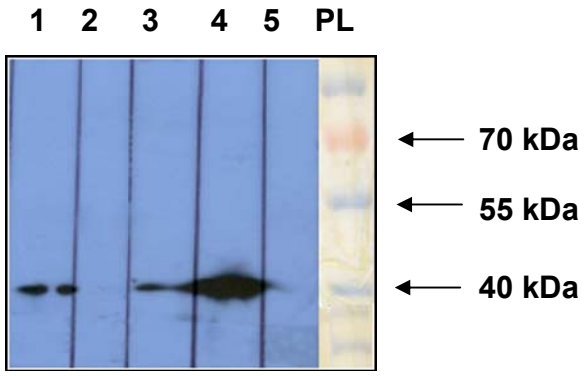

Fig 16: Western blot hybridization of Adh5p in *S. cerevisiae* strain W303-1A and *S. cerevisiae* Invsc. The 40 kDa purified Adh5p expressed in *S. cerevisiae* Invsc is represented in (**lane 1**) while the expression of *S. cerevisiae* Invsc at time 0 is represented in (**lane 2**). Purified Adh5p expressed in *S. cerevisiae* strain W303-1A (**lane 3**). Lysed *S. cerevisiae* W303-1A cells expressed for 8 hours (**lane 4**) and expression in *S. cerevisiae* W303-1A at time 0 (**lane 5**). Prestained page blue protein ladder (Fermentas) (**lane 6**).

After comparing Adh5p purified from both *S. cerevisiae* W303-1A and *S. cerevisiae* Invsc it was decided to continue large-scale purification of Adh5p expressed in *S. cerevisiae* strain W303-1A. However, before large-scale purification was performed Adh5p was expressed in *S. cerevisiae* W303-1A and purified using Ni-NTA Spin Columns provided by Qiagen. The purified Adh5p was verified on SDS-PAGE and stained with silver stain method (Merril, 1990). The Silver stained SDS-PAGE in **Fig 17** illustrates the expression at time 0. The lysed cells were diluted tenfold before being loaded onto SDS gel which showed three prominent bands at 75 kDa, 40 kDa and 35 kDa respectively. SDS-PAGE illustrated in **Fig 14** was performed on crude concentrated extract. The method used in **Fig 17** is much more sensitive and would cause prominent indistinguishable bands if cellular extract is not diluted in order to be compared to the purified Adh5p. After purification only one band at 40 kDa was left. All other proteins were eluted from the sample at baseline imidazole concentrations (20 mM).

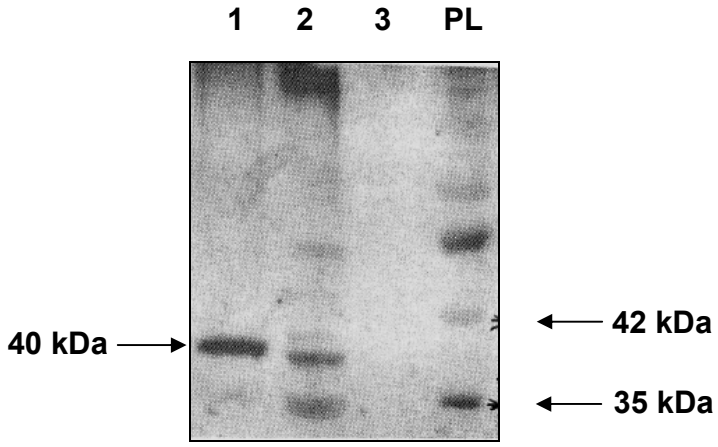

Fig 17: SDS-PAGE analysis of purified Adh5p using Ni-NTA Spin Columns, illustrating Adh5p at 40 kDa, harvested at 8 hours expression (**lane 1**). *S. cerevisiae* W303-1A lysed after 8 hours of Adh5p expression (**lane 2**). Sample taken prior to induction of *S. cerevisiae* W303-1A with *GAL1* promoter (**lane 3**). Fermentas unstained protein ladder can be interpreted in lane **PL.**

3 *FPLC* purification

Adh5p was passed through a column containing immobilized Ni^{2+}, which binds the polyhistidine tag. All untagged proteins passed through the column at approximately 20% conductivity. Protein was measured under spectrophotometric conditions and absorbed at $A_{280.}$ **Fig 18** illustrates the elution process as the concentration of imidazole increased. The salts out compete the tightly bound protein for the matrix. This induces the shift from stationary phase to mobile phase, causing the protein to elute into solution. When the protein is released from the stationary phase to the mobile phase, the spectrophotometric instrument (ÄKTAprime™) will detect a sudden increase of A_{280}.

The pYES2::*ADH5*-N-terminal constructs containing the integrated 6X His-tag were expressed and lysed after 8 hours of expression. Expression was induced in YP plus 2% galactose medium, at 30°C in a shaking incubator oscillating at 200 rpm. After purifying Adh5p using an ÄKTAprime™ with 5 ml HisTrap™ FF

columns (Invitrogen) as matrix the Adh5p was removed from the non-bound protein fraction. All remaining imidazole was removed with dialysis and confirmed with SDS-PAGE followed by Western blot analysis (**Fig 19**). Adh5p expressed in *S. cerevisiae* W303-1A lab strain was purified using fast protein liquid chromatography (FPLC) ÄKTAprime™ technologies. The enzyme was over-expressed with a His-tag at the N-terminal of the protein, and the preferred method of purification was Ni^{2+} affinity chromatography.

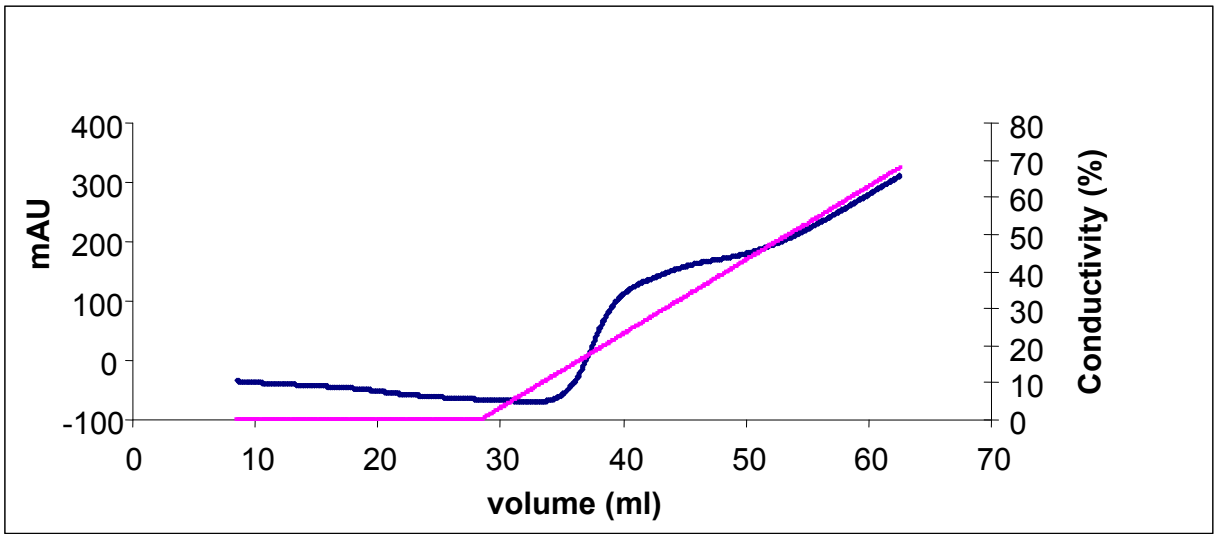

Fig 18: Adh5p elution profile. The blue line represents the A_{280} and the pink line the linear gradient of imidazole. When the conductivity reached 20% the protein shifted to mobile phase. This resulted in the elution of Adh5p to be used in downstream kinetic experiments.

After dialysis of purified Adh5p, the efficiency of purification and protein yield was determined with SDS-PAGE and Western blot analysis. The Western blot verified that no contaminating proteins were purified. Coomassie blue and silver staining showed no other proteins. After a separate purification, protein standards were incorporated to pre-equilibrate a Sefadex H200 gel matrix (Sigma Aldrich). Purified Adh5p was thereafter run on the equilibrated matrix, and elution profiles were compared to those of the six individual standards. The

native size through interpretation of elution profiles captured by FPLC software was determined as 158 kDa.

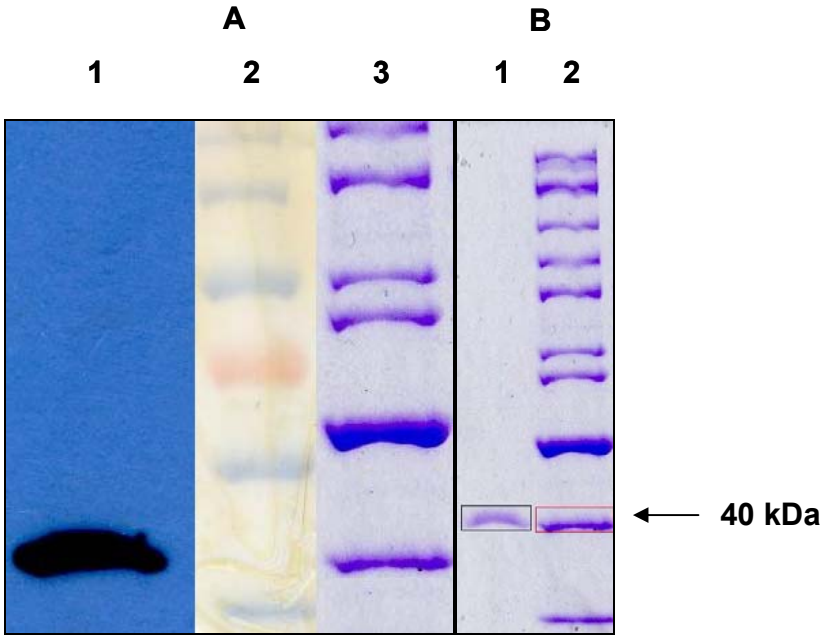

Fig 19: **A:** Western blot analysis of purified Adh5p after dialysis illustrating the purified Adh5p at 40 kDa after 8 hours expression (**lane 1**). The prestained protein ladder was compared to the unstained protein ladder from SDS-PAGE. Prestained protein ladder has a tendency to denature resulting in false band sizes (**lane 2** and **lane 3**). **B**: Purified Adh5p (**lane 1**) and unstained protein ladder (**lane 2**).

Protein concentration after purification was determined using a Micro BCA™ protein assay kit supplied by Pierce. Standard curve was constructed from a dilution range provided by the manufacturer (**Fig 20**). Protein concentration was calculated as 1 mg ml^{-1}.

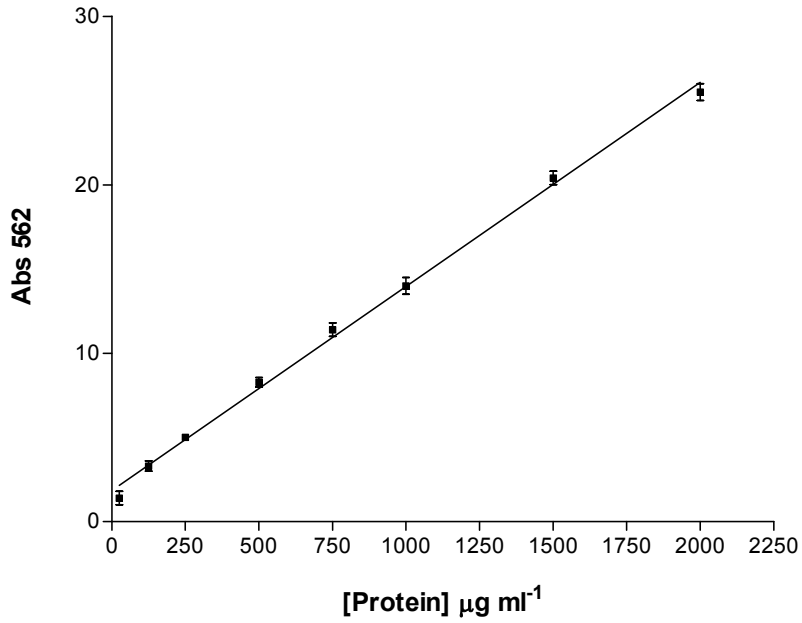

Fig 20: BCA standard curve. The theoretical absorbance is annotated on the Y axis and the protein concentration on the X axis. Curve was constructed from dilution range provided by the manufacturer. The graph represents a linear curve recorded at A_{562}.

Adh5p characterization

3.1 Parameters optimization

Before Adh5p could be characterized, co-factor dependence had to be determined and pH and temperature optimized. By optimizing all the variables in the enzymatic reaction, the reaction rate can be performed at a maximum velocity, delivering the optimum results.

3.2 Co-factor

Characterization assays were monitored on a micro-titre plate reader and measured at A_{340}. NAD^+ becomes reduced and accepts an H^+ atom the reduced shape (NADH) will result in an increase of $A_{340.}$ If NADH is oxidized the spectrophotometer will measure the decrease in NADH concentrations, resulting in a decrease of A_{340}. Classical YADHs either utilize NAD^+ or NADH, while the two cinnamyl Adhps utilize $NADP^+$ and NADPH.

3.2.1 Ethanol oxidation

Unsure of the substrate specificity of Adh5p towards aldehydes and alcohols, four co-factors involved in all other yeast alcohol dehydrogenases were used.
NAD^+ or $NADP^+$ is used as co-factor during the oxidation of ethanol to acetaldehyde. The co-factor reduction was monitored on a micro-titre plate reader at $A_{340.}$ Data retrieved clearly indicated NAD^+ as preferred co-factor (**Fig 21**).

3.2.2 Acetaldehyde reduction

Substrate specificity towards acetaldehyde as substrate was monitored using NADH and NADPH as co-factors. The A_{340} was monitored on a micro-titre plate reader. The results showed no significant oxidation of either NADH or NADPH.

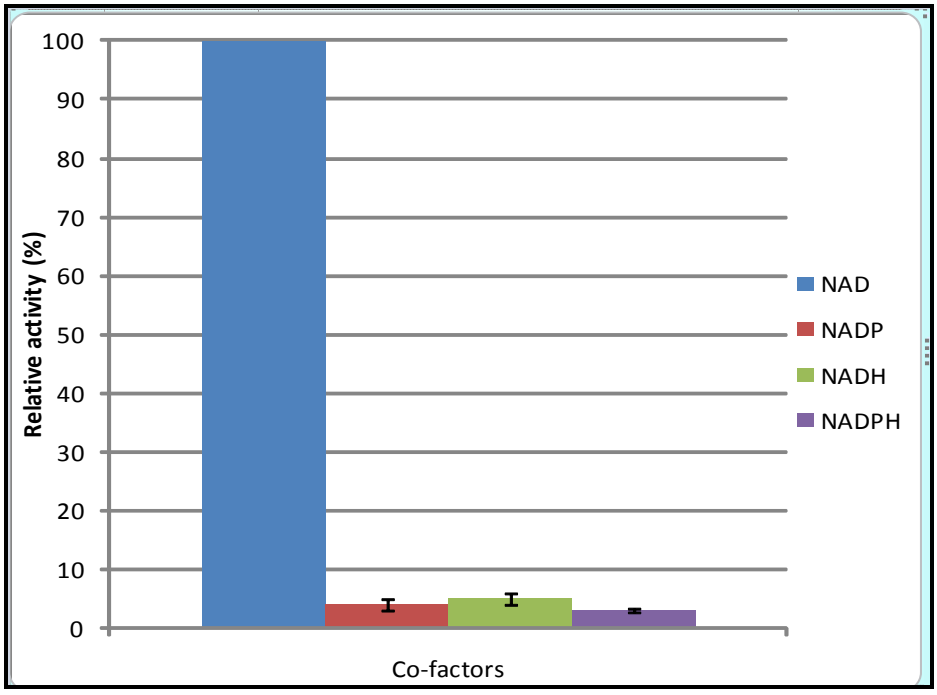

Fig 21: Data profile illustrating the relative activity in percentage towards the four co-factors utilized in YADHs. NAD^+ was plotted as 100% and the other co-factors' conversion rates are plotted against NAD^+.

The bar graph in **Fig 21** illustrates the dependence of Adh5p towards all four co-factors. The relative activity towards NAD^+ as co-factor is significantly higher than the others. These results are conclusive that Adh5p utilizes NAD^+ as co-factor.

3.3 pH optimization

From the conclusive results retrieved in the co-factor determination study, it was decided to continue with NAD^+ as co-factor, thus representing the oxidation of ethanol and other alcohols back to acetaldehyde and respective aldehydes. **Fig 22** shows the relative activity of Adh5p at various pH. As the pH increased from pH 6 the relative activity also increased proportionally. Optimum pH was reached at approximately 8.8, concurring with literature stating that the optimum pH for the oxidative reaction in most yeast alcohol dehydrogenase is in the vicinity of pH 7.5 to pH 9 (Zanon et al. 2007).

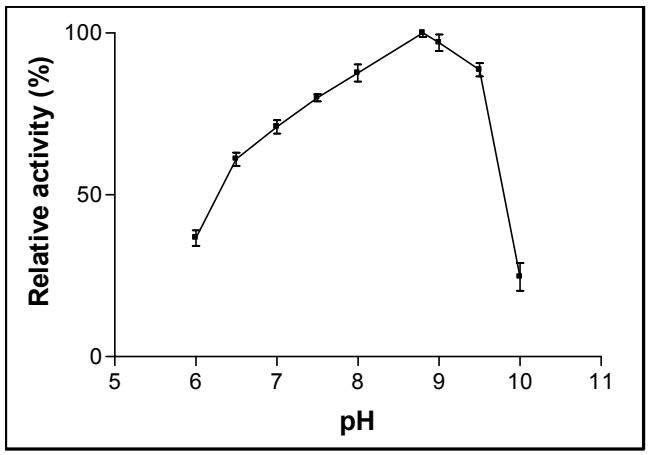

Fig 22: Optimum pH of Adh5p determined at 30°C with ethanol as substrate and NAD^+ as co-factor. The data demonstrates the optimum pH at 8.8 with a rapid decline visible when the pH exceeds 9. The error bars indicate the standard deviations calculated from triplicate experiments to be less than 10%.

3.4 Temperature optimization

The oxidative pathway was implemented to determine the optimum temperature of Adh5p during oxidation of ethanol to acetaldehyde. The experimental procedure was much the same as that of the optimum pH determination. After determining the optimum pH, as well as the suitable co-factor, these data sets were then used to calculate the optimum temperature of the reaction. Optimum activity was determined at 30°C. However, enzyme activity increased gradually from 17°C to 30°C. When the temperature exceeded 30°C the activity rapidly decreased to less than 10% of the maximum oxidative catalytic activity reached (**Fig 23**).

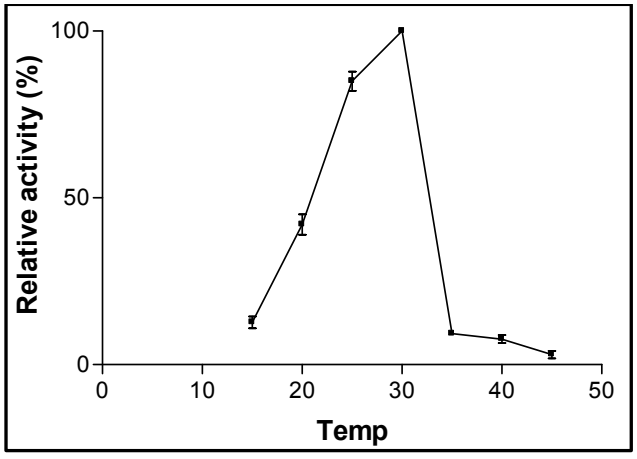

Fig 23: Optimum temperature of Adh5p determined at 30°C with ethanol as substrate and NAD^+ as co-factor. The optimum activity was plotted as 100% and the rest of the data plotted relative to it with a standard deviation of less than 10%.

3.5 Substrate optimization

Literature suggests that the classical Adhps are capable of oxidizing alcohols containing more than two carbons (Dickinson et al. 2003). To substantiate whether Adh5p is also capable of oxidizing longer un-branched alcohols, experiments were performed at the optimum pH and temperature conditions.

Adh1p and Adh2p have been characterized and established as capable of oxidizing various secondary alcohols, such as propanol, propan-2-ol, butanol, pentanol, decanol, hexanol and ethanol (Dickinson et al. 2003). As the number of carbon atoms in the backbone of the alcohol increases, the relative activity decreases. When branched alcohols were introduced to the enzyme's (active site, the activity decreased more rapidly as the chain length increased (Dickinson et al. 2003).

The relative activity of Adh5p towards alcohols ranging from two to ten carbons in chain length can be seen in **Fig 24**. As the carbon length of an alcohol increases, the solubility in a polar solution decreases. Ethanol is miscible in water, while decanol is completely insoluble in any polar solution without a solvent present. Marcinkeviciene and co-workers (2006) tested the effect of various solvents on the stability and activity of Adh2p and Adh3p. It was concluded that Dimethyl sulfoxide (DMSO) and Dimethylformamide (DMF) at concentrations of between 5% and 10% had no effect on the activity of the enzyme. It was further established that decanol and octanol dissolved completely in 0.5% DMSO.

The effect of 0.5% DMSO on enzyme (Adh5p) activity was tested. Assays were performed on Adh5p towards ethanol as substrate containing 0.5% DMSO and 1% DSMO respectively. The DMSO had no effect on the activity of Adh5p. Alcohols such as propan-2-ol, pentanol and butanol are soluble in polar solutions at low concentration. DMSO was only added to hexanol and decanol (Marcinkeviciene et al. 2006).

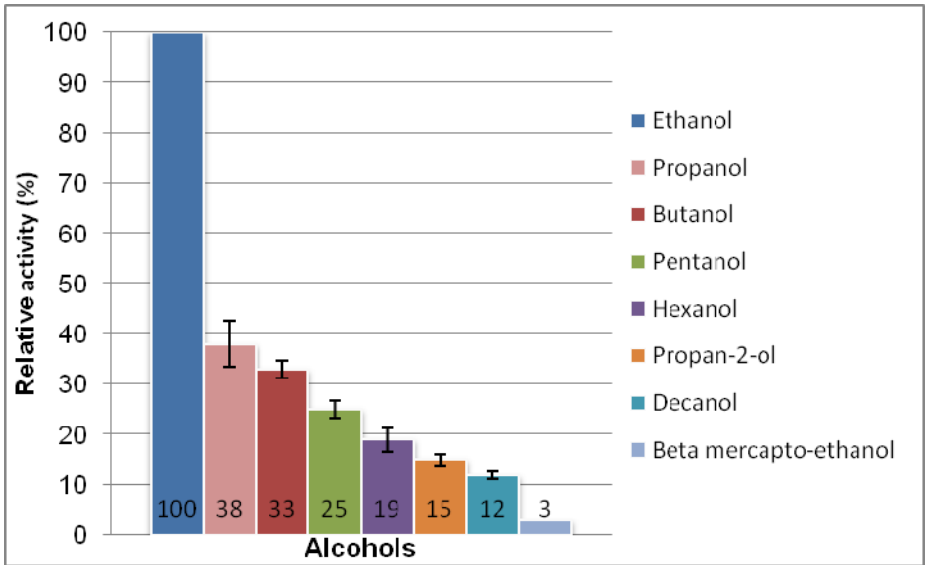

Fig 24: Illustration of the substantial difference in relative activity in % of Adh5p when exposed to alcohols increasing in chain length. Standard deviations calculated are less than 12%.

3.6 Substrate specificity

Characterization was performed under aerobic conditions at optimized parameters. Catalysis was initiated by the addition of NAD^+ as co-factor. The purified Adh5p showed no activity towards aldehydes as substrate with NADH or NADPH as co-factors. In the kinetic characterization of Adh5p the two variables were NAD^+ concentrations and substrate (alcohol) concentrations.

Every substrate had to be characterized on various predetermined alcohol and co-factor concentrations. Michaelis-Menten describes the kinetics of many enzymes and this kinetic model is relevant to situations where very simple kinetics can be assumed, (i.e. there is no intermediate or product inhibition, and there is no allostericity or cooperativity). The Michaelis–Menten equation relates the initial reaction rate v_0 to the substrate concentration [S] (Mathews et al. 2000). The corresponding graph is a hyperbolic function and the maximum rate is described as V_{max}. The equation describes the rates of irreversible reactions. A steady state solution for a chemical equilibrium modeled with Michaelis–

Menten kinetics can be obtained with the Goldbeter–Koshland equation (Mathews et al. 2000).

Data was plotted in graph pad prism 3. All reference/blank samples were subtracted from the A_{340} of every test sample. It was monitored throughout the study and the blank values did not show any significant fluctuation, thus little to no chemical reduction of NAD^+ took place.

The characterization data can be seen in **Fig 25 – Fig 36**. Characterization graphs are arranged in alcohols ascending in chain length. Adh5p was assayed on both substrate and co-factor level. The kinetics is based on Michael-Menten kinetics. Adh5p was characterized to determine the substrate specificity and the efficiency of the enzyme. This was performed on various alcohols, increasing in chain length and branching. The data presented in **Fig 25 – Fig 36** was performed in triplicate. Michaelis-Menten kinetics wasincluded to calculate the kinetic constants of each data set, these constants can be seen in **table 4**.

Adh5p, similar to homologous alcohol dehydrogenases, is primarily restricted to un-branched alcohols. The turnover efficiency of Adh5p decreased as the alcohol's chain length increased (**Fig 25** to **Fig 36**). It further decreased when the branched alcohols were introduced as illustrated in **Fig 27**. The enzyme is most efficient with ethanol as substrate, as seen in **table 4** and **Fig 25**. All the characterization data coincides with published data obtained on Adh1p and Adh2p. Leskovac and co-workers (2002) compared and calculated kinetic data reported by Ganzhorn and co-workers (1987) of Adh1p and Adh2p. When Adh5p is compared to Adh1p and Adh2p (**table 5**), it can be concluded that Adh5p is not as kinetically efficient as Adh1p or Adh2p. Less substrate is converted to product per second than in Adh1p and Adh2p.

The Michaelis constants calculated for Adh5p are much lower than Adh2p. The lower K_m indicates that Adh5p has a much higher affinity toward ethanol. However, the turnover number is much lower than Adh2p seen in **table 5**. This

signifies that the substrate binds tightly to the cleft. The binding occurs in such an orientation that prolongs the protonation and deprotonation of amino acids critical in the proton relay system mentioned in chapter one**.**

3.7 Ethanol characterization

The oxidation of ethanol to acetaldehyde was monitored through the reduction of NAD^+ to NADH. The reduction of the co-factor was monitored at A_{340}. The kinetic parameters were calculated at a fixed NAD^+ concentration as seen in **Fig 25**. The kinetic parameters were also calculated at a fixed ethanol concentration as seen in **Fig 26**. The parameters can be seen in **table 4**.

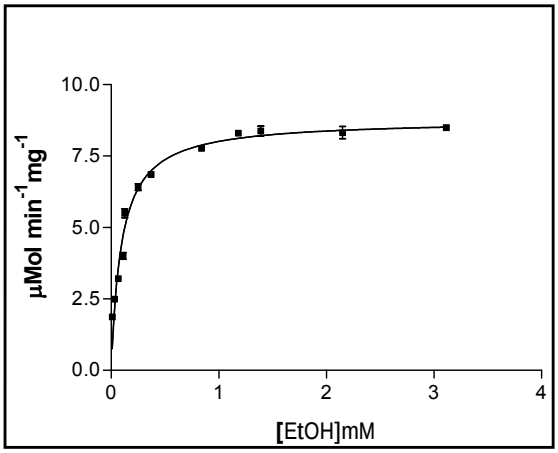

Fig 25: Kinetics of Adh5p towards ethanol as substrate in mM, specific activity is expressed in µMol min^{-1} mg^{-1}. The data follows Michaelis-Menten steady state kinetics. Parameters were kept at 30°C, pH 8.8. The graph indicates a clear turnover of substrate to product. Enzyme saturation occurred at relatively low concentrations, approximately 3 mM ethanol.

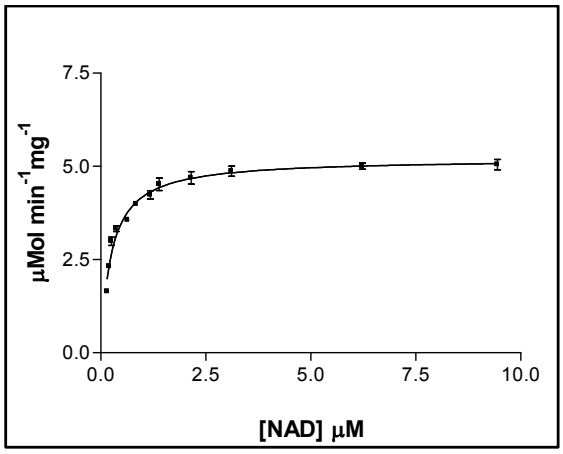

Fig 26: Enzyme kinetics illustrating the 1st and 2nd order reaction progress curve of the characterization based on NAD^+ as substrate at fixed ethanol concentration. Parameters were kept at 30°C, pH 8.8. The graph indicates a clear turnover of substrate to product. Enzyme saturation occurred at relatively low concentrations, approximately 5 µM NAD^+. The V_{max} determined in the NAD^+ characterization is much lower than characterization data presented in **Fig 25**.

3.8 Propan-2-ol characterization

Dickinson and co-workers (2003) illustrated the effect of longer branched and un-branched alcohols on the activity of Adh1p and Adh2p. The introduction of branched alcohols into the active site caused a rapid decrease in catalytic activity. The affinity of Adh5p towards propan-2-ol is much lower, as seen with ethanol. The kinetic curves can be seen in **Fig 27** at fixed alcohol concentrations. The graph represented by **Fig 28** illustrates the activity at fixed co-factor concentration. The parameters can also be seen in **table 4**.

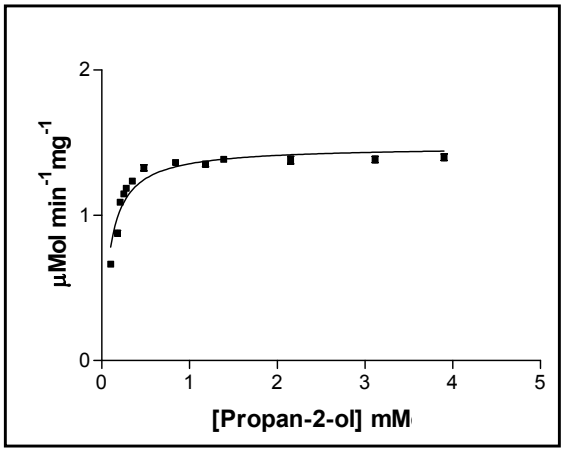

Fig 27: Enzyme kinetics illustrating the 1st and 2nd order reaction progress curve of the characterization based on propan-2-ol as substrate at fixed co-factor concentration. Parameters were kept at 30°C, pH 8.8. Enzyme saturation occurred at low concentrations, approximately 3 mM propan-2-ol. The enzyme proved a very insufficient catalyst of propan-2-ol. This is due to the branched backbone of the alcohol.

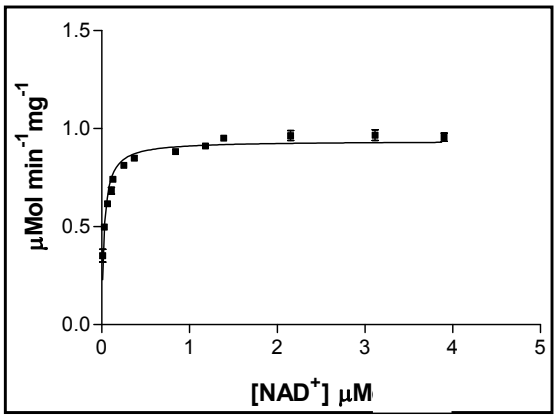

Fig 28: 1st and 2nd order reaction progress curve of the characterization based on NAD^+ as substrate. Parameters were kept at 30°C, pH 8.8. Enzyme saturation occurred at low concentrations, approximately 3 mM NAD^+. The enzyme proved a very insufficient catalyst of propan-2-ol. This is due to the branched backbone of the alcohol.

3.9 Butanol characterization

The oxidation of butanol was monitored at A_{340}. The kinetic parameters were calculated at fixed NAD^+ concentration as seen in **Fig 29**. The kinetic parameters were also calculated at a fixed butanol concentration as seen in **Fig 30**. The parameters can be seen in **table 4**. The V_{max} recorded in **Fig 29** (3.6 µMol min^{-1} mg^{-1}) is lower than ethanol. The recorded V_{max} for ethanol is 8.5 µMol min^{-1} mg^{-1}. The enzyme is less affinitive towards butanol than ethanol. The K_m recorded for butanol (0.12 mM) is slightly higher than ethanol (0.1 mM).

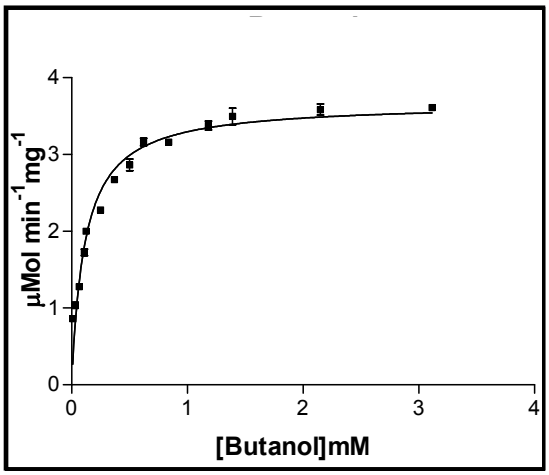

Fig 29: Kinetics of butanol as substrate in mM, the specific activity was calculated in µMol min^{-1} mg^{-1} Adh5p. Enzyme saturation occurred at approximately 3 mM butanol. Parameters were kept at 30°C, pH 8.8. The activity towards butanol is higher than towards propan-2-ol. This signifies the effect of branched alcohols on the activity of Adh5p. The butanol chain length is longer than propan-2-ol. However, butanol is not branched.

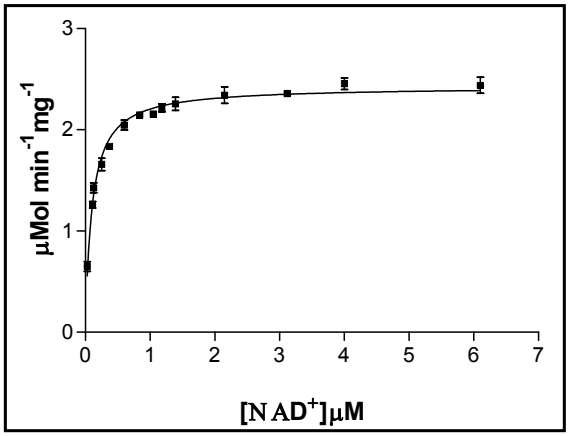

Fig 30: 1st and 2nd order reaction progress curve of the characterization based on NAD^+ as substrate. Enzyme saturation occurred at approximately 3 mM NAD^+. Parameters were kept at 30°C, pH 8.8.

3.10 Pentanol characterization

The oxidation of pentanol was monitored through the reduction of NAD^+ to NADH. Kinetic parameters were calculated at fixed NAD^+ concentration as seen in **Fig 31**. The kinetic parameters were also calculated at a fixed pentanol concentration as seen in **Fig 32**. The kinetic parameters can be seen in **table 4**. The V_{max} recorded in **Fig 31** (2.7 µMol min^{-1} mg^{-1}) is lower than ethanol (8.5 µMol min^{-1} mg^{-1}). The chain length clearly has an effect on the efficiency of Adh5p. The binding potential of the substrate decreased as the K_m value increased when pentanol was introduced.

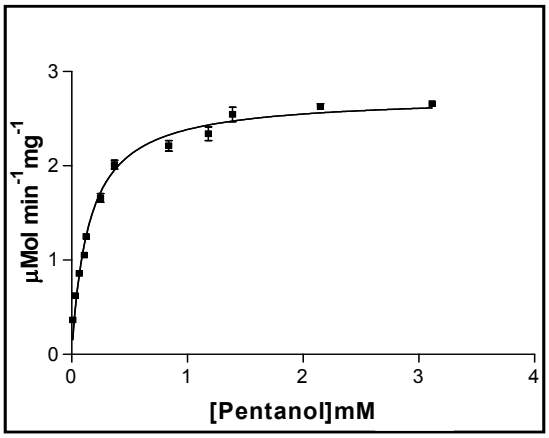

Fig 31: Kinetics of pentanol as substrate in mM, the specific activity was calculated in µMol min^{-1} mg^{-1} Adh5p. Enzyme saturation occurred at approximately 3 mM pentanol. Parameters were kept at 30°C, pH 8.8. The activity towards pentanol is higher than towards propan-2-ol. However, ethanol is the preferred substrate.

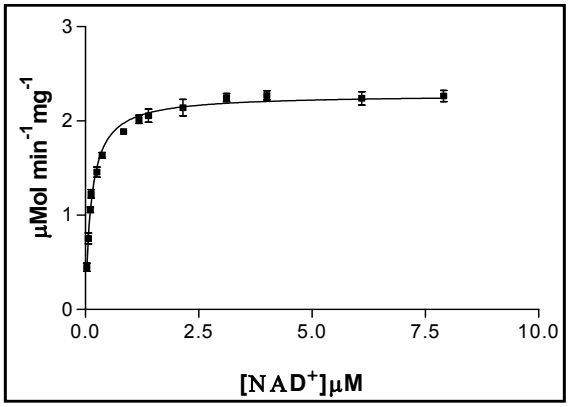

Fig 32: 1st and 2nd order reaction progress curve of the characterization based on NAD^+ as substrate. Enzyme saturation occurred at approximately 3 mM NAD^+. Parameters were kept at 30°C, pH 8.8.

3.11 Hexanol characterization

The oxidation of hexanol was monitored through the reduction of NAD^+ to NADH. The reduction of the co-factor was monitored at A_{340}. The kinetic parameters were calculated at a fixed NAD^+ concentration as seen in **Fig 33**. The kinetic parameters were also calculated at a fixed hexanol concentration as seen in **Fig 34**. The kinetic parameters can be seen in **table 4**. The V_{max} recorded in **Fig 33** (2.4 µMol min^{-1} mg^{-1}) is lower than ethanol (8.5 µMol min^{-1} mg^{-1}). The data presented in **Fig 33** (hexanol) is similar to **Fig 31** (pentanol). The increase in chain length by one carbon shows no dramatic decrease in activity.

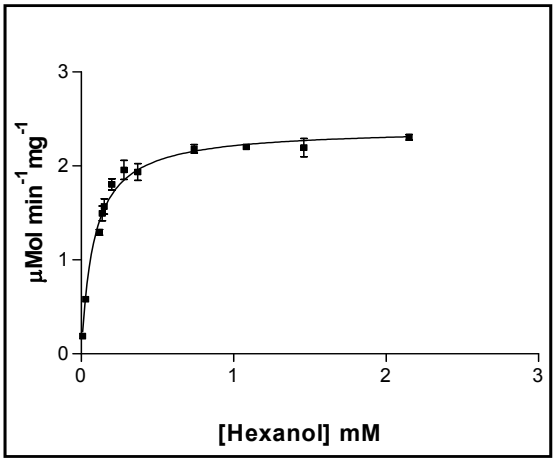

Fig 33: Kinetics of hexanol as substrate in mM, the specific activity was calculated in µMol min^{-1} mg^{-1} Adh5p. Enzyme saturation occurred at approximately 2 mM hexanol. Parameters were kept at 30°C, pH 8.8. The activity towards hexanol is higher than towards propan-2-ol. However, ethanol is the preferred substrate.

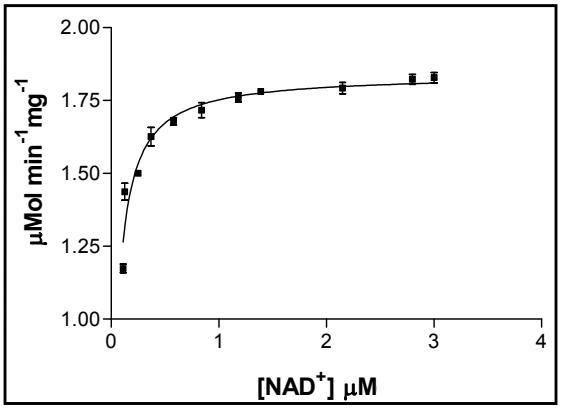

Fig 34: 1st and 2nd order reaction progress curve of the characterization based on NAD^+ as substrate. Enzyme saturation occurred at approximately 3 mM NAD^+. Parameters were kept at 30°C, pH 8.8.

3.12 Decanol characterization

The oxidation of decanol was monitored through the reduction of NAD^+ to NADH. Kinetic parameters were calculated at a fixed NAD^+ concentration as seen in **Fig 35**. The kinetic parameters were also calculated at a fixed decanol concentration as seen in **Fig 36**. The kinetic parameters can be seen in **table 4**. The V_{max} recorded in **Fig 35** (0.85 µMol min^{-1} mg^{-1}) is tenfold lower than ethanol (8.5 µMol min^{-1} mg^{-1}). The turnover number (K_{cat}/K_m mM s^{-1}) decreased dramatically when longer or branched alcohols were used as substrate. Decanol and propan-2-ol are the least efficient substrates utilized by Adh5p.

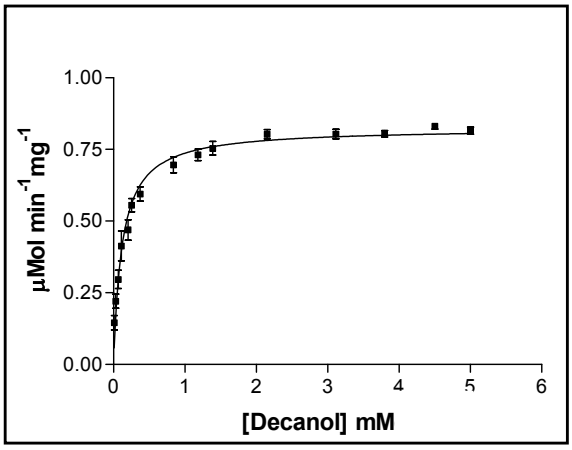

Fig 35: Kinetics of decanol as substrate in mM, the specific activity was calculated in µMol min^{-1} mg^{-1} Adh5p. Enzyme saturation occurred at approximately 3 mM decanol. Parameters were kept at 30°C, pH 8.8. The enzyme is not capable of oxidizing decanol. This alcohol has a 10-carbon chain length. The affinity towards decanol is the lowest of all the substrates used in this study. The K_m is double that recorded for ethanol.

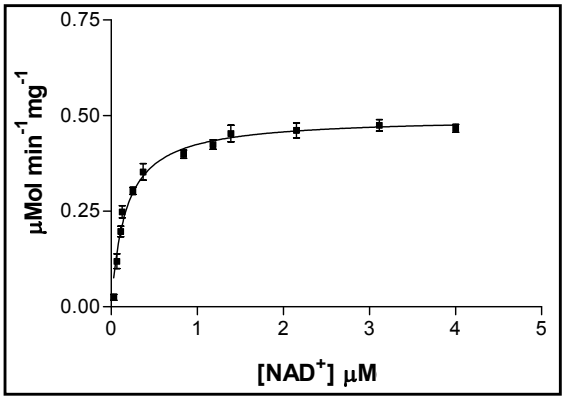

Fig 36: 1st and 2nd order reaction progress curve of the characterization based on NAD^+ as substrate. Enzyme saturation occurred at approximately 3 mM NAD^+. Parameters were kept at 30°C, pH 8.8. The reduction of NAD^+ was extremely low. No significant signs of reduction were recorded.

After various assays it can be determined by interpretation of the kinetic data presented in **Fig 25** that Adh5p participates in the oxidation of ethanol to acetaldehyde. The other yeast alcohol dehydrogenase in *S. cerevisiae* primarily responsible for the oxidation localized in the cytosol is Adh1p and Adh2p (**table 5;** Dickinson and Monger, 1972; Schopp and Aurich, 1976; Ganzhorn et al. 1987; Murali and Creaser,1986; Leskovac et al. 2002; Trivedi et al. 2005).

Table 4. Kinetic parameters of Adh5p calculated per active site. Enzymatic activities were measured in 50 mM Sodium Phosphate, pH 8.8. K_m and V_{max} values were determined by interpretation of steady state kinetic curves.

Parameter	Ethanol	Propan-2-ol	Butanol	Pentanol	Hexanol	Decanol
[1]K_m mM	0.1 ± 0.002	0.2 ± 0.009	0.12 ± 0.005	0.132 ± 0.007	0.138 ± 0.01	0.2 ± 0.013
[1]V_{max} µMol min^{-1} mg^{-1}	8.5	1.4	3.6	2.7	2.4	0.85
[1]K_{cat} s^{-1}	0.145±0.001	0.023 ± 0.005	0.061 ± 0.001	0.046 ± 0.003	0.041 ± 0.002	0.014 ± 0.003
[1]K_{cat}/K_m mM.s^{-1}	1.45	0.119	0.508	0.348	0.290	0.0725
[2]K_m µM	0.18 ± 0.001	0.09 ± 0.003	0.132 ± 0.006	0.15 ± 0.006	0.15 ± 0.01	0.125 ± 0.01
[2]V_{max} µMol $min^{-1}$$mg^{-1}$	5	1	3.2	1.8	1.8	0.5
[2]K_{cat} s^{-1}	5 ± 0.07	1 ± 0.1	3.27 ± 0.08	1.84 ± 0.1	1.84 ± 0.09	0.512 ± 0.04
[2]K_{cat}/K_m µM.s^{-1}	28.44	11.11	24.8	12.28	12.28	4.09

[1] Michaelis constant for alcohol at fixed co-factor concentrations
[2] Michaelis constants for co-factor at fixed alcohol concentrations

Table 5. Data retrieved from different studies. The purpose of this table is to compare data between the various K_m and V_{max} values of Adh1p, Adh2p and now characterized Adh5p to ethanol as substrate.

Ethanol	[a]Adh1p	[a]Adh2p	Adh5p
K_m µM	1700	810	100
V_{max} µMol min^{-1} mg^{-1}	20000	160	8.5
K_{cat} s^{-1}	340	130	0.145
K_{cat}/K_m $mM^{-1}s^{-1}$	20	160	1.45

[a] Calculated from data of Ganzhorn et al. 1987; Dickinson and Monger, 1972; Schopp and Aurich, 1976; Murali and Creaser,1986; Leskovac et al. 2002; Trivedi et al. 2005

The total enzyme concentration was 1 mg ml^{-1}, the amount of enzyme added in the assay was 0.01 mg in 20 µl. K_{cat} was determined by dividing the V_{max} of every reaction by the total enzyme concentration, calculated from the tetrameric molecular weight of Adh5p (158 kDa) and the amount in grams of enzyme added. All K_{cat}/K_m values were calculated per dimer, thus per catalytic site, and not as the active tetramer. The molecular weight of the dimer was calculated as 75296.1 g Mol^{-1}.

The longer chain length of the other alcohols indicates that the orientation at which the substrate binds the cleft has an extreme effect on the catalytic efficiency. The orientation of the substrate is directly propositional to the positioning of the functional groups of the substrate.

The kinetic parameters listed in **table 5** show the differences retrieved from past studies and those recorded in this study. Adh5p has a much higher affinity towards ethanol than Adh1p and Adh2p. The turnover number of substrate to product is significantly lower. Compared to Adh1p and Adh2p, Adh5p is much less efficient at turning substrate over to product.

4 Construction of *adh* triple deletion mutant

Wild type *S. cerevisiae* is capable of utilizing both glucose and ethanol as carbon source due to the presence of both Adh1p and Adh2p. These enzymes are primary responsible for redox reactions involved in ethanol metabolism. *S. cerevisiae* is capable of utilizing ethanol as a carbon source.

A triple deletion mutant was constructed to restrict oxidative activity as well as monitor the influence on growth in an *adh1, adh2* and *adh3* null background, when Adh5p is active under expression of the *ADH1* promoter. *ADH5* expression levels are known to be low and under natural conditions. The activity is masked by *ADH1* and *ADH2* expression. For this reason an *adh1, adh2* and *adh3* null background was constructed to eliminate the three

dominant dehydrogenases in ethanol metabolism. *S. cerevisiae* double deletion strain ∆*adh2, adh3* (*S. cerevisiae* strain D∆23) (De Smidt, 2007) was used to construct the triple deletion mutant. Transformation of a ~4 kb PCR product (a*dh1*∆::*LEU2*) in which *ADH1* open reading frame was replaced by the marker gene *LEU2* (**Fig 37**). The *adh1*∆::*LEU2* product was amplified by primer combinations *ADH1*-1F and *ADH1*-1R.

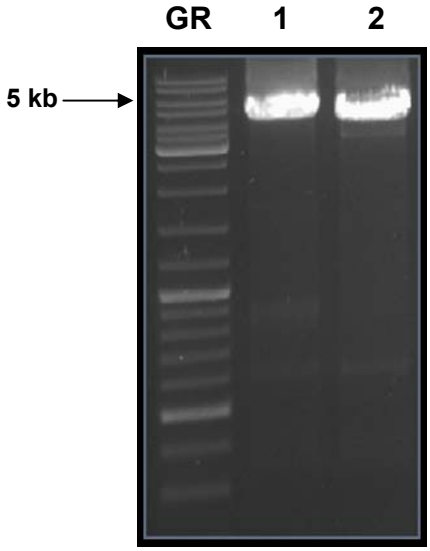

Fig 37: PCR amplicons representing the a*dh1*∆::*LEU2* ~4 kb fragment amplified with primer set *ADH1*-1F and *ADH1*-1R. Lane **GR** is represented by a 1 kb DNA ruler supplied by Fermentas.

Transformants were selected on –UTL (Ura^-, Trp^- and Leu^-) plates. Genomic DNA was extracted from each colony and used as template for PCR screening, to detect the *adh1*∆::*LEU2* integration. The PCR screening was performed to detect *ADH5* (~1.1 kb), *ADH4* (~1.4 kb), and to confirm that the wild type alleles of *ADH1, ADH2* and *ADH3* are not present (**Fig 39B**). The screening to detect the deleted genes of *adh1, adh2* and *adh3* can be seen in **Fig 38, Fig 39A** and **Fig 40**. PCR was designed to amplify substituted genes with the corresponding markers. Thus the target gene is replaced with the target marker. PCR results

show a band corresponding to each marker size. The desired band amplified confirms the deletion of the gene. The screening results for *adh1*∆::*LEU2* are shown in **Fig 38** the *LEU2* marker is ~1.7 kb. Visualization of the ~1.7 kb band indicated that the gene was deleted and replaced by *LEU2.* After confirming the deletion of *adh1*∆::*LEU2* six clones were selected for screening, a*dh3*∆::*TRP1* (~1.5 kb) (**Fig 39A**) and a*dh2*∆::*URA3* which is ~1.5 kb in size (**Fig 40**).

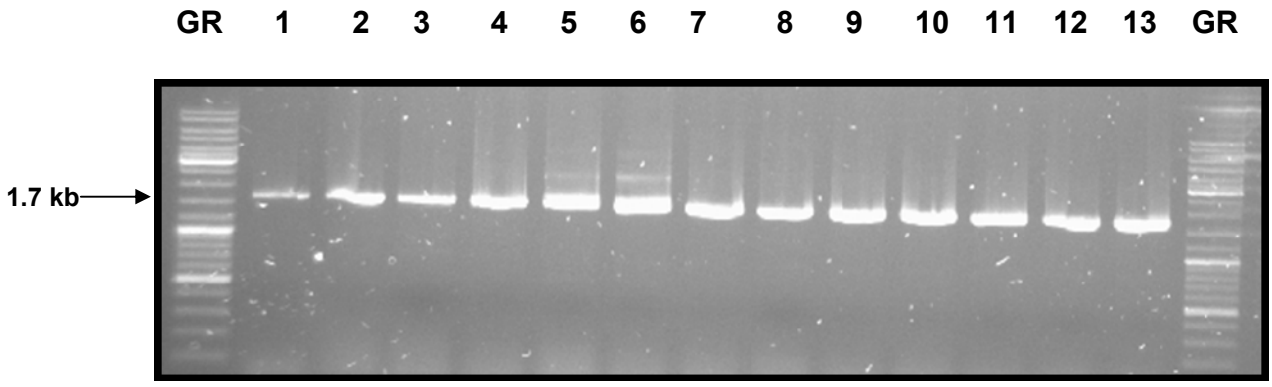

Fig 38: PCR profile of clones screened for a*dh1*∆::*LEU2* replacement. 1 kb DNA ruler (**GR**) and gel electrophoresis of clones screened for a*dh1*∆::*LEU2* (**lane 1 – 13**) delivering a ~1.7 kb fragment when amplified with *ADH1-2F*/LEU2-1R . Visualization of this band indicates the deletion of *ADH1* by replacing the gene with a selective marker (*LEU2*).

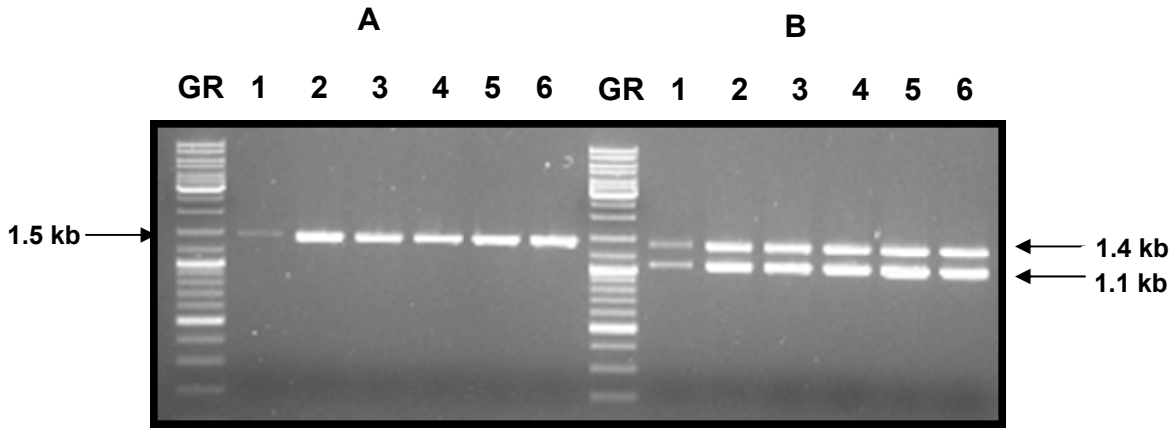

Fig 39: **A:** Gel electrophoresis illustrating PCR profiles of triple deletion mutant clones screened for the a*dh3*Δ::*TRP1* deletion (**A**) and intact *ADH4* and *ADH5* genes. **B:** Multiplex PCR reaction, containing primer sets to amplify *ADH1* – *ADH5* ORFs. As expected no amplification was visible for the *ADH1*, *ADH2* and *ADH3* genes, while the intact *ADH4* and *ADH5* genes were represented by amplicons of ~1.4 kb for *ADH4* and ~1.1 kb for *ADH5* in length respectively (**lane 1 – 6**).

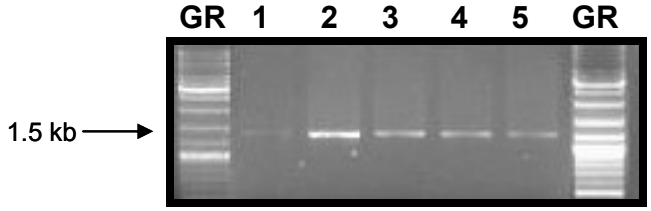

Fig 40: PCR results applied to genomic DNA extracted from triple deletion mutant, lacking *ADH1, ADH2* and *ADH3*. Primers were used to amplify the a*dh2*Δ::*URA3* deletion identified at ~1.5 kb. Visualization of this band indicates the deletion of *ADH2* by replacing the gene with a selective marker (*URA3*).

The final goal was to design a vector containing the *ADH5* open reading frame flanked on the 5' and 3' side with the *ADH1* promoter and terminator regions respectively. The flanking regions were amplified using a pGEM®-T Easy

plasmid containing the *ADH1* gene (De Smidt, 2007) as template. This resulted in a 5 kb construct containing the backbone of pGEM®-T Easy. 1 kb fragments upstream and downstream of *ADH1* (**Fig 41**). Primer combinations *ADH1*-MH-R (*Hin*dIII) and *ADH1*-MH-F (*Xba*I) were used to propagate the region. Thus through the PCR process *ADH1* was removed from the construct.

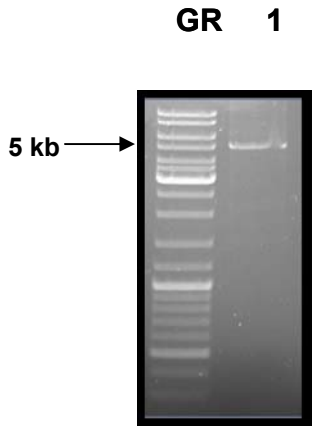

Fig 41: Gel electrophoresis illustrating PCR profiles using *ADH1*-MH-R (*Hin*dIII) and *ADH1*-MH-F (*Xba*I). 5 kb amplicon containing the 1 kb *ADH1* promoter region, 1 kb *ADH1* terminator region and pGEM®-T Easy backbone can be seen in (**lane 1**). DNA gene ruler (**GR**) (Fermentas).

The PCR product was purified, digested with *Dpn*I (to digest the template DNA), separated on an agarose gel, and purified with the Biospin gel extraction kit (Bioflux). *ADH5* was amplified with *ADH5*-Forward-*Hin*dIII and *ADH5*-Reverse-*Xba*I primers. Ligated into the PCR product produced in the above section. Delivering a ~6.1 kb product (3 kb pGEM®-T Easy backbone, 2 kb flanking regions and ~1.1 kb *ADH5*) when digested with *Xba*I and *Hin*dIII (**Fig 42**).

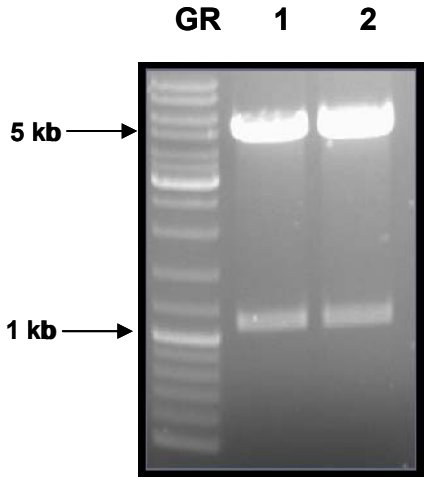

Fig 42: Gel electrophoresis of two clones (pGEM®-T Easy plus promoter, terminator and *ADH5* gene). The 5 kb band represents the pGEM®-T backbone illustrated in **Fig 41**. The *ADH5* gene is represented by the ~1.1 kb bands visualized in both **lanes 1** and **2.** DNA gene ruler (**GR**) (Fermentas).

The pRS vector series were used for expression of the target gene *ADH5* in *S. cerevisiae.* The two plasmids used, pRS413 which is a singlecopy plasmid and pRS423 a multicopy plasmid. The constructs were ligated into both the single and multicopy vectors and transformed into *S. cerevisiae TΔ123 (adh1, adh2, adh3* null). Cloning of the two products (*TΔ123*::*ADH5*_S and *TΔ123*::*ADH5*_M) was verified by digestion with *Bam*HI (**Fig 43**).

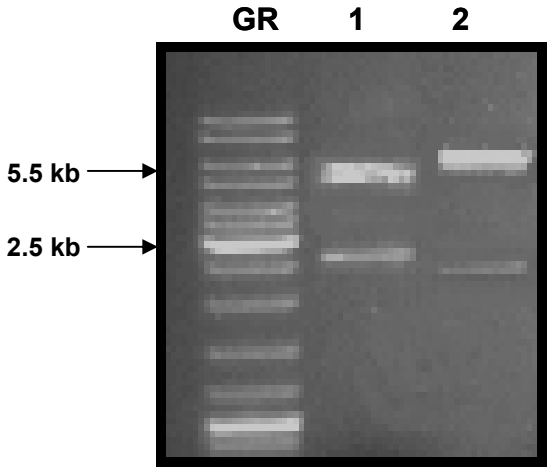

Fig 43: Gel electrophoresis of two clones after ligation into pRS413 and pRS423 respectively. Clones were digested with *Bam*HI. pRS413, delivered a ~2.5

kb and ~5.5 kb band respectively (**lane 1**). pRS423, delivered a ~2.1 kb and ~6.5 kb band respectively (**lane 2**).

The digestion of both products with *Bam*HI yielded a ~2.5 kb and a ~5.5 kb fragment for pRS413, and a ~2.1 kb and ~6.5 kb fragment for pRS423. Following confirmation of correct plasmid construction the single and multicopy plasmids were transformed into *S. cerevisiae TΔ123,* producing *S. cerevisiae TΔ123*::*ADH5*_singlecopy and *S. cerevisiae TΔ123*::*ADH5*_multicopy strains. These strains were subsequently used for growth studies. *In vitro* studies proved Adh5p less efficient than Adh1p, in both ethanol oxidation and acetaldehyde reduction. Thus the singlecopy pRS413 under regulation of the *ADH1* promoter will be less efficient than pRS423. The substrate utilization and the amount of substrate converted to product per second are substantially lower than that of Adh1p. Thus even when expressed at Adh1p levels the enzyme's efficiency will not be sufficient enough to have a dramatic effect on ethanol metabolism. pRS423 was used to monitor the cellular growth under over-expressed conditions. The completed vectors can be seen in **Fig 44** and **Fig 45**. Apart from the differences based on the yeast origin of replication both vectors are identical.

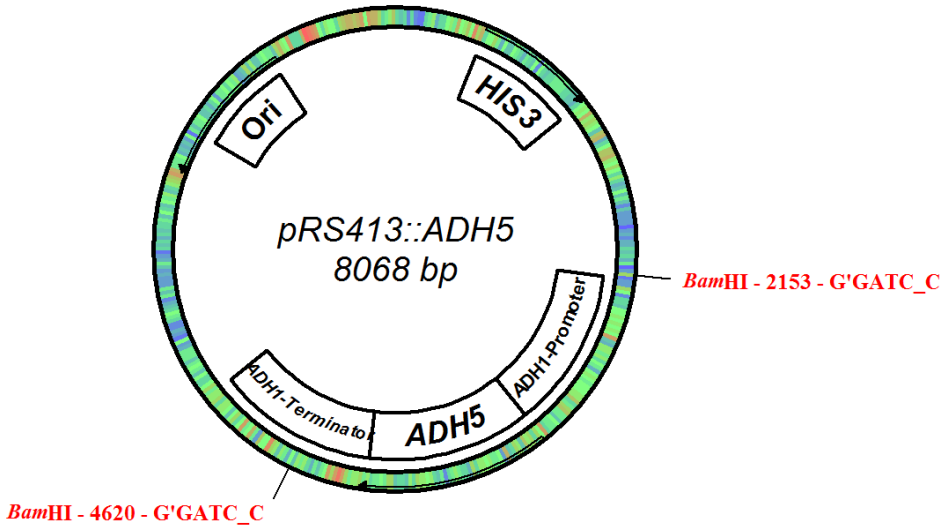

Fig 44: pRS413::*ADH5.* Finalized vector in circular configuration with *ADH5* flanked with the *ADH1* promoter and *ADH1* terminator regions. *HIS3* is the selective marker utilized by both pRS413 and pRS423. The transformed strain has the capability to grow in histidine-deficient media due to vector's capability for selection on histidine.

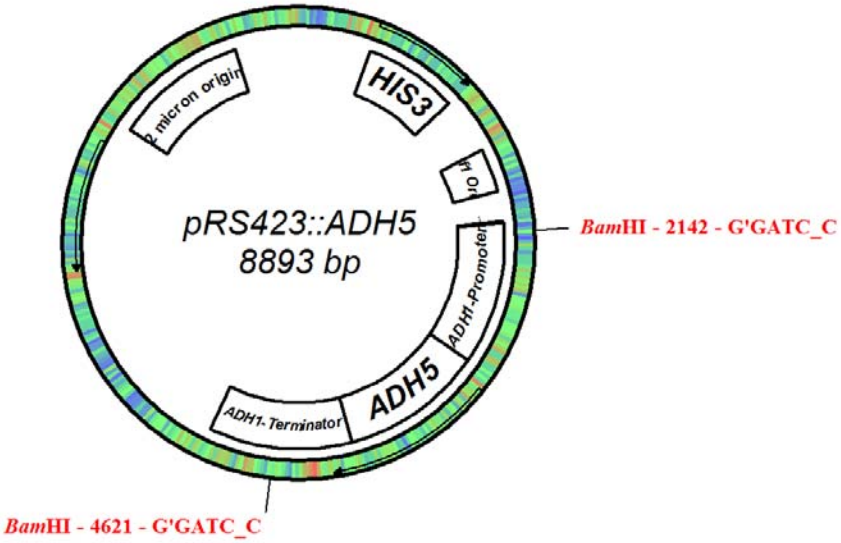

Fig 45: pRS423::*ADH5.* Finalized vector in circular configuration with *ADH5* flanked with the *ADH1* promoter and *ADH1* terminator regions. *HIS3* is the selective marker utilized by both pRS413 and pRS423. The transformed strain has the capability to grow in histidine-deficient media due to vector's capability for selection on histidine.

5 Growth studies

5.1 Shake flask cultivation

Shake flask cultivations were performed as described in Chapter 2 section 14. Data retrieved from shake flask cultivation clearly demonstrated that *S. cerevisiae* Q1, and *S. cerevisiae* W303-1A are capable of growth on both glucose and ethanol as carbon sources. Neither the pRS413::*ADH5* singlecopy (*S. cerevisiae T*Δ*123*::*ADH5*_S) nor pRS423::*ADH5* multicopy (*S. cerevisiae*

TΔ123::*ADH5*_M) strains showed any growth when compared to *S. cerevisiae* Q1 and *S. cerevisiae* W303-1A (**Fig 46**).

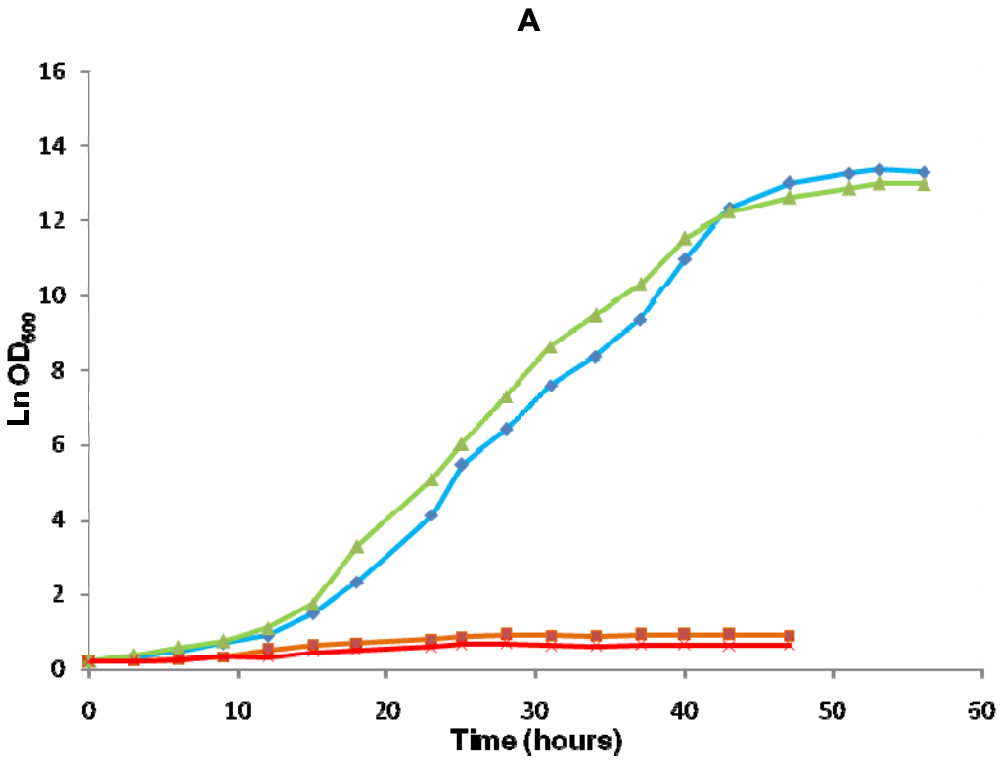

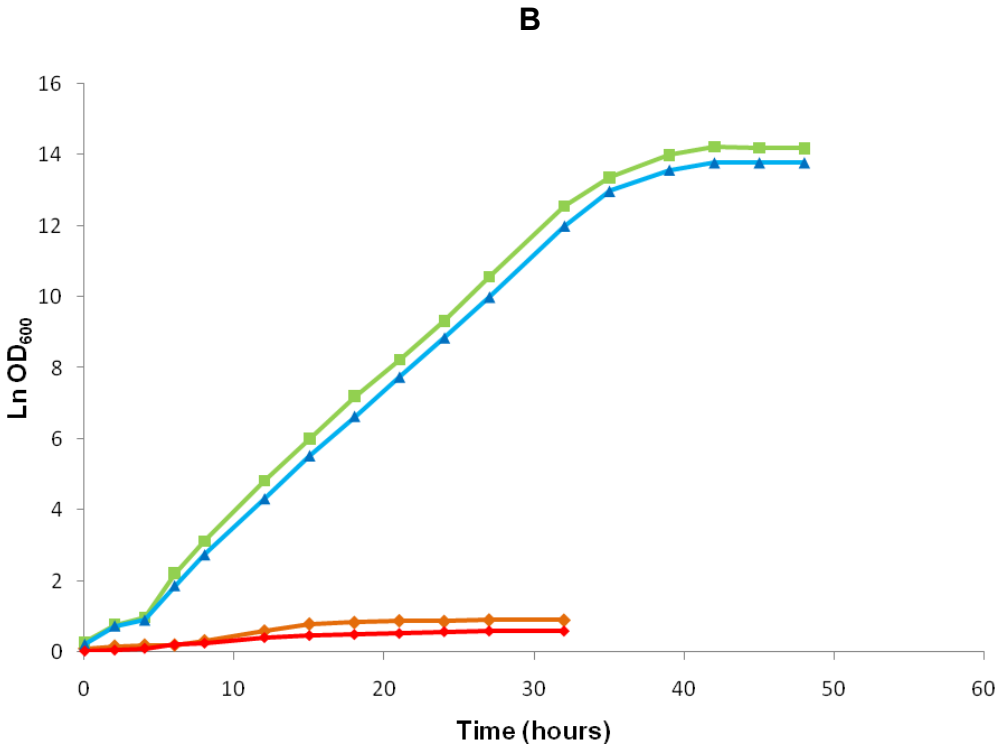

Fig 46: Growth profiles of *S. cerevisiae* W303-1A, *S. cerevisiae* Q1, *S. cerevisiae* *TΔ123*::*ADH5*_S and *S. cerevisiae* *TΔ123*::*ADH5*_M on glucose or ethanol as carbon sources. Strains were grown in chemically defined medium in shake flasks at 30°C. **A**: *S. cerevisiae* W303-1A (**green**), *S. cerevisiae* Q1 (**blue**), *S. cerevisiae* *TΔ123*::*ADH5*_S (**red**) and *S. cerevisiae* *TΔ123*::*ADH5*_M (**orange**) grown on 7 g l^{-1} ethanol. **B**: Illustrates growth of *S. cerevisiae* W303-1A (**green**), *S. cerevisiae* Q1 (**blue**), *S. cerevisiae* *TΔ123*::*ADH5*_S (**red**) and *S. cerevisiae* *TΔ123*::*ADH5*_M (**orange**) on 8 g l^{-1} glucose as carbon source.

5.2 Bioreactor cultivation

The Biostat B plus system was incorporated for growth of *S. cerevisiae* W303-1A, *S. cerevisiae* Q1, *S. cerevisiae* *TΔ123*::*ADH5*_S and *S. cerevisiae* *TΔ123*::*ADH5*_M. Growth was monitored under aerobic conditions with an oxygen transfer rate (pO_2) of 30%. The oxygen transfer rate was controlled by stirrer speed at 201 rpm. Growth was monitored on 7 g l^{-1} ethanol or 8 g l^{-1} glucose as carbon sources. The growth of *S. cerevisiae* W303-1A and *S. cerevisiae* Q1 on 7 g l^{-1} ethanol can be seen in **Fig 47**.

5.2.1 Growth on 7 g l^{-1} ethanol

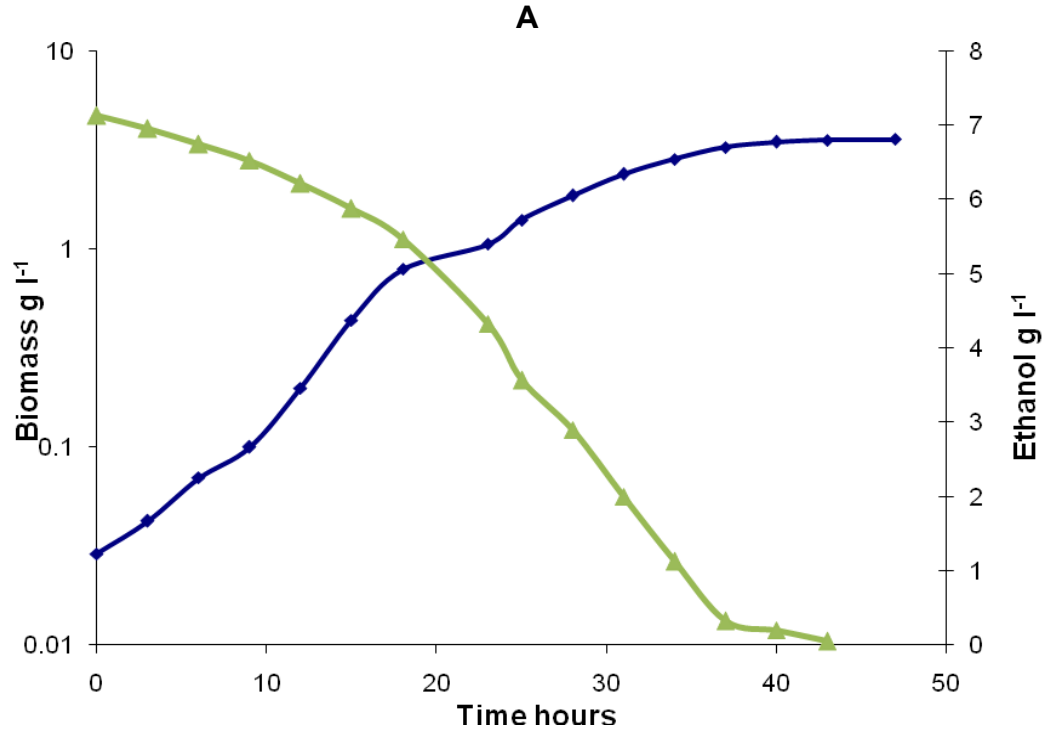

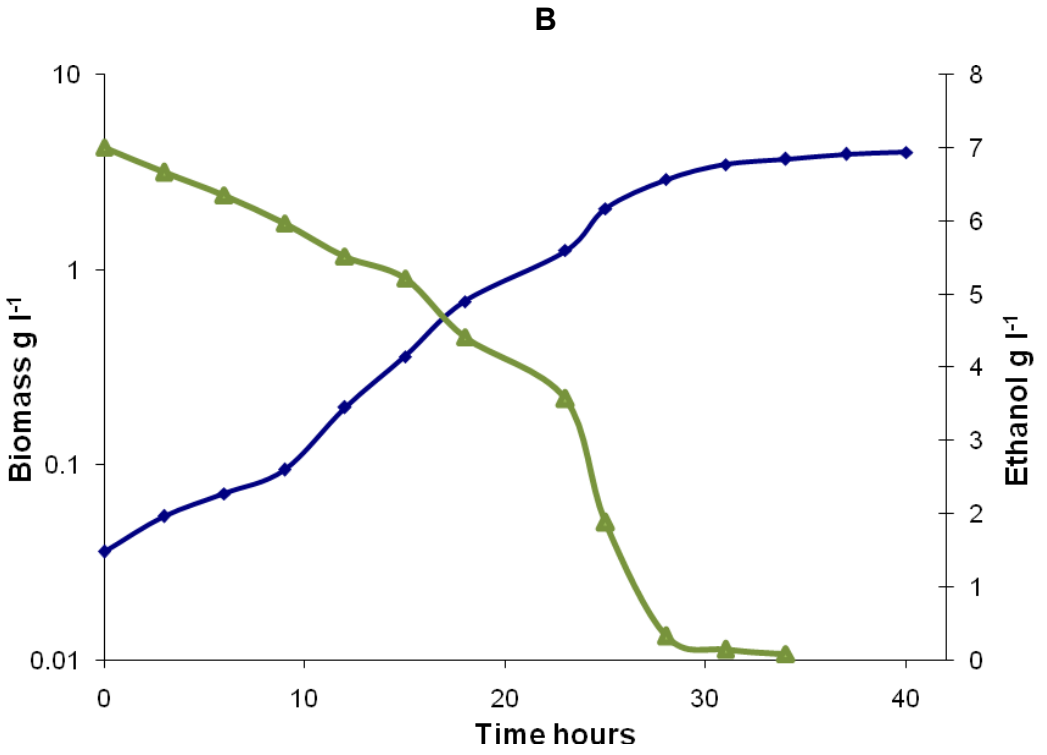

Fig 47: Curves **A+B** illustrate biomass (**blue**) over time, on ethanol (**green**) as carbon source. **A:** Growth of *S. cerevisiae* Q1 on ethanol as carbon source indicates an increase in biomass with a decrease in ethanol to approximately 0.07 g l^{-1}. **B**: Growth of *S. cerevisiae* W303-1A on 7 g l^{-1} ethanol, ethanol depletion takes place at a quicker rate than that of *S. cerevisiae* Q1.

Growth of *S. cerevisiae T∆123* strains, with expression under regulation of the *ADH1* promoter can be seen in **Fig 48**. Both *S. cerevisiae T∆123*::*ADH5*_S and *S. cerevisiae T∆123*::*ADH5*_M showed oxidation of ethanol. However, no comparison can be made when these data sets are compared to *S. cerevisiae* W303-1A and *S. cerevisiae* Q1 in **table 6**. Both these strains have low biomass yield coefficients, below 0.07g.

A

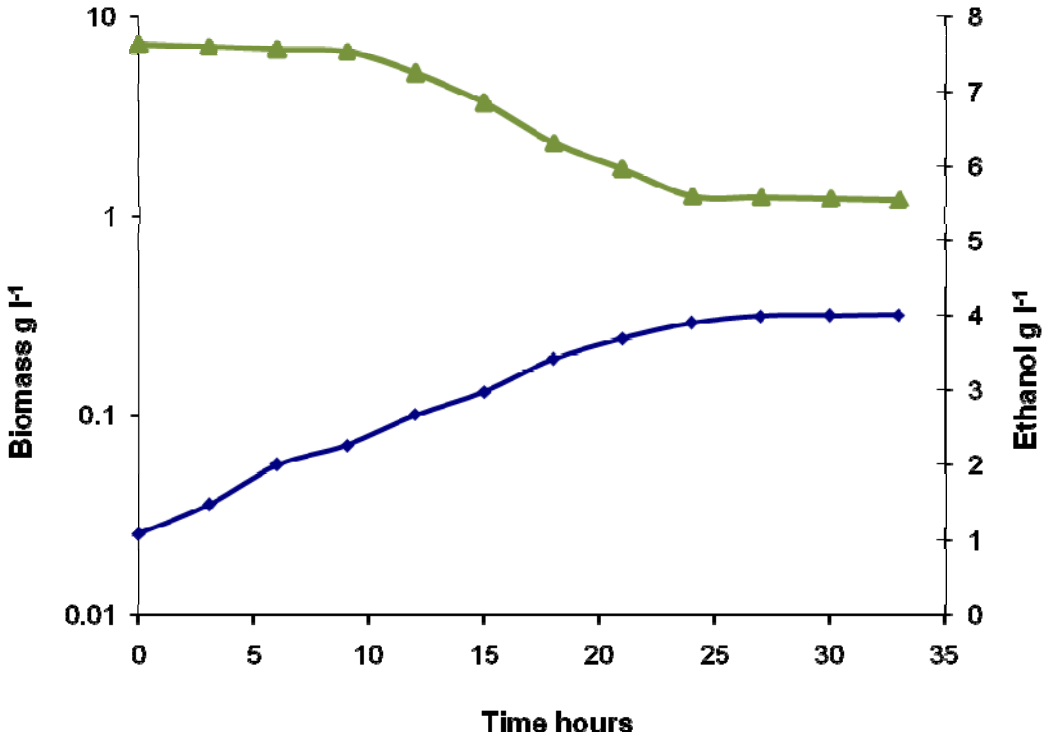

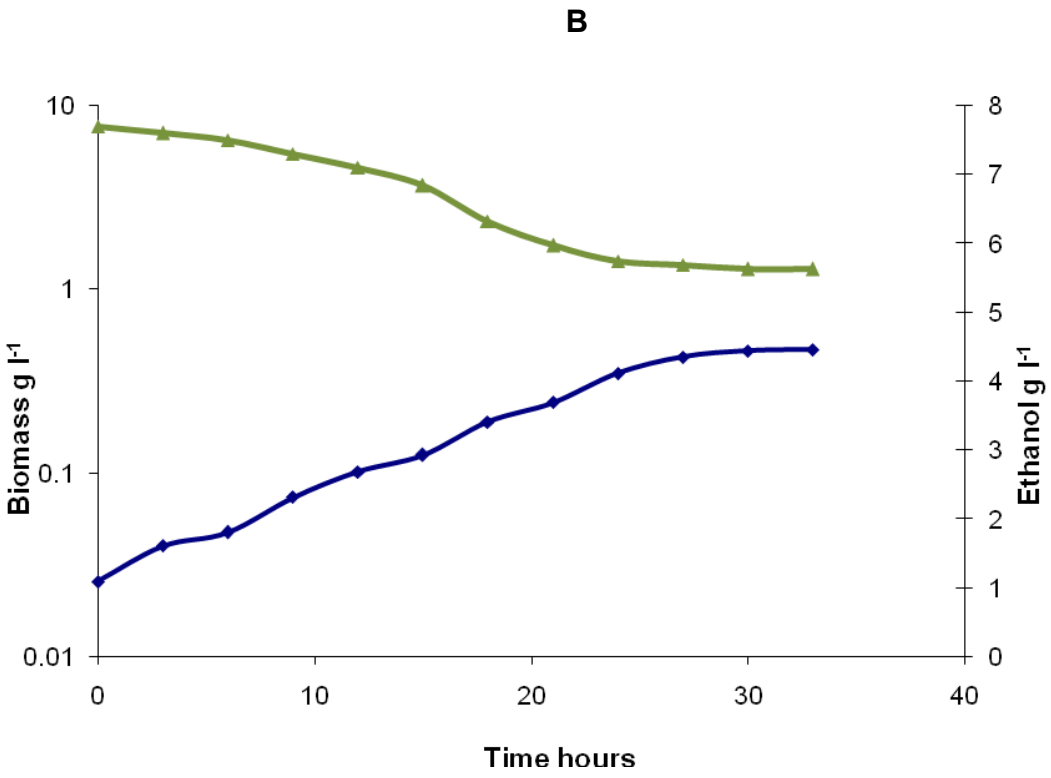

Fig 48: Graphs **A** and **B** represent the growth studies performed on both *S. cerevisiae T∆123*::*ADH5*_S and *S. cerevisiae T∆123*::*ADH5*_ M. **A:** Biomass formation (**blue**) and ethanol consumption (**green**) of *S. cerevisiae T∆123*::*ADH5*_S. Biomass yield is tenfold lower than that of *S. cerevisiae* W303-1A and *S. cerevisiae* Q1. 2 g of ethanol was utilized. **B:** Biomass formation (**blue**) and ethanol consumption (**green**) of *S. cerevisiae T∆123*::*ADH5*_M.

Table 6. *S. cerevisiae* strain W303-1A, *S. cerevisiae* Q1, *S. cerevisiae T∆123*::*ADH5*_S and *S. cerevisiae T∆123*::*ADH5*_M. Growth parameters are listed below.

	W303-1A	**Q1**	***T∆123::ADH5_S***	***T∆123::ADH5_M***
[1]$\mu_{max\ ethanol}$, h^{-1}	0.180	0.198	0.072 ± 0.003	0.091
[2]$Y_{x/s\ ethanol}$	0.569	0.5	0.04 ± 0.004	0.061 ± 0.007

[1] Maximum specific growth rate on carbon substrate stated, calculated by linear regression analysis of exponential growth data (μ_{max})
[2] Biomass yield coefficient (g dry biomass/g carbon substrate) ($Y_{x/s}$)

5.2.2 Growth on 8 g l^{-1} glucose

Growth curves of *S. cerevisiae* W303-1A and *S. cerevisiae* Q1 can be seen in **Fig 49**. The growth parameters can be seen in **table 7**. The graphs in **Fig 49** illustrate the formation of biomass with the depletion of glucose as carbon source. When the glucose drops below 7 g l^{-1} the ethanol pathway is activated and ethanol is consumed as primary carbon source. This continues into late exponential and stationary phase. Enzymes responsible for this process, Adh1p and Adh2p, are expressed in *S. cerevisiae* W303-1A (**A**). Adh1p is expressed in the *S. cerevisiae* Q1 (**B**).

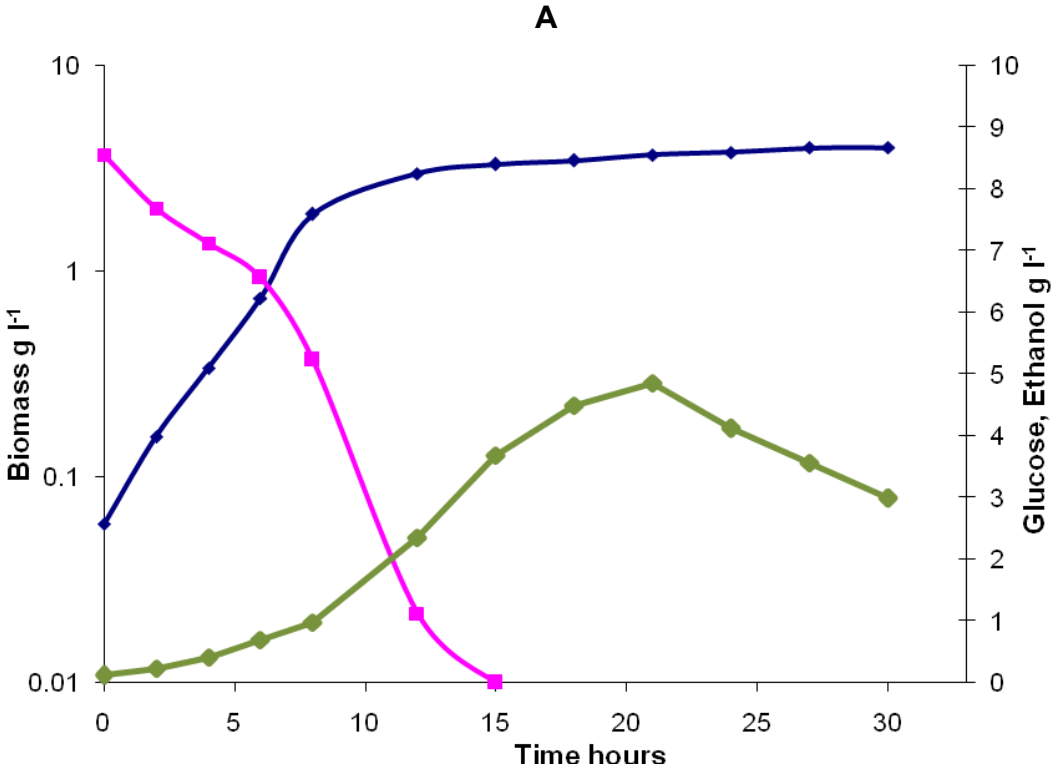

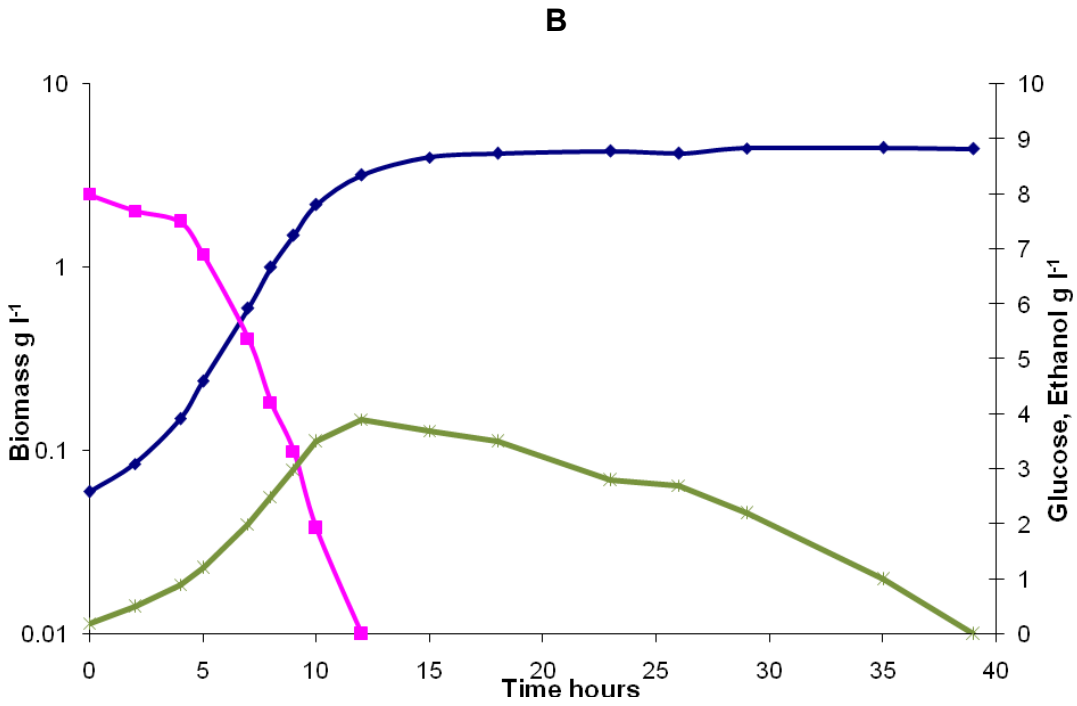

Fig 49: Graphs **A** and **B** represent the growth studies performed on both *S. cerevisiae* W303-1A and *S. cerevisiae* Q1 with 8 g l^{-1} glucose as carbon source. Biomass (**blue**) vs. ethanol (**green**) formation and glucose (**purple**) depletion. Ethanol pathway was activated as glucose concentration decreased. Adh1p and Adh2p are primarily responsible for the ethanol metabolism in *S. cerevisiae* W303-1A (**A**). Adh1p is responsible for the ethanol metabolism in *S. cerevisiae* Q1 (**B**).

Fig 49 results were compared to results retrieved from **Fig 50**. Both *S. cerevisiae T*Δ*123*::*ADH5*_S and *S. cerevisiae T*Δ*123*::*ADH5*_M, showed little to no resemblance to that of *S. cerevisiae* W303-1A or *S. cerevisiae* Q1 seen in (**Fig 50**). $\mu_{max,}$ biomass, ethanol and acetaldehyde yield coefficients can be seen in **table 7**.

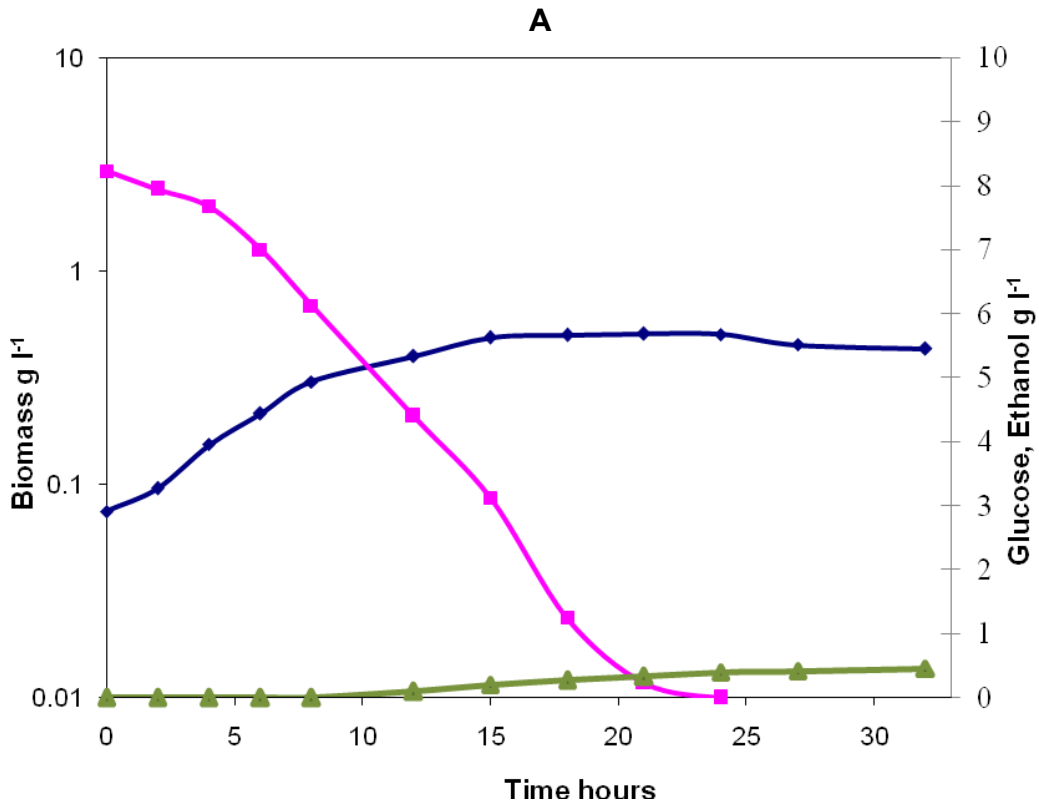
A
10
1
0.1
0.01
Biomass g l-1
10
9
8
7
6
5
4
3
2
1
0
Glucose, Ethanol g l-1
0
5
10
15
20
25
30
Time hours

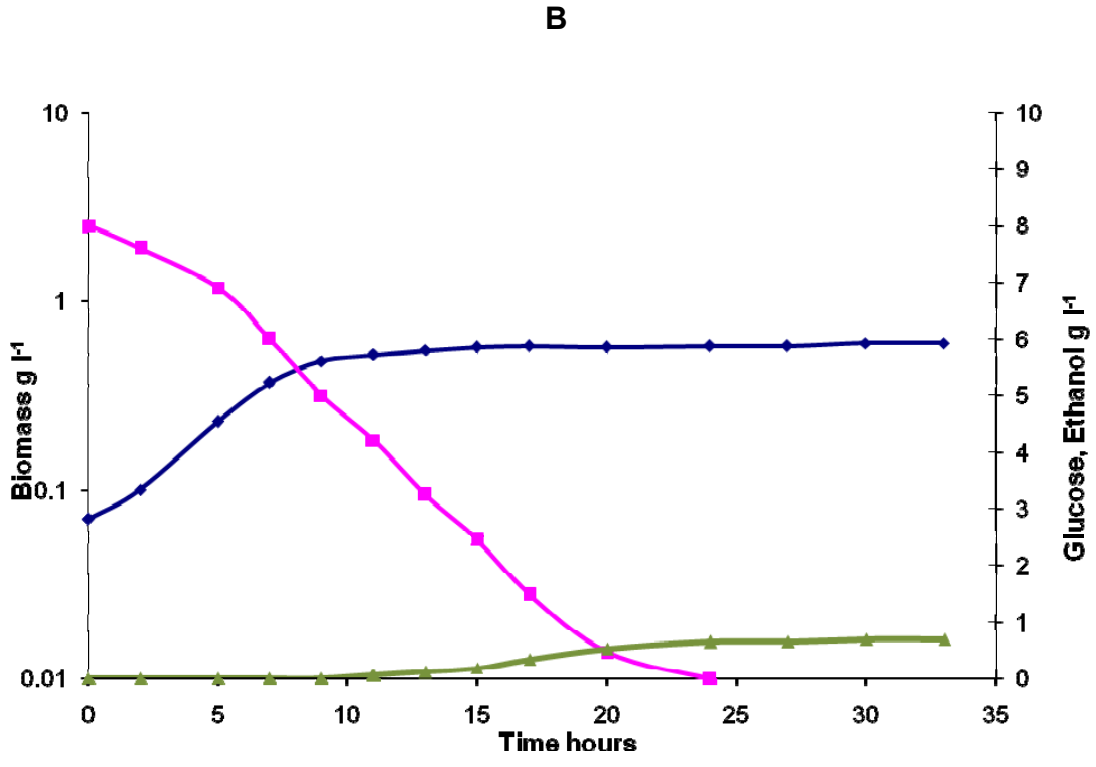
B
10
1
0.1
0.01
Biomass g l-1
10
9
8
7
6
5
4
3
2
1
0
Glucose, Ethanol g l-1
0
5
10
15
20
25
30
35
Time hours

Fig 50: Graphs **A** and **B** represent the growth studies performed on both *S. cerevisiae T∆123*::*ADH5*_S and *S. cerevisiae T∆123*::*ADH5*_ M, 8 g l^{-1} glucose as carbon source. Biomass (**blue**) vs. ethanol (**green**) formation and glucose (**purple**) depletion for both the singlecopy vector (**A**), and multicopy expression (**B**). Glucose depletion took place after approximately 20 hours, where max biomass yield was identified. Ethanol production started after 7 hours of incubation. The ethanol formation rate in the multicopy expression is slightly higher.

Acetaldehyde and glycerol analyses were performed on both *S. cerevisiae T∆123*::*ADH5*_S and *S. cerevisiae T∆123*::*ADH5*_M samples (**Fig 51**). The results can be seen in **Fig 51**. The accumulation of toxic acetaldehyde is a clear indication that Adh5p lacks the ability to reduce this toxic compound. Accumulation can lead to cellular death.

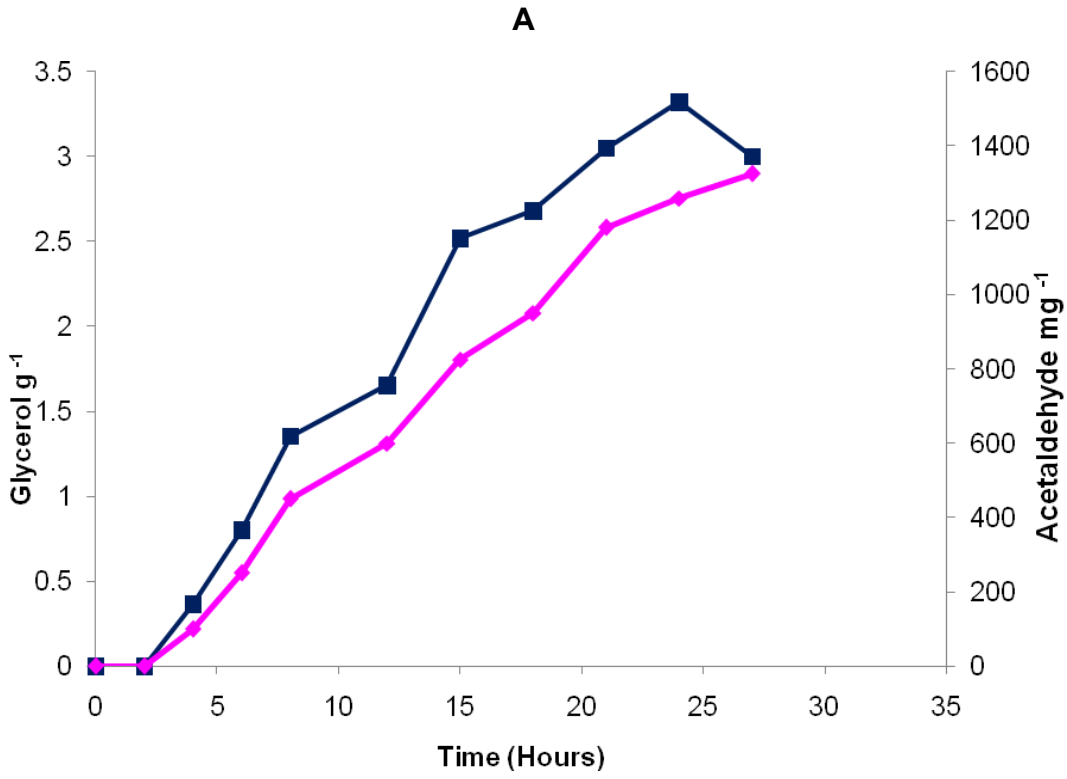

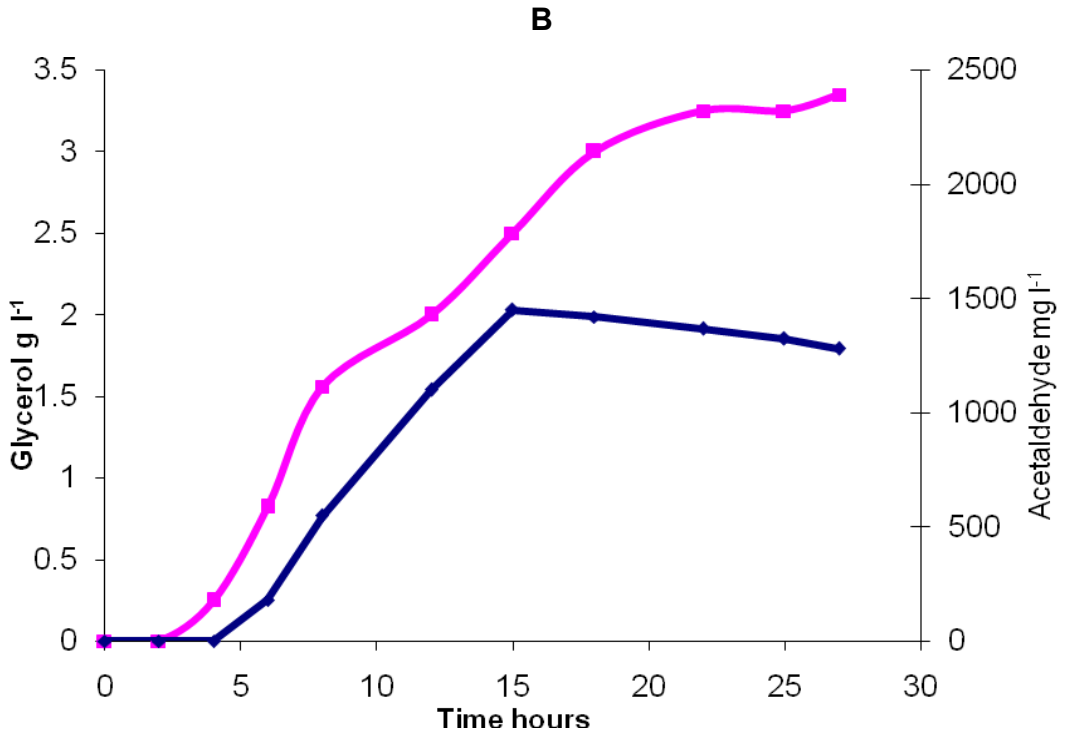

Fig 51: Analysis curves illustrating acetaldehyde (**blue**) and glycerol (**purple**) accumulation in both *S. cerevisiae T*Δ*123*::*ADH5*_S (**A**) and *S. cerevisiae T*Δ*123*::*ADH5*_ M (**B**). Acetaldehyde concentrations increased in both strains. A clear indication that acetaldehyde is being formed and not catalyzed by Adh5p. The glycerol concentrations also increased in both strains.

Table 7. Growth parameters of *S. cerevisiae* W303-1A, *S. cerevisiae* Q1, *S. cerevisiae T*Δ*123*::*ADH5*_S and *S. cerevisiae T*Δ*123*::*ADH5*_M in bioreactor batch cultures grown on glucose.

	W303-1A	***Q1***	***T*Δ*123::ADH5_S***	***T*Δ*123::ADH5_M***
[1]$\mu_{max\ glucose}$, h^{-1}	0.424	0.376	0.178 ± 0.004	0.207 ± 0.005
[2]$Y_{x/s\ glucose}$	0.277	0.255	0.030 ± 0.007	0.050 ± 0.001
[2]$Y_{x/s\ ethanol}$	0.338	0.400	1.106 ± 0.01	0.717 ± 0.03
[3]$Y_{ethanol/s}$	0.365	0.351	0.055 ± 0.008	0.083 ± 0.004
[4]$Y_{acetaldehyde/s}$	ND	ND	0.180 ± 0.001	0.118 ± 0.003

Maximum specific growth rate on carbon substrate stated, calculated by linear regression analysis of exponential growth data (μ_{max})

[2] Biomass yield coefficient (g dry biomass/g carbon substrate) ($Y_{x/s}$)

[3] Ethanol yield coefficient (g ethanol produced/g glucose assimilated)

[4] Acetaldehyde yield coefficient (g acetaldehyde produced/g glucose assimilated)

Adhp expression was verified at various time intervals. Cells were lysed and enzyme activity was tested on the crude extract. Protein concentrations of *S. cerevisiae* Q1, *S. cerevisiae* *TΔ123*::*ADH5*_S and *S. cerevisiae* *TΔ123*::*ADH5*_M were determined and compared. The relative activity was compared to the respective biomass yield of each strain.

Table 8. Expression of Adh5p and Adh1p on ethanol and glucose as carbon sources respectively.

	Q1	***TΔ123::ADH5_S***	***TΔ123::ADH5_M***
	Adh1p	**Adh5p**	**Adh5p**
[1][E] $_{EtOH}$ ($\mu g.ml^{-1}$)	279.844	192.887	228.145
[1][E] $_{Glu}$ ($\mu g.ml^{-1}$)	300.056	150.126	178.326
[2][E] $_{EtOH}$ ($\mu g.ml^{-1}$)	300.541	195.654	285.558
[2][E] $_{Glu}$ ($\mu g.ml^{-1}$)	315.234	139.261	186.321
[3]Biomass yield	3.65	0.31	0.47
[4]**Biomass yield**	4.00	0.5	0.61

[1]Protein concentrations at time 15 hours for Q1, singlecopy expression and multicopy expression on ethanol as carbon source
[2]Protein concentrations at time 21 hours for Q1, singlecopy expression and multicopy expression on ethanol as carbon source
[3]Max biomass yields on ethanol
[4]Max biomass yields on glucose

Growth studies performed on *S. cerevisiae* W303-1 and *S. cerevisiae* Q1 showed high biomass yields. Furthermore, both these strains were capable of growth on ethanol as carbon source. Together with the production ethanol when glucose levels become insufficient. In accordance with De Smidt, 2007, Adh1p is capable of ethanol metabolism in the absence of other Adh proteins. This can be seen in data reported on *S. cerevisiae* Q1 in this study.

Growth of *S. cerevisiae* *TΔ123*::*ADH5*_S and *S. cerevisiae* *TΔ123*::*ADH5*_M under aerobic conditions showed low biomass yields. Biomass yield on ethanol as carbon source was tenfold lower than *S. cerevisiae* Q1. Enzyme activity was tested for both Adh5p and Adh1p. In both cases protein was active and capable of oxidizing ethanol. However, studies shown in this thesis proved the lack of

Adh5p's ability to reduce toxic acetaldehyde to ethanol. A total of 2 g ethanol was utilized, and 0.2 g was produced. Increased acetaldehyde concentrations were the dominant factor that leads to cellular death. *In vitro* studies concluded that Adh5p is capable of oxidizing ethanol to acetaldehyde. However, the catalytic efficiency per unit enzyme is much lower than Adh1p and Adh2p. The amount of substrate converted to product in the second order reaction for Adh5p is less than that of Adh1p.

In vivo studies proved that Adh5p cannot maintain cellular homeostasis when introduced as sole enzyme responsible for ethanol metabolism. Biomass was harvested and cells were lysed to determine protein concentrations in *S. cerevisiae* Q1, *S. cerevisiae T∆123*::*ADH5*_S and *S. cerevisiae T∆123*::*ADH5*_M. Protein concentration can be seen in **table 8**. Although it is not the most accurate method it still indicates a clear relationship between the expression levels.

Chapter 4: Summary

In the past few decades much research has been conducted on yeast alcohol dehydrogenases with emphasis on their role in *S. cerevisiae*. There are seven known Adh proteins that were identified in *S. cerevisiae*. Six of them are intensively studied on gene and translational level. After sequencing of *S. cerevisiae* chromosome II (Feldman et al. 1994), *ADH5* was identified which is 76% and 77% identical to *ADH1* and *ADH2* respectively. Later studies on global localization on genes showed that *ADH5* is localized in the cytoplasm (Hue et al. 2003). No further research has been performed on *ADH5*.

In this study Adh5p was over-expressed, purified and characterized towards its primary substrate, ethanol, and preferred co-factor NAD^+. Furthermore, in-depth kinetic studies were performed using various alcohols, increasing in chain length and branching. Adh5p is capable of oxidizing alcohols from two carbons to ten carbons. However, the catalytic efficiency decreases with increasing chain length. Results showed that Adh5p functions *in vitro* the same as Adh1p and Adh2p, sharing a primary substrate (ethanol). Adh1p and Adh2p are capable of converting more substrate per unit enzyme per second Adh5p.

The second part of this study was to determine if Adh5p could substitute the catalytic function of Adh1p *in vivo*. For this purpose, *ADH5* expression needed to be similar to Adh1p levels in the cell. Thus an expression vector was used containing *ADH5* gene flanked with the promoter and terminator regions of *ADH1*. *S. cerevisiae T∆123* was constructed with *ADH4* and *ADH5* still intact. *S. cerevisiae T∆123* was transformed with a pRS413 and pRS423 construct containing the *ADH1* promoter and terminator fused to the *ADH5* ORF. Growth was monitored in chemically defined media containing 7 g l^{-1} ethanol or 8 g l^{-1} glucose. Growth parameters were also compared to the *S. cerevisiae* W303-1A and the *adh* quadruple deletion strain (Q1) containing only *ADH1*. The *S. cerevisiae T∆123*::*ADH5*_S and *S. cerevisiae T∆123*::*ADH5*_M constructs were capable of limited growth on both glucose and ethanol as carbon sources.

When comparing the biomass yield of *S. cerevisiae T∆123*::*ADH5*_S and *S. cerevisiae T∆123*::*ADH5*_M to the biomass yield for both *S. cerevisiae* W303-1A and *S. cerevisiae* Q1 the constructs delivered a much lower biomass yield. To verify the expression of Adh5p, a Micro BCA™ protein assay kit supplied by Pierce (Smith et al. 1985) was used. Protein concentrations were determined at various time intervals. Cell homogenization was standardized, *S. cerevisiae* Q1 cells were diluted to fit the OD_{600} obtained for both the *S. cerevisiae T∆123*::*ADH5*_S and *S. cerevisiae T∆123*::*ADH5*_M strains.

To conclude, Adh5p is capable of oxidizing various alcohols, but ethanol is its primary substrate. Furthermore Adh5p is not capable of replacing Adh1p in cellular metabolic function. The low turnover number illustrated by Adh5p and the lack thereof to reduce acetaldehyde is the most prominent cause of cellular death. Unlike Adh1p, Adh5p is not capable of reducing acetaldehyde to ethanol and thus not capable of NAD^+ - NADH regeneration.

Chapter 5: Opsomming

Gedurende die afgelope paar jaar is daar baie navorsing gedoen op gis *ADH*, hoofsaaklik die van *S. cerevisiae*. Daar is tans sewe *ADH's* geïdentifiseer in *S. cerevisiae*, ses van die sewe is reeds gekarakteriseer en baie navorsing is reeds gedoen op *geen* vlak. Dit was egter na Feldman en sy kollegas in 1994 bevestig het dat een van die *ADH's (ADH5)*, wat tot op hede nog geen navorsing op gedoen is nie, sekere verwantskappe deel met Adh1p en Adh2p, op basispaaropeenvolgende vlak, naamlik 76% en 77%. Geen navorsing was tot op hede op *ADH5* gedoen nie.

In hierdie studie was Adh5p uitgedruk en gekarakteriseer teenoor die proteïen se primêre substraat, naamlik etanol en ko-faktor naamlik NAD^+. Diepgaande studies was uitgevoer op verskeie ander substrate, alkohole wat se koolstof lengte toeneem vanaf twee tot tien koolstof atome. Hoe langer die alkohol, hoe vinniger neem die effektiwiteit van die ensiem af. Resultate wys dat Adh5p dieselfde funksioneer as Adh1p en Adh2p. Die hoof- en kritieke verskil is dat Adh1p en Adh2p die vermoë besit om meer substraat per eenheid ensiem om te skakel per sekonde as Adh5p, en is dus baie meer effektief is as Adh5p.

Die tweede helfte van die studie was om te bepaal of Adh5p die funksie van Adh1p kan oorneem *in vivo*. *ADH5* uitdrukkingsvlakke moes dus verhoog word sodat dit vergelykbaar kan wees met *ADH1* vlakke. 'n Uitdrukkingsplasmied was gemaak wat die *ADH5* geen bevat, gekoppel aan die promotor en termineerder gebiede van *ADH1*. Die konstruk was in die *T∆123* mutant in getransformeer. Die getransformeerde gisstam, *S. cerevisiae T∆123*::*ADH5*_S en *S. cerevisiae T∆123*::*ADH5*_M, was daaropvolgend gebruik om die groeikromme te monitor in chemies gedefinieerde medium. Die media het 7 g l^{-1} etanol of 8 g l^{-1} glukose bevat. Groeiparameters van die delesiekonstrukte was vergelyk met *S. cerevisiae* W303-1A en *S. cerevisiae* Q1 stamme.

Wanneer daar vergelykinge getref word tussen die biomassa-opbrengs van albei verwysingsstamme en die delesiekonstrukte kan daar afgelei word dat die biomassa-opbrengs van die konstrukte sowat tien maal laer is. Proteïen konsentrasies was op verskeie tydsintervalle geneem om sodoende die hoeveelheid proteïen in elke stam te kan vergelyk. Die konsentrasies van al die stamme waar Adh1p uitgedruk is, was vergelykbaar met die van die konstrukte.

Om saam te vat, Adh5p is wel in staat daarvan om verskeie alkohole te oksideer, maar etanol is wel die primêre substraat. Adh5p is nie in staat om asetaldehied te reduseer nie en dus lei dit tot ‘n toename van die toksiese produk wat lei tot die afsterwing van die sel. Adh5p kan dus nie NAD^+ - NADH herwin nie, maar speel tog ’n belangrike rol in etanol metabolisme sodat gisselle onder optimum kondisies kan funksioneer.

References

Bakker, B., Bro, C., Kotter, P., Luttik, M. A. H., van Dijken, J. P. and Pronk, J. T. (2000). The Mitochondrial Alcohol Dehydrogenase Adh3p Is Involved in a Redox Shuttle in *Saccharomyces cerevisiae. Journal of bacteriology*. **2000**, 4730–4737.

Bennetzen, J. and Hall, B. D. (1982). The primary structure of the *Saccharomyces cerevisiae* gene for alcohol dehydrogenase. *The journal of biological chemistry*. **257**, 3018 – 3025.

Blumberg, H., Eisen, A., Sledziewski, A., Bader, D. and Young, E. T. (1987). Two Zinc fingers of a yeast regulatory protein shown by genetic evidence to be essential for its function. *Nature*. **328**, 443 – 445.

Branden, C., Jornvall, H., Eklund, H. and Furugren, B. (1975). Alcohol dehydrogenase, in The Enzymes (Boyer, P. D, ed) 3rd edn. **11**, 103 – 190. *Academic Press, New York.*

Brzezinski, B. and Zundel, G. (1996). The role of water and proton transfer processes in hydrogen-bonded chains with large proton polarizability. *Faraday Discuss Chemical Society.* **103**, 363 – 370.

Chen, D. C., Yang, B. C. and Kuo, T. T. (1992). One-step transformation of yeast in stationary phase. *Current Genetics*. **21,** 83-84.

Cook, P. F. and Cleland, W. W. (1981). pH variation of isotope effects in enzyme-catalyzed reactions. *Biochemistry.* **20**, 1797 - 1805.

De Bolle, X., Vinals, C., Fastrez, J. and Feytmans, E. (1997). Bivalent cations stabilize yeast alcohol dehydrogenase I. *Biochemical Journal*. **323**, 409 – 413.

De Smidt O. (2007). Molecular and physiological aspects of alcohol dehydrogenases in the ethanol metabolism of *Saccharomyces cerevisiae.* Ph.D. thesis, University of the Free State.

Dickinson, F. M. and Dack, S. (2001). The activity of yeast ADH1 and ADHII with long-chain alcohols and diols. *Chemico-biological interactions*. 130 - 132, 417 – 423.

Dickinson, J. R., Eshantha, L., Salgado, J. and Hewlins, M. J. E. (2003). The catabolism of amino acids to long chain and complex alcohols in *Saccharomyces cerevisiae. The journal of biological chemistry*. **10**, 8028 – 8034.

Dickinson, F. M. and Monger, G. P. (1972). A study of the kinetics and mechanism of yeast alcohol dehydrogenase with a variety of substrate. *Biochemical Journal*. **131,** 261 – 270.

Drewke, C. and M. Ciriacy. (1988). Over-expression, purification and properties of alcohol dehydrogenase IV from *Saccharomyces cerevisiae*. *Biochimica et Biophysica Acta*. **950,** 54 -60.

Eckert, M. and Zundel, G. (1988). Energy surface and proton polarizability of hydrogen-bonded chains: an ab initio treatment with respect to the charge conduction in biological systems. *Journal of Physical Chemistry.* **92**, 7016 – 7023.

Ehrt, S. and Schnappinger, D. (2003). Isolation of Plasmids from *E. coli* by Boiling Lysis. *Humana Press*. **235,** 79 – 82.

Entian, K. D. and Kotter, P. (1998). Yeast mutants and plasmid collections. Yeast gene analysis, *Academic Press*. **26,** 431 – 449.

Fairbanks, G., Steck, T. L. and Wallach, D. F. H. (1971). Electrophoretic analysis of the major polypeptides of the human erythrocyte membrane. *Biochemistry*. **10**, 2606 – 2617.

Fan, F. and Plapp, B. V. (1999). Probing the affinity and specificity of alcohol dehydrogenase 1 for co-enzyme. *Biochemistry and Biophysics*. **367**, 240 – 249.

Feldmann, H., Aigle, M., Aljinovic, G., Andre, B., Baclet, M. C., Barthe, C., Baur, A., Becam, A. M., Biteau, N., Boles, E., et al. (1994). Complete DNA sequence of yeast chromosome II. *EMBO Journal* **13,** 5795 – 5809.

Ganzhorn, A. J., Green, D. W., Hershey, A. D., Gould, R. M and Plapp, B. V. (1987). Kinetic characterization of yeast alcohol dehydrogenase. Amino acid residue 294 and substrate specificity. *The journal of biological chemistry*. **262**, 3754 – 3761.

Gonzalez, E., Fernandez, M. R., Larroy, C., Sola, L., Pericas, A. M., Pares, X. and Biosca, J. A. (2000). Characterization of a (2R,3R)-2.3-Butanediol dehydrogenase as the *Saccharomyces cerevisiae YAL060W* gene product. *The journal of biological chemistry*. **275,** 35876 – 35885.

Harris, J. I. (1964)**.** The structure and catalytic activity of thiol dehydrogenases. *Structure and activity of enzymes.* (Goodwin TW, Harris, J. I and Hartley, B. S, eds), 97 – 109. *Academic Press,* New York.

Heick, H. M. C., Willemot, J. and Begin-heick, N. (1969). The subcellular localization of alcohol dehydrogenase activity in baker's yeast. *Biochimica et Biophysica Acta*. **191,** 493–501.

Hue, W. K., Falvo, J. V., Gerke, L. C, Carroll, A. S, Howson, R. W., Weissman, J. S. and O'Shea, E. K. (2003). Global analysis of protein localization in budding yeast. *Nature.* **425,** 686 – 691.

Jornvall, H. (1994). The alcohol dehydrogenase system. In Towards a Molecular Basis of Alcohol Use and Abuse (Jansson, B., Jornvall, H., Rydberg, U., Terenius, L. and Vallee, B. L., eds.), 221 - 229, Birkhauser Verlag, Basel.

Jornvall, H., Persson, M. and Jeffery, J. (1981). Alcohol and polyol dehydrogenases are both divided into two protein types, and structural properties cross-relate the different enzyme activities within each type. *Proceedings of National Academy of Sciences USA.* **78,** 4226–4230.

Jornvall, H. (1977). Differences between alcohol dehydrogenases. Structural properties and avolutionary aspects. *European Journal of Biochemistry*. **72,** 443 – 452.

Kallberg, Y., Oppermann, U., Jornvall, H. and Persson, B. (2002). Short-chain dehydrogenase / reductases (SDRs). Coenzyme-based functional assignments in completed genomes. *FEBS*. **269**, 4409 – 4417.

Keller, B., Volkmann, A., Wilckens, T., Moeller, G. and Adamski, J. (2006). Bioinformatic identification and characterization of new member of short-chain dehydrogenase/reductase superfamily. *Molecular and cellular endocrinology*. **248**, 56 -60.

Klinman, J. P. (1974). Acid-based catalysis in yeast alcohol dehydrogenase reaction. *The journal of biological chemistry***. 7**. 2569 – 2573.

Labuschagne, M. and Albertyn, J. A. (2007). Cloning of an epoxide hydroxylase-encoding gene from *Rhodotorula mucilaginosa* and functional expression in *Yarrowia lipolytica*. *Yeast.* **24**, 69-78.

Larroy, C., Fernendez, M. R., Gonzalez, E., Pares, X. and Biosca, J. A. (2002a). Characterization of the *Saccharomyces cerevisiae YMR318C (ADH6)* gene product as a broad specificity NADPH-dependent alcohol dehydrogenase: relevance in aldehyde reduction. *Biochemical Journal*. **361**, 163 – 172.

Larroy, C., Pares, X. and Biosca, J. A. (2002b). Characterization of a *Saccharomyces cerevisiae* alcohol dehydrogenase (ADHVII), a member of the cinnamyl alcohol dehydrogenase family. *European Journal of Biochemistry.* **269**, 5738 – 5745.

Leskovac, L., Trivi, S. and Anderson, B. M. (1998). Use of competitive dead-end inhibitors to determine the chemical mechanism of action of yeast alcohol dehydrogenase. *Molecular and Cellular Biochemistry.* **178,** 219–227.

Leskovac, V., Trivic, S. and Pericin, D. (2002). The three Zinc-containing alcohol dehydrogenases from baker's yeast, *Saccharomyces cerevisiae. FEMS* yeast research. **2**, 481 – 494.

Lutstorf, U. and Megnet, R. (1968). Multiple forms of alcohol dehydrgenase in *Saccharomyces cerevisiae.* I. Physiological control of ADH-2 and properties of ADH-2 and ADH-4. *Archives of Biochemistry and Biophysics.* **126**, 933 – 944.

Magonet, E., Hayen, P., Delforge, D., Delaive, E. and Remacle, J. (1992). Importance of the structural Zinc atom for the stability of yeast alcohol dehydrogenase. *Biochemical Journal*. **287**, 361 – 365.

Mahler, H. R. and Douglas, J. (1957). Mechanism of enzyme-catalyzed oxidation-reduction reactions. I. An Investigation of the yeast alcohol dehydrogenase reaction by means of the isotope rate effect. *Journal of the American Chemical Society.* **79**, 1159 – 1166.

Marcinkeviciene, L., Bachmatova, I. and Meškys, R. (2006). Stability, activity and substrate specificity of alcohol dehydrogenases in media containing organic solvents. *BIOLOGIJA*. **3**, 38 – 42.

Mathews, C. K., van Holde, K. E. and Ahern, K. G. (2000). Biochemistry third edition. *Addison Wesley Longman.*

Men, L. and Wang, Y. (2006). The oxidation of yeast alcohol dehydrognase 1 by hydrogen peroxide *in vitro*. *Journal of proteome research*. **6**, 216 – 225.

Merril, C. R. (1990). Silver staining of proteins and DNA. *Nature*. **343**, 779 – 780.

Murali, C. and Creaser, E. H. (1986). Protein engineering of alcohol dehydrogenase 1. Effects of two amino acid changes in the active site of yeast ADH1. IRL. *Press limited Oxford England*.

Nadolny, C. and Zundel, G. (1997). Fourier transform infrared spectroscopic studies of protin transfer processes and the dissociation of Zn2+ bound water in alcohol dehydrogenases. *FEBS*. **247**, 914 – 919.

Nishimura, A.,Morita, A., Nishimura, Y. and Sugino, Y. (1990). A rapid and highly efficient method for preparation of competent *Escherichia coli* cells. *Nucleic Acid Research* **18:20**, 6169.

Orgel, L. E. (1960). An introduction to transition-metal chemistry: ligand-field theory. *John Wiley and Sons.*

Russell, D. W., Smith, M., Williamson, V. M. and Young, E. T. (1983). Nucleotide sequence of the yeast alcohol dehydrogenase II gene. *The journal of biological chemistry*. **258,** 2674 – 2682.

Sambrook, J. and Russell, D. W. (2001). Preparation of Plasmid DNA by Large-scale Boiling Lysis. *Molecular Cloning, 3rd edition*.

Schopp, W. and Aurich, H. (1976). Kinetics and reaction mechanism of yeast alcohol dehydrogenase with long chain primary alcohols. *Biochemical Journal.* **157,** 15 – 22.

Smith, P. K., Krohn, R. I., Hermanson, G. T., Mallia, A. K., Gartner, F. H., Provenzano, M. D., Fujimoto, E. K., Goeke, N. M., Olson, B. J. and Klenk, D. C. (1985). Measurements of protein using bicinchoninic acid. *Analytical Biochemistry.* **150**, 76 – 85.

Sund, H. and Theorell, H. (1963). Alcohol dehydrogenases. 25–83. *In* P. D. Boyer, H. Lardy, and K. Myrba¨ck (ed.), The enzymes, 2nd ed., vol. 7. *Academic Press*, London, United Kingdom.

Tamura, K., Dudley, J., Nei, M. and Kumar, S. (2007). *MEGA4*: Molecular Evolutionary Genetics Analysis (MEGA) software version 4.0. *Molecular Biology and Evolution.* **24**, 1596-1599.

Thomas, J. and Rothstein, R. (1989). Elevated recombination rates in transcriptionally activated DNA. *Cell.* **56**, 619-630.

Thompson, J. D., Gibson, T. J., Plewniak, F., Jeanmougin, F. and Higgins, D. G. (1997). The ClustalX windows interface: flexible strategies for

multiple sequence alignment aided by quality analysis tools. *Nucleic Acids Research.* **25**, 4876-4882.

Thomson, J. M., Burgan, M. F., De Kee, W. D., Li, T., Aris, J. P. and Benner, S. A. (2005). Resurrecting ancestral alcohol dehydrogenases from yeast. *Nature genetics*. **37**, 630 – 635.

Trivedi, A., Heinemann, M., Spiess, A. C., Duassmann, T. and Buchs, J. (2005). Optimization of adsorptive immobilization of alcohol dehydrogenases. *Journal Bioscience and Bioengineering.* **4**, 340 – 347.

Vallee, B. L. and Falchuk, K. H. (1993). The biochemical basis of Zinc physiology. *Physiological Reviews.* **73,** 79 – 118.

Walther, K. and Schuller, H. J. (2001). Adr1 and Cat8 synergistically activate the glucose-regulated alcohol dehydrogenase gene *ADH2* of the yeast *Saccharomyces cerevisiae. Microbiology*. **147**, 2037 – 2044.

Wiesenfeld, M., Schimpfessel, L. and Crokaert, R. (1975). Multiple forms of mitochondrial alcohol dehydrogenase in *Saccharomyces cerevisiae. Biochimica et Biophysica Acta.* **405,** 500 – 512.

Williamson, V. M. and Paquin, C. E. (1987). Homology of *Saccharomyces cerevisiae ADH4* to an iron-activated alcohol dehydrogenase from *Zymomonas mobilis. Molecular and General Genetics.* **209,** 374 – 381.

Williamson, V. M., Bennetzen, J., Young, E. T., Nasmyth, K. and Hall, B. D. (1980). Isolation of the structural gene for alcohol dehydrogenase by genetic complementation in yeast. *Nature*. **283,** 214 – 216.

Wills, C., Kratofil, P. and Martin, T. (1982). Functional mutants of yeast alcohol dehydrogenase, *Basic Life Sciences.* **19,** 305 – 329.

Wratten, C. C. and Cleland, W. W. (1963). Product inhibition studies on yeast and liver alcohol dehydrogenase. *Biochemistry*. **2**, 935 – 941.

Young, E. T. and Pilgrim, D. (1985). Isolation and DNA sequence of *ADH3*, a nuclear gene encoding the mitochondrial isozyme of alcohol dehydrogenase in *Saccharomyces cerevisiae. Molecular Cell Biology*. **5,** 3024 – 3334.

Zanon, P. J., Peres, M. F. S. and Gatt'as, E. A. L. (2007). Colorimetric assay of ethanol using alcohol dehydrogenase from dry baker's yeast. *Enzyme and Microbial Technology.* **40**, 466 – 470.

Zundel, G. (1969). Hydration and intermolecular interaction – infrared Investigations with polyelectrolyte membranes. *Academic Press, New York and MIR Moscow, 1972.*